University of Alberta

Applications of Wavelet Bases to Numerical Solutions
of Elliptic Equations

by

Wei Zhao

A thesis submitted to the Faculty of Graduate Studies and Research
in partial fulfillment of the requirements for the degree of

Doctor of Philosophy
in
Mathematics

Department of Mathematical and Statistical Sciences

Fall 2010
Edmonton, Alberta

Examining Committee

Rong-Qing Jia, Mathematics

Yau Shu Wong, Mathematics

Bin Han, Mathematics

Jos Derksen, Chemical and Materials Engineering

Yuesheng Xu, Mathematics, Syracuse University

To my parents

Abstract

In this thesis, we investigate Riesz bases of wavelets and their applications to numerical solutions of elliptic equations.

Compared with the finite difference and finite element methods, the wavelet method for solving elliptic equations is relatively young but powerful. In the wavelet Galerkin method, the efficiency of the numerical schemes is directly determined by the properties of the wavelet bases. Hence, the construction of Riesz bases of wavelets is crucial. We propose different ways to construct wavelet bases whose stability in Sobolev spaces is then established. An advantage of our approaches is their far superior simplicity over many other known constructions. As a result, the corresponding numerical schemes are easily implemented and efficient. We apply these wavelet bases to solve some important elliptic equations in physics and show their effectiveness numerically. Multilevel algorithm based on preconditioned conjugate gradient algorithm is also developed to significantly improve the numerical performance. Numerical results and comparison with other existing methods are presented to demonstrate the advantages of the wavelet Galerkin method we propose.

Acknowledgements

My first and foremost gratitude goes to my supervisor, Professor Rong-Qing Jia, for his patient guidance, constantly encouragement and generous support in many ways during my graduate studies. Without him, this thesis would not have been completed or written. His insightful suggestions and constructive criticisms helped me to improve my research skills and contributed greatly to this thesis.

I thank Professor Bin Han and Professor Yau Shu Wong for all their help. Numerous stimulating discussions with them on wavelet constructions and scientific computing have been invaluable.

I also thank Professor Jos Derksen and Professor Yuesheng Xu for serving on my thesis committee and providing valuable feedbacks.

I am grateful to my friends Jiafen Gong, Hanqing Zhao and Xiaosheng Zhuang for inspiring and in-depth discussions on my research and various kinds of help.

Finally, I am deeply and forever indebted to my parents for their love, support and encouragement throughout my entire life.

Contents

List of Tables

List of Figures

Chapter 1

Introduction

1.1 Preliminary

Wavelets have been proven to be a powerful tool in signal and image processing such as image compression and denoising. In recent years, the wavelet method for numerical solutions of partial differential equations (PDEs) has been developed. For the numerical treatment of elliptic equations, the efficiency of the wavelet preconditioning techniques is directly determined by the properties of the wavelet bases. Riesz bases of spline wavelets are more suitable for numerical solutions of PDEs than the classical orthogonal or biorthogonal wavelets. Spline wavelets with short support were investigated by Jia, Wang and Zhou in [26] and by Han and Shen in [21]. Jia [23] constructed spline wavelets on the interval $[0,1]$ with homogeneous boundary conditions. For polygonal domains, Riesz bases of C^1 spline wavelets were constructed by Davydov and Stevenson [17] on quadrangulation, and by Jia and Liu [25] on arbitrary triangulations. The rigorous wavelet theory provides us a guide to design reliable algorithms for solving elliptic equations. In this thesis, we focus on constructions of spline wavelet bases which provide efficient preconditioners for numerical solutions of elliptic equations. The numerical schemes based on our wavelet bases are simple, efficient and reliable. We implement our algorithms in C and use gcc to compile them. Numerical results are provided to demonstrate the efficiency and effectiveness of the wavelet Galerkin method we propose.

We use $\mathbb{N}$, $\mathbb{Z}$, $\mathbb{R}$ and $\mathbb{C}$ to denote the set of positive integers, integers, real numbers and complex numbers, respectively.

For $s \in \mathbb{N}$, the s-dimensional Euclidean space is denoted by $\mathbb{R}^s$. The inner product in $\mathbb{R}^s$ is defined by

$$x \cdot y := x_1 y_1 + x_2 y_2 + \cdots + x_s y_s,$$

for $x = (x_1, x_2, \ldots, x_s), y = (y_1, y_2, \ldots, y_s) \in \mathbb{R}^s$. Let $\mathbb{N}_0 := \mathbb{N} \cup \{0\}$. An element of $\mathbb{N}_0^s$ is called a multi-index. The length of a multi-index $\mu = (\mu_1, \mu_2, \ldots, \mu_s) \in \mathbb{N}_0^s$ is given by $|\mu| := \mu_1 + \mu_2 + \cdots + \mu_s$. For $\mu = (\mu_1, \mu_2, \ldots, \mu_s) \in \mathbb{N}_0^s$ and $x = (x_1, x_2, \ldots, x_s) \in \mathbb{R}^s$, define $x^\mu := x_1^{\mu_1} x_2^{\mu_2} \cdots x_s^{\mu_s}$. A polynomial is a finite sum of the form $\sum_\mu c_\mu x^\mu$ with c_μ being complex numbers. The degree of a polynomial $q = \sum_\mu c_\mu x^\mu$ is defined to be $\deg q := \max\{|\mu| : c_\mu \neq 0\}$. We use Π_k to denote the linear space of all polynomials of degree at most k.

Let Ω be a (Lebesgue) measurable subset of $\mathbb{R}^s$. Suppose f is a complex-valued (Lebesgue) measurable function on Ω. For $1 \le p < \infty$, let

$$\|f\|_{L_p(\Omega)} := \left(\int_\Omega |f(x)|^p dx \right)^{1/p},$$

and let $\|f\|_{L_\infty(\Omega)}$ denote the essential supremum of $|f|$ on Ω. We omit the reference Ω if there is no ambiguity. For $1 \le p \le \infty$, by $L_p(\Omega)$ we denote the Banach space of all measurable functions f on Ω such that

$\|f\|_{L_p(\Omega)} < \infty$. For $p = 2$, $L_2(\Omega)$ is a Hilbert space with the inner product given by $\langle f, g\rangle := \int_\Omega f(x)\overline{g(x)}dx$, $f, g \in L_2(\Omega)$.

For a vector $y = (y_1, y_2, \ldots, y_s) \in \mathbb{R}^s$, let D_y denote the differential operator given by

$$D_y f(x) := \lim_{t\to 0} \frac{f(x+ty) - f(x)}{t}, \quad x \in \mathbb{R}^s.$$

Let $e_1, e_2, \ldots, e_s$ be the unit coordinate vectors in $\mathbb{R}^s$. For $j = 1, 2, \ldots, s$, we write D_j for D_{e_j}. For a multi-index $\mu = (\mu_1, \mu_2, \ldots, \mu_s)$, we use D^μ to denote the differential operator $D_1^{\mu_1} D_2^{\mu_2} \cdots D_s^{\mu_s}$.

Suppose Ω is a (nonempty) open subset of $\mathbb{R}^s$. Let $C(\Omega)$ be the linear space of all continuous functions on Ω. By $C_c(\Omega)$ we denote the linear space of all continuous functions on Ω with compact support contained in Ω. For an integer $r \geq 0$, we use $C^r(\Omega)$ to denote the linear space of those functions f on Ω for which $D^\alpha f \in C(\Omega)$ for all $|\alpha| \leq r$. Let $C^\infty(\Omega) := \bigcap_{r=0}^\infty C^r(\Omega)$ and $C_c^\infty(\Omega) := C_c(\Omega) \cap C^\infty(\Omega)$.

For $m \in \mathbb{N}_0$, the Sobolev space $H^m(\Omega)$ is defined by

$$H^m(\Omega) := \{u \in L_2(\Omega) : D^\alpha u \in L_2(\Omega) \text{ for all } |\alpha| \leq m\},$$

where $D^\alpha u$ exists in the distributional sense, i.e.,

$$\langle D^\alpha u, \phi\rangle = (-1)^{|\alpha|}\langle u, D^\alpha \phi\rangle$$

for all $\phi \in C_c^\infty(\Omega)$. $H^m(\Omega)$ is a Hilbert space with inner product given by

$$\langle u, v\rangle_{H^m} := \sum_{|\alpha|\leq m} \langle D^\alpha u, D^\alpha v\rangle \text{ for } u, v \in H^m(\Omega).$$

We define the norm and semi-norm in $H^m(\Omega)$ by

$$\|u\|_{H^m} := \sqrt{\langle u, u\rangle_{H^m}} \text{ for } u \in H^m(\Omega)$$

and

$$|u|_{H^m} := \sqrt{\sum_{|\alpha|=m} \langle D^\alpha u, D^\alpha u \rangle} \text{ for } u \in H^m(\Omega),$$

respectively. Let $H_0^m(\Omega)$ be the closure of $C_c^\infty(\Omega)$ with respect to the norm $\|\cdot\|_{H^m}$ in $H^m(\Omega)$. The norm and semi-norm in $H_0^m(\Omega)$ are inherited from $H^m(\Omega)$.

Now suppose that Ω is a bounded and connected open subset of $\mathbb{R}^s$, and its boundary $\partial\Omega$ is Lipschitz continuous (see [20] for details). By Poincaré-Friedrichs inequality (see, e.g., [19]), the norm and semi-norm in $H_0^m(\Omega)$ are equivalent in the sense that

$$C_1|u|_{H^m} \leq \|u\|_{H^m} \leq C_2|u|_{H^m}$$

for $u \in H_0^m(\Omega)$ and some positive constants C_1 and C_2 independent of u.

Consider the elliptic equation of order $2m$, $m \in \mathbb{N}$, with homogenous boundary conditions given by

$$\begin{cases} Lu = f & \text{in} \quad \Omega, \\ u = 0, \dfrac{\partial u}{\partial n} = 0, \ldots, (\dfrac{\partial}{\partial n})^{m-1} u = 0 & \text{on} \quad \partial\Omega, \end{cases} \tag{1.1.1}$$

where

$$L = \sum_{|\alpha|,|\beta| \leq m} (-1)^{|\beta|} D^\beta (a_{\alpha\beta}(x) D^\alpha),$$

and $(\frac{\partial}{\partial n})^{m-1} u$ denotes the $(m-1)^{th}$ derivative of u in the direction normal to the boundary $\partial\Omega$. We assume that $a_{\alpha\beta} \in C(\Omega)$, $f \in L_2(\Omega)$ and there exists a positive constant λ independent of x and ξ such that

$$\sum_{|\alpha|=|\beta|=m} a_{\alpha\beta}(x) \xi^{\alpha+\beta} \geq \lambda |\xi|^{2m}, \ \ x \in \Omega, \xi \in \mathbb{R}^s.$$

In fact, the last assumption defines the ellipticity of the deferential operator L. We will develop the wavelet Galerkin method for solving (1.1.1) efficiently.

1.2 The Galerkin Method

Let us consider the variational formulation of equation (1.1.1):

$$\text{find } u \in H_0^m(\Omega) \text{ with } a(u,v) = l(v) \text{ for all } v \in H_0^m(\Omega), \tag{1.2.1}$$

where

$$a(u,v) := \sum_{|\alpha|,|\beta| \le m} \int_\Omega a_{\alpha\beta}(x)(D^\alpha u(x))(D^\beta v(x))dx$$

and

$$l(v) := \int_\Omega f(x)v(x)dx.$$

If there exists a unique solution to equation (1.2.1), this solution is called the weak solution. Note that the classical solution satisfies (1.2.1), and the weak solution satisfies (1.1.1) if it lies in $C^{2m}(\Omega)$.

The bilinear form $a(u,v)$ is continuous if

$$a(u,v) \le C_1 \|u\|_{H^m} \|v\|_{H^m} \tag{1.2.2}$$

holds true for all $u, v \in H_0^m(\Omega)$ and some positive constant C_1 independent of u and v.

$a(u,v)$ is called coercive if for $u \in H_0^m(\Omega)$ there exists a positive constant C_2 independent of u such that

$$a(u,u) \ge C_2 \|u\|_{H^m}^2. \tag{1.2.3}$$

Suppose $a(u,v)$ is continuous and coercive, by the Lax-Milgram theorem (see, e.g., [5]), the unique solvability of equation (1.2.1) is guaranteed.

Now we assume all functions are real-valued and the bilinear form $a(\cdot,\cdot)$ is symmetric. To apply the Galerkin method to solve equation (1.2.1) numerically, we take a finite dimensional subspace V_n to approximate $H_0^m(\Omega)$ and seek $u_n \in V_n$ such that

$$a(u_n, v) = l(v), \qquad \forall v \in V_n. \tag{1.2.4}$$

The dimension of V_n increases as n increases. Suppose $\dim V_n = d_n$ where d_n is a positive integer and $\Phi_n = \{\phi_{n,1}, \ldots, \phi_{n,d_n}\}$ is a basis of V_n. Then for each positive integer i, $1 \le i \le d_n$, (1.2.4) holds true, i.e.,

$$a(u_n, \phi_{n,i}) = l(\phi_{n,i}), \qquad i = 1, 2, \ldots, d_n. \tag{1.2.5}$$

Since $u_n \in V_n$, we seek $y_{n,1}, \ldots, y_{n,d_n} \in \mathbb{R}$ such that $u_n := \sum_{i=1}^{d_n} y_{n,i}\phi_{n,i}$ satisfies the linear system (1.2.5). Thus we can write (1.2.5) in the following matrix form:

$$A_n y_n = \xi_n \tag{1.2.6}$$

where $A_n = (a(\phi_{n,i}, \phi_{n,j}))_{1\le i,j\le d_n}$, $y_n = (y_{n,i})^T_{1\le i\le d_n}$ and $\xi_n = (l(\phi_{n,i}))^T_{1\le i\le d_n}$. A_n is called the stiffness matrix. By solving (1.2.6), we obtain an approximate solution to (1.2.1).

The condition number $\kappa(A_n)$ of A_n usually deteriorates as n increases. Hence A_n becomes ill-conditioned when n is large. An ill-conditioned matrix usually results in very slow convergence for classical iterative methods. This motivates us to propose the wavelet Galerkin method.

1.3 The Wavelet Galerkin Method

In brief, the wavelet Galerkin method proceeds by choosing a proper basis, called a wavelet basis, of the approximate space V_n such that the condition number of the stiffness matrix associated with this basis is relatively small and uniformly bounded (independent of the level n). This leads us to study Riesz bases in Hilbert spaces.

Let H be a Hilbert space. The inner product of two elements u and v in H is denoted by $\langle u, v\rangle$. The norm of an element u in H is given by $\|u\| := \sqrt{\langle u, u\rangle}$. Let J be a countable index set. A sequence $(v_j)_{j\in J}$ in the Hilbert space H is said to be a Bessel sequence if there exists a positive constant C such that the inequality

$$\Big\| \sum_{j\in J} c_j v_j \Big\| \le C \Big(\sum_{j\in J} |c_j|^2 \Big)^{1/2}$$

holds for every sequence $(c_j)_{j\in J}$ with only finitely many nonzero terms. A sequence $(v_j)_{j\in J}$ in H is said to be a Riesz sequence if there exist two positive constants C_1 and C_2 such that the inequalities

$$C_1 \Big(\sum_{j\in J} |c_j|^2 \Big)^{1/2} \le \Big\| \sum_{j\in J} c_j v_j \Big\| \le C_2 \Big(\sum_{j\in J} |c_j|^2 \Big)^{1/2}$$

hold for every sequence $(c_j)_{j\in J}$ with only finitely many nonzero terms. We call C_1 a Riesz lower bound and C_2 a Riesz upper bound. If $(v_j)_{j\in J}$ is a Riesz sequence in H and the linear span of $(v_j)_{j\in J}$ is dense in H, then $(v_j)_{j\in J}$ is said to be a Riesz (or stable) basis of H. If $(v_j)_{j\in J}$ is a Riesz basis of H, then the condition number of the matrix $(\langle v_j, v_k\rangle)_{j,k\in J}$ is no bigger than C_2^2/C_1^2. See [42] for details.

Note that $H_0^m(\Omega)$ is a Hilbert space with the inner product given by $\langle u, v\rangle_{H^m}$ for $u, v \in H_0^m(\Omega)$. In order to solve equation (1.2.1) using the wavelet

Galerkin method, we first formulate a sequence of finite dimensional subspaces $(V_n)_{n\geq n_0}$ of $H_0^m(\Omega)$ such that $V_n \subset V_{n+1}$ for all $n \geq n_0$ and $\bigcup_{n=n_0}^{\infty} V_n$ is dense in $H_0^m(\Omega)$ where n_0 is a positive integer. In general, we choose an appropriate basis $\Phi_n := \{\phi_{n,j}^i, j \in J_n^i, 1 \leq i \leq r\}$ for V_n. Here r is a positive integer, whereas $\{\phi^1, \dots, \phi^r\}$ are real-valued functions, and

$$\phi_{n,j}^i(x) := \phi^i(2^n x - j), j \in J_n^i, 1 \leq i \leq r, x \in \Omega$$

for some index set $J_n^i, 1 \leq i \leq r$.

Then we construct a suitable subspace W_n of V_{n+1}, called a wavelet space, such that V_{n+1} is the direct sum of V_n and W_n for $n \geq n_0$. Similarly, W_n is constructed by a number of functions $\{\psi^1, \dots, \psi^t\}$ where t is a positive integer. Specifically, let

$$\psi_{n,k}^i(x) := \psi^i(2^n x - k), k \in K_n^i, 1 \leq i \leq t, x \in \Omega$$

for some index set $K_n^i, 1 \leq i \leq t$, and $\Gamma_n := \{\psi_{n,k}^i, k \in K_n^i, 1 \leq i \leq t\}$ forms a basis of W_n. $\psi^1, \dots, \psi^{t-1}$ and ψ^t are called wavelets.

By the construction, we have

$$V_n = V_{n_0} + W_{n_0} + \cdots + W_{n-1}.$$

Therefore $\Psi_n := \Phi_{n_0} \bigcup (\bigcup_{k=n_0}^{n-1} \Gamma_k)$ forms a basis of V_n other than Φ_n. Let $\Psi := \Phi_{n_0} \bigcup (\bigcup_{k=n_0}^{\infty} \Gamma_k)$. We normalize Ψ_n and Ψ with respect to the H^m norm in the sense that the H^m norm of each basis function is a constant independent of n. And we use Ψ_n^{norm} and Ψ^{norm} to denote the normalized Ψ_n and Ψ, respectively. Under certain conditions, Ψ^{norm} forms a Riesz basis of $H_0^m(\Omega)$.

An application of a general result in chapter 4 of [42] gives the following proposition, which relates the Riesz basis of $H_0^m(\Omega)$ and the condition number of the associated stiffness matrix.

Proposition 1.1. *If Ψ^{norm} is a Riesz basis of $H_0^m(\Omega)$ and $a(u,v)$ is both continuous and coercive, then the condition number of the stiffness matrix associated with Ψ_n^{norm}, i.e., $B_n := (a(\chi,\psi))_{\chi,\psi\in\Psi_n^{norm}}$, is uniformly bounded.*

Proof. For $n > n_0$, let $\lambda_{max}(B_n)$ and $\lambda_{min}(B_n)$ be the maximal and minimal eigenvalues of B_n. Then the condition number $\kappa(B_n) = \lambda_{max}(B_n)/\lambda_{min}(B_n)$. For any eigenvalue $\lambda(B_n)$ of B_n, there exists a column vector $z = (a_\psi)_{\psi\in\Psi_n^{norm}}$ such that $\lambda(B_n) = z^T B_n z/z^T z$. Ψ is a Riesz basis of $H_0^m(\Omega)$, then there exist two positive constants C_1 and C_2 such that

$$C_1 z^T z \le \Big\| \sum_{\psi\in\Psi_n^{norm}} (a_\psi \psi) \Big\|_{H^m}^2 \le C_2 z^T z.$$

The fact that $a(u,v)$ is continuous and coercive implies

$$\begin{aligned} C_3 \Big\| \sum_{\psi\in\Psi_n^{norm}} (a_\psi \psi) \Big\|_{H^m}^2 &\le a\Big(\sum_{\psi\in\Psi_n^{norm}} (a_\psi \psi), \sum_{\psi\in\Psi_n^{norm}} (a_\psi \psi) \Big) \\ &\le C_4 \Big\| \sum_{\psi\in\Psi_n^{norm}} (a_\psi \psi) \Big\|_{H^m}^2 \end{aligned}$$

for some positive constants C_3 and C_4 independent of n. Therefore,

$$C_1 C_3 z^T z \le a\Big(\sum_{\psi\in\Psi_n^{norm}} (a_\psi \psi), \sum_{\psi\in\Psi_n^{norm}} (a_\psi \psi) \Big) \le C_2 C_4 z^T z.$$

Note that

$$z^T B_n z = a\Big(\sum_{\psi\in\Psi_n^{norm}} (a_\psi \psi), \sum_{\psi\in\Psi_n^{norm}} (a_\psi \psi) \Big).$$

We have

$$C_1 C_3 z^T z \le z^T B_n z \le C_2 C_4 z^T z.$$

Thus

$$C_1 C_3 \le \lambda(B_n) = z^T B_n z/z^T z \le C_2 C_4.$$

Consequently $\kappa(B_n) = \lambda_{max}(B_n)/\lambda_{min}(B_n) \leq (C_2C_4)/(C_1C_3)$, i.e. $\kappa(B_n)$ is uniformly bounded. $\square$

In order to solve equation (1.2.1) efficiently, this proposition guides us to construct a Riesz basis of $H_0^m(\Omega)$ since the condition number of the stiffness matrix associated with Riesz basis is uniformly bounded. Therefore, our goal is to construct a Riesz basis of $H_0^m(\Omega)$ such that the condition number of the associated stiffness matrix is as small as possible.

1.4 Organization of this Thesis

Here is the outline of this thesis.

Chapter 1 gives an overview of the wavelet Galerkin method for numerical solutions of elliptic equations. The elliptic equations with homogeneous boundary conditions and the Galarekin method are introduced. In order to apply the wavelet Galerkin method to solve the corresponding variational problems, we relate Riesz bases in Sobolev spaces and the condition numbers of the associated stiffness matrices. Thus we make clear that our goal is to construct proper Riesz bases of wavelets in Sobolev spaces.

Chapter 2 discusses wavelets on the interval. We formulate approximate subspaces $(V_n)_{n\geq 1}$ of $H_0^2(0,1)$ based on Hermite cubic splines. By orthogonality with respect to $\langle u'', v'' \rangle$, wavelet spaces $(W_n)_{n\geq 1}$ are constructed. We analyze the properties of the finite element bases of $(V_n)_{n\geq 1}$ and establish the stability of the wavelet bases in $H_0^2(0,1)$. These wavelet bases are applied to numerical solutions to the Euler-Bernoulli equation.

Chapter 3 studies the wavelet Galerkin method for the second-order elliptic equations with variable coefficients in the two-dimensional space. We first construct stable wavelet bases in $H_0^1((0,1)^2)$, and then apply the associated preconditioning technique in the finite difference method, instead of the finite element method, for solving general second-order elliptic equations with rough variable coefficients. The numerical results and comparison with classical multigrid algorithms are provided.

Chapter 4 investigates Riesz bases of wavelets in $H_0^2((0,1)^2)$ and their applications to numerical solutions of the Biharmonic equation and general elliptic equations of fourth order. Stable wavelet bases are constructed in the one-dimensional case and then extended to the two-dimensional case by tensor products. The characterization of Riesz bases in Hilbert spaces is proposed. Automatic multilevel algorithm is developed for solving the Biharmonic equation with error estimates in the energy norm. We compare our method with many other popular numerical methods from different point of view such as number of iterations, relative residue reduction and computational cost.

Chapter 5 highlights our main contributions and indicates possible directions for future research.

Chapter 2

Wavelet Bases on the Interval and Applications

2.1 Introduction

In this chapter, we investigate stable wavelet bases of Hermite cubic splines on the interval. These wavelet bases are suitable for numerical solutions of differential equations of the fourth order.

Orthogonal wavelets were constructed by Daubechies in [16], while biorthogonal wavelets were investigated by Dahmen and Micchelli in [15]. Chui and Wang [12] initiated the study of semi-orthogonal wavelets. In order to deal with problems with bounded domains, Daubechies wavelets were adapted to the interval $[0, 1]$ by Cohen, Daubechies and Vial [13]. Chui and Quak adapted semi-orthogonal wavelets to the interval $[0, 1]$ in [11], and the Riesz basis property was established by Jia in [22]. Dahmen, Han, Jia and Kunoth [14] constructed biorthogonal multiwavelets on the basis of Hermite cubic splines and adapted them to the interval $[0, 1]$.

However, in order to solve differential equations, the orthogonality in the energy norm is more desirable than that in the L_2 norm. The orthogonality with respect to $\langle u', v' \rangle$ instead of $\langle u, v \rangle$ were considered in [10] and [24]. Christon and Roach [10] discussed wavelets on the basis of linear finite elements. Jia and Liu [24] constructed wavelet bases using Hermite cubic splines and applied them to numerical solutions to the Sturm-Liouville equation with Dirichlet boundary conditions. In [9], Chen, Wu and Xu proposed a general construction of wavelets according to the orthogonality with respect to $\langle u^{(m)}, v^{(m)} \rangle$, where m is a positive integer. Based on these wavelet bases, the multilevel augmentation methods provided a very fast solution for a class of differential equations whose highest order term has a constant coefficient.

Here we consider the fourth-order differential equations of the type

$$\begin{cases} (a(x)u'')''(x) - (b(x)u')' + c(x)u(x) = f(x) \text{ for } x \in (0,1), \\ u(0) = u(1) = u'(0) = u'(1) = 0, \end{cases} \tag{2.1.1}$$

where $a(x)$ is a positive continuous function satisfying $K_1 \leq a(x) \leq K_2$ for all $x \in [0,1]$ and positive constants K_1 and K_2. $b(x) \geq 0$, $c(x) \geq 0$ and $f \in L_2(0,1)$. Hence we use the orthogonality with respect to $\langle u'', v'' \rangle$. For simplicity, we apply the wavelet bases to numerical solutions to the Euler-Bernoulli beam equation, i.e.,

$$\begin{cases} (a(x)u'')''(x) = f(x) \text{ for } x \in (0,1), \\ u(0) = u(1) = u'(0) = u'(1) = 0. \end{cases} \tag{2.1.2}$$

To solve the Euler-Bernoulli beam equation by the Galerkin finite element method, we must use at least a cubic polynomial expansion over the individual elements, and require a C^1 solution. Therefore, we choose Hermite cubic splines which have good interpolation property. Although the associated wavelet bases are the same as those in [9], the constructions were independent and the numerical schemes are different. The aim of this chapter is to illustrate classical constructions of wavelets and relevant numerical schemes by solving relatively simple examples and help further understanding the wavelet Galerkin methods in more complicated cases afterwards.

2.2 Wavelets on the Interval

Recall that $L_2(0,1)$ denotes the space of all square-integrable real-valued functions on $(0,1)$. The inner product in $L_2(0,1)$ is defined as

$$\langle u, v\rangle := \int_0^1 u(x)v(x)dx, \;\; u, v \in L_2(0,1).$$

$H^2(0,1)$ is the space of all functions u in $L_2(0,1)$ for which (the distributional derivative) $u'' \in L_2(0,1)$. The norm in $H^2(0,1)$ is defined as

$$\|u\|_{H^2} := \left(\int_0^1 \Big[\big(u(x)\big)^2 + \big(u'(x)\big)^2 + \big(u''(x)\big)^2 \Big] dx \right)^{1/2}, \;\; u \in H^2(0,1),$$

and the semi-norm is given by

$$|u|_{H^2} := \left(\int_0^1 \big(u''(x)\big)^2 dx \right)^{1/2}, \;\; u \in H^2(0,1).$$

$H_0^2(0,1)$ is the closure of $C_c^\infty(0,1)$ with respect to the norm $\|\cdot\|_{H^2}$ in $H^2(0,1)$. The norm and semi-norm in $H_0^2(0,1)$ are inherited from $H^2(0,1)$ and equivalent.

For $n \geq 1$, let V_n be the space of those cubic splines $v \in C^1[0,1]$ for which $v(0) = v(1) = v'(0) = v'(1) = 0$ and

$$v|_{(j/2^n,(j+1)/2^n)} \in \Pi_3|_{(j/2^n,(j+1)/2^n)} \text{ for } j = 0, \ldots, 2^n - 1.$$

The dimension of V_n is $2^{n+1} - 2$.

Moreover,

- V_n's are nested, i.e., $V_1 \subset V_2 \subset \cdots \subset V_n \subset \cdots$;
- $\bigcup_{n=1}^{\infty} V_n$ is dense in $H_0^2(0,1)$.

We first find a basis for V_n.

Consider the Hermite cubic splines given by

$$\phi_1(x) = \begin{cases} (x+1)^2(1-2x) & \text{for} \quad -1 \leq x < 0, \\ (1-x)^2(2x+1) & \text{for} \quad 0 \leq x \leq 1, \\ 0 & \text{for} \quad \mathbb{R} \setminus [-1,1], \end{cases}$$

and

$$\phi_2(x) = \begin{cases} x(x+1)^2 & \text{for} \quad -1 \leq x < 0, \\ x(x-1)^2 & \text{for} \quad 0 \leq x \leq 1, \\ 0 & \text{for} \quad \mathbb{R} \setminus [-1,1]. \end{cases}$$

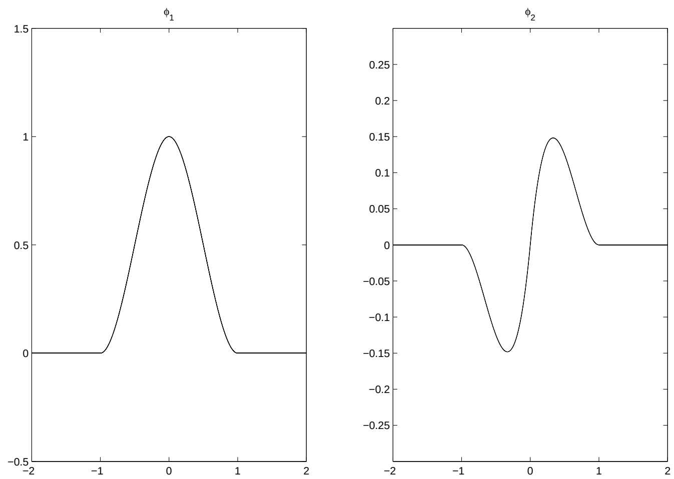

FIGURE 2.1: Hermit Cubic Splines

ϕ_1 and ϕ_2 satisfy the following refinement equations:

$$\begin{aligned} \phi_1(x) = &\ \frac{1}{2}\phi_1(2x+1) + \frac{3}{4}\phi_2(2x+1) + \phi_1(2x) \\ &+\frac{1}{2}\phi_1(2x-1) - \frac{3}{4}\phi_2(2x-1) \\ \phi_2(x) = &\ -\frac{1}{8}\phi_1(2x+1) - \frac{1}{8}\phi_2(2x+1) + \frac{1}{2}\phi_2(2x) \\ &+\frac{1}{8}\phi_1(2x-1) - \frac{1}{8}\phi_2(2x-1). \end{aligned} \tag{2.2.1}$$

Note that ϕ_1 is an even function, and ϕ_2 is an odd function. Moreover, ϕ_1 and ϕ_2 have continuous first derivatives on $\mathbb{R}$ satisfying:

$$\phi_1(0) = 1, \phi_1'(0) = 0, \phi_2(0) = 0, \phi_2'(0) = 1,$$

$$\phi_1(j) = 0, \phi_1'(j) = 0, \phi_2(j) = 0, \phi_2'(j) = 0,$$

for $j \in \mathbb{Z} \setminus \{0\}$. Thus, for $f \in C^1(\mathbb{R})$,

$$u = \sum_{j\in\mathbb{Z}} f(j)\phi_1(\cdot - j) + \sum_{j\in\mathbb{Z}} f'(j)\phi_2(\cdot - j)$$

is a Hermite interpolation of f on $\mathbb{Z}$, i.e., $u(j) = f(j)$ and $u'(j) = f'(j)$ for all $j \in \mathbb{Z}$.

For $0 \le x \le 1$ and $n \ge 1$, define

$$\phi_{n,j}(x) := \begin{cases} \phi_1(2^n x - (j+1)/2) & \text{for} \quad j = 1, 3, 5, \ldots, 2^{n+1} - 3, \\ \phi_2(2^n x - j/2) & \text{for} \quad j = 2, 4, 6, \ldots, 2^{n+1} - 2. \end{cases}$$

Let $\Phi_n := \{\phi_{n,j}, j = 1, 2, \ldots, 2^{n+1} - 2\}$. It is easy to check that Φ_n is a basis of V_n.

Next we construct wavelet space $W_n \subset V_{n+1}$ such that

$$\int_0^1 v''(x)w''(x)dx = 0, \;\; \forall v \in V_n \;\text{ and }\; w \in W_n. \tag{2.2.2}$$

Then V_{n+1} is the direct sum of V_n and W_n, and the dimension of W_n is $\dim(V_{n+1}) - \dim(V_n) = (2^{n+2} - 2) - (2^{n+1} - 2) = 2^{n+1}$.

Suppose $\psi \in W_n$, then there exists a sequence $(b(j))_{j=1,2,\ldots,2^{n+2}-2}$ such that $\psi = \sum_{j=1}^{2^{n+2}-2} b(j)\phi_{n+1,j}$ on $[0, 1]$ since $W_n \subset V_{n+1}$ and Φ_{n+1} is a basis of V_{n+1}. By (2.2.2), we have

$$\int_0^1 \Big(\sum_{j=1}^{2^{n+2}-2} b(j)\phi_{n+1,j}\Big)''(x)\phi''_{n,k}(x)dx = 0, \;\text{ for }\; k = 1, 2, \ldots, 2^{n+1} - 2.$$

This linear system can be written in the following matrix form:

$$T\mathbf{b} = \mathbf{0}, \tag{2.2.3}$$

where $T = (\langle \phi''_{n,k}, \phi''_{n+1,j} \rangle)_{1 \le k \le 2^{n+1}-2, 1 \le j \le 2^{n+2}-2}$ and $\mathbf{b}$ is the column vector $(b(1), b(2), \ldots, b(2^{n+2}-2))^T$. Note that

$$\phi''_1(x) = \begin{cases} -12x - 6 & \text{for} \quad -1 < x < 0, \\ 12x - 6 & \text{for} \quad 0 < x < 1, \\ 0 & \text{for} \quad \mathbb{R} \setminus [-1, 1], \end{cases}$$

and

$$\phi''_2(x) = \begin{cases} 6x + 4 & \text{for} \quad -1 < x < 0, \\ 6x - 4 & \text{for} \quad 0 < x < 1, \\ 0 & \text{for} \quad \mathbb{R} \setminus [-1, 1]. \end{cases}$$

The $(2^{n+1} - 2) \times (2^{n+2} - 2)$ matrix T has the following form by direct computation,

$$T = (\mathbf{0}, \mathbf{0}, *, *, \mathbf{0}, \mathbf{0}, *, *, \cdots, *, *, \mathbf{0}, \mathbf{0}),$$

i.e., for $0 \le l \le 2^n - 1$, the $4l + 1$ and $4l + 2$ columns of T are zero vectors, and $*$ stands for a non-zero vector. Therefore, (2.2.3) has 2^{n+1} linearly independent solutions e_{4l+1} and e_{4l+2} for $0 \le l \le 2^n - 1$, where e_i is the ith unit vector in $\mathbb{R}^{2^{n+2}-2}$. Correspondingly, $\phi_{n+1,4l+1}, \phi_{n+1,4l+2} \in W_n$ for $0 \le l \le 2^n - 1$, and they form a basis of W_n by their linear independence and $\dim(W_n) = 2^{n+1}$. Let

$$\psi_1(x) = \phi_1(2x + 1) \ \text{ and } \ \psi_2(x) = \phi_2(2x + 1) \ \text{ for } \ x \in \mathbb{R}.$$

For $0 \le x \le 1$ and $n \ge 1$, define

$$\psi_{n,j}(x) := \begin{cases} \psi_1(2^n x - (j + 1)/2) & \text{for} \quad j = 1, 3, 5, \ldots, 2^{n+1} - 1, \\ \psi_2(2^n x - j/2) & \text{for} \quad j = 2, 4, 6, \ldots, 2^{n+1}. \end{cases}$$

Then $\Gamma_n := \{\psi_{n,j}, j = 1, 2, \ldots, 2^{n+1}\}$ is a basis of W_n.

To avoid treating the term V_1 every time separately, we define $W_0 := V_1$, $\psi_{0,1} := \phi_1(2x-1)$ and $\psi_{0,2} := \phi_2(2x-1)$. Since V_{n+1} is a direct sum of V_n and W_n, we have the following decomposition:

$$V_{n+1} = W_0 + W_1 + \cdots + W_n.$$

Note that V_n is orthogonal to W_n with respect to $\langle u'', v'' \rangle$. Thus W_m is orthogonal to W_n with respect to $\langle u'', v'' \rangle$ for $m \neq n$.

Moreover,

$$\langle \psi''_{n,j}, \psi''_{n,k} \rangle = 0 \text{ for } 1 \leq j, k \leq 2^{n+1} \text{ and } j \neq k. \tag{2.2.4}$$

Indeed, if $|j-k| \geq 2$, $\mathrm{supp}(\psi''_{n,j}) \cap \mathrm{supp}(\psi''_{n,k}) = \emptyset$. If j is an even number, $\mathrm{supp}(\psi''_{n,j}) \cap \mathrm{supp}(\psi''_{n,j+1}) = \emptyset$. Thus in these two cases, (2.2.4) holds. If j is an odd number, (2.2.4) is true because $\langle \phi''_1, \phi''_2 \rangle = 0$.

Consequently, $\bigcup_{n=0}^{\infty} \Gamma_n$ is an orthogonal basis of $H_0^2(0,1)$ with respect to $\langle u'', v'' \rangle$. Similarly $\Psi_n := \bigcup_{k=0}^{n-1} \Gamma_k$ is an orthogonal basis of V_n with respect to $\langle u'', v'' \rangle$.

2.3 The Finite Element and Wavelet Bases

In this section, we discuss the properties of the finite element bases $(\Phi_n)_{n \geq 1}$ and the wavelet bases $(\Psi_n)_{n \geq 1}$.

Proposition 2.1. *For $n \geq 1$,*

$$2^{n/2}\Phi_n := \{2^{n/2}\phi_{n,j}, j = 1, 2, \ldots, 2^{n+1} - 2\}$$

is a Riesz basis of V_n in the L_2 space.

Proof. Let $p_3(x)$ be a cubic polynomial defined on $[x_0, x_0+h]$ satisfying:

$$p_3(x_0) = a_0, p_3(x_0+h) = a_1, p_3'(x_0) = b_0, \text{and } p_3'(x_0+h) = b_1,$$

where x_0, h, a_0, a_1, b_0 and b_1 are real numbers. Then

$$p_3(x) = ax^3 + bx^2 + cx + d,$$

where

$$\begin{aligned}
a &= \frac{2(a_0-a_1)}{h^3} + \frac{b_0+b_1}{h^2}, \\
b &= \frac{3(a_1-a_0)(2x_0+h)}{h^3} - \frac{(3x_0+2h)b_0 + (3x_0+h)b_1}{h^2}, \\
c &= \frac{6(a_0-a_1)x_0(x_0+h)}{h^3} - \frac{(x_0+h)(3x_0+h)b_0 + x_0(3x_0+2h)b_1}{h^2}, \\
d &= \frac{a_0(x_0+h)^2(h-2x_0) + x_0^2 a_1(2x_0+3h)}{h^3} \\
&\quad - \frac{x_0(x_0+h)^2 b_0 + (x_0+h)x_0^2 b_1}{h^2}.
\end{aligned}$$

Therefore,

$$\begin{aligned}
\int_{x_0}^{x_0+h} p_3^2(x)dx = \; & \frac{h}{210}(54a_0a_1 + 22a_0hb_0 - 13a_0hb_1 + 13a_1hb_0 + 78a_0^2 \\
& -22a_1hb_1 - 3h^2b_0b_1 + 78a_1^2 + 2h^2b_0^2 + 2h^2b_1^2).
\end{aligned} \tag{2.3.1}$$

Suppose $f = \sum_{j=1}^{2^{n+1}-2} 2^{n/2} x_{n,j}\phi_{n,j}$, $g = \sum_{j=1}^{2^{n+1}-2} x_{n,j}\phi_{n,j}$ and $h = 1/2^n$, then

$$\|f\|_{L_2}^2 = 2^n \int_0^h g^2(x)dx + \sum_{j=2}^{2^n-1} 2^n \int_{(j-1)h}^{jh} g^2(x)dx + 2^n \int_{(2^n-1)h}^{1} g^2(x)dx.$$

Note that $g(0)=0, g(h)=x_{n,1}, g'(0)=0$ and $g'(h)=x_{n,2}/h$, by (2.3.1) we have

$$\begin{aligned} 2^n\int_0^h g^2(x)dx &= \frac{1}{210}(78x_{n,1}^2+2x_{n,2}^2-22x_{n,1}x_{n,2}) \\ &= \begin{pmatrix} x_{n,1} & x_{n,2} \end{pmatrix} \begin{pmatrix} \frac{13}{35} & -\frac{11}{210} \\ -\frac{11}{210} & \frac{1}{105} \end{pmatrix} \begin{pmatrix} x_{n,1} \\ x_{n,2} \end{pmatrix}. \end{aligned}$$

Since the maximal and minimal eigenvalues of the matrix

$$\begin{pmatrix} \frac{13}{35} & -\frac{11}{210} \\ -\frac{11}{210} & \frac{1}{105} \end{pmatrix}$$

are $4/21+\sqrt{1565}/210$ and $4/21-\sqrt{1565}/210$, respectively,

$$C_1(x_{n,1}^2+x_{n,2}^2) \le 2^n\int_0^h g^2(x)dx \le C_2(x_{n,1}^2+x_{n,2}^2), \tag{2.3.2}$$

where $C_1 = 4/21-\sqrt{1565}/210 > 0$ and $C_2 = 4/21+\sqrt{1565}/210 > 0$.

An analogous argument gives

$$C_3(x_{n,2^{n+1}-3}^2+x_{n,2^{n+1}-2}^2) \le 2^n\int_{(2^n-1)h}^1 g^2(x)dx \le C_4(x_{n,2^{n+1}-3}^2+x_{n,2^{n+1}-2}^2) \tag{2.3.3}$$

for some positive constants C_3 and C_4 independent of n.

For $j=2,3,\ldots,2^n-1$, we have $g((j-1)h)=x_{n,2j-3}$, $g(jh)=x_{n,2j-1}$, $g'((j-1)h)=x_{n,2j-2}/h$ and $g'(jh)=x_{n,2j}/h$, hence by (2.3.1)

$$2^n\int_{(j-1)h}^{jh} g^2(x)dx = \vec{x}_{n,j}^T M\vec{x}_{n,j},$$

where $\vec{x}_{n,j}$ is the column vector $(x_{n,2j-3}, x_{n,2j-1}, x_{n,2j-2}, x_{n,2j})^T$ and

$$M = \begin{pmatrix} \frac{13}{35} & \frac{9}{70} & \frac{11}{210} & -\frac{13}{420} \\ \frac{9}{70} & \frac{13}{35} & \frac{13}{420} & -\frac{11}{210} \\ \frac{11}{210} & \frac{13}{420} & \frac{1}{105} & -\frac{1}{140} \\ -\frac{13}{420} & -\frac{11}{210} & -\frac{1}{140} & \frac{1}{105} \end{pmatrix}.$$

Since the maximal and minimal eigenvalues of M are $31/120 + \sqrt{941}/120$ and $103/840 - \sqrt{421}/168$, respectively, we have

$$\begin{aligned} & C_5(x_{n,2j-3}^2 + x_{n,2j-2}^2 + x_{n,2j-1}^2 + x_{n,2j}^2) \le 2^n \textstyle\int_{(j-1)h}^{jh} g^2(x)dx \\ & \le C_6(x_{n,2j-3}^2 + x_{n,2j-2}^2 + x_{n,2j-1}^2 + x_{n,2j}^2), \end{aligned} \tag{2.3.4}$$

where $C_5 = 103/840 - \sqrt{421}/168 > 0$ and $C_6 = 31/120 + \sqrt{941}/120 > 0$.

Consequently, by (2.3.2), (2.3.3) and (2.3.4),

$$C_7 \sum_{j=1}^{2^{n+1}-2} x_{n,j}^2 \le \|f\|_{L_2}^2 \le C_8 \sum_{j=1}^{2^{n+1}-2} x_{n,j}^2,$$

where

$$C_7 = \min\{C_1 + C_5, 2C_5, C_5 + C_3\} \text{ and } C_8 = \max\{C_2 + C_6, 2C_6, C_6 + C_4\}.$$

This completes the proof. $\square$

The stability of the finite element basis in L_2 leads to the uniform boundedness of the condition number of the mass matrix. However, if we discretize (2.1.1) using the finite element basis, the resulting linear system is ill-conditioned. In fact, we need to look for a basis such that the condition number of the stiffness matrix is relatively small and uniformly bounded.

The following theorem and proposition 1.1 indicate that the wavelet bases constructed in the previous section meet our need.

Theorem 2.2.

$$\bigcup_{n=0}^{\infty} 2^{n/2-2n}\Gamma_n := \bigcup_{n=0}^{\infty} \{2^{n/2-2n}\psi_{n,j}, j = 1, 2, \ldots, 2^{n+1}\}$$

is a Riesz basis of $H_0^2(0,1)$.

Proof. Suppose $f = \sum_{n=0}^{\infty} 2^{n/2-2n} \sum_{j=1}^{2^{n+1}} x_{n,j}\psi_{n,j}$. Since $\bigcup_{n=0}^{\infty} \Gamma_n$ is an orthogonal basis of $H_0^2(0,1)$ with respect to $\langle u'', v''\rangle$, we have

$$|f|_{H^2}^2 = \sum_{n=0}^{\infty} \sum_{j=1}^{2^{n+1}} x_{n,j}^2 2^n \langle 2^{-2n}\psi''_{n,j}, 2^{-2n}\psi''_{n,j}\rangle.$$

If j is an odd number,

$$2^n \langle 2^{-2n}\psi''_{n,j}, 2^{-2n}\psi''_{n,j}\rangle = 192.$$

If j is an even number,

$$2^n \langle 2^{-2n}\psi''_{n,j}, 2^{-2n}\psi''_{n,j}\rangle = 64.$$

Therefore,

$$64 \sum_{n=0}^{\infty} \sum_{j=1}^{2^{n+1}} x_{n,j}^2 \leq |f|_{H^2}^2 \leq 192 \sum_{n=0}^{\infty} \sum_{j=1}^{2^{n+1}} x_{n,j}^2.$$

This in connection with the equivalence of the H^2 norm and semi-norm gives the desired result. ∎

2.4 Applications

The variational problem of equation (2.1.1) is to find $u \in H_0^2(0,1)$ such that

$$a(u,v) = \langle f, v\rangle \quad \forall v \in H_0^2(0,1), \tag{2.4.1}$$

where $a(u,v) = \langle a(x)u'', v''\rangle + \langle b(x)u', v'\rangle + \langle c(x)u, v\rangle$. We assume that $a(x)$, $b(x)$ and $c(x)$ are continuous functions on $[0,1]$ satisfying $a(x) > 0$ and $b(x), c(x) \geq 0$ for all $x \in [0,1]$.

For $u, v \in H_0^2(0,1)$, by the Schwarz inequality,

$$\begin{aligned} |a(u,v)| &\leq C_1(\|u''\|_{L_2}\|v''\|_{L_2} + \|u'\|_{L_2}\|v'\|_{L_2} + \|u\|_{L_2}\|v\|_{L_2}) \\ &\leq C_1\|u\|_{H^2}\|v\|_{H^2}, \end{aligned}$$

where $C_1 = \max_{x\in[0,1]}\{a(x), b(x), c(x)\}$. On the other hand, $a(u,u) \geq C_2|u|_{H^2}^2$ where $C_2 = \min_{x\in[0,1]}\{a(x)\}$. The equivalence of the H^2 norm and semi-norm gives $a(u,u) \geq C_3\|u\|_{H^2}^2$ where C_3 is a positive constant independent of u. Hence $a(u,v)$ is continuous and coercive, and by the Lax-Milgram theorem, existence and uniqueness of the solution are guaranteed for (2.4.1).

The corresponding Galerkin approximation problem for (2.4.1) is to find $u_n \in V_n$ such that

$$a(u_n, v) = \langle f, v\rangle \quad \forall v \in V_n. \tag{2.4.2}$$

Note that we have two bases for V_n. One is the finite element basis Φ_n and the other one is the wavelet basis Ψ_n. We normalize these two bases such that the H^2 semi-norm of each basis functions is 1 as follows.

$$\begin{aligned}\Phi_n^{norm} &:= \Big\{\frac{1}{2\sqrt{6}}2^{-3n/2}\phi_{n,j}, j \text{ is odd}\Big\}\bigcup\Big\{\frac{1}{2\sqrt{2}}2^{-3n/2}\phi_{n,j}, j \text{ is even}\Big\};\\ \Psi_n^{norm} &:= \bigcup_{k=0}^{n-1}\bigg(\Big\{\frac{1}{8\sqrt{3}}2^{-3k/2}\psi_{k,j}, j \text{ is odd}\Big\}\bigcup\Big\{\frac{1}{8}2^{-3k/2}\psi_{k,j}, j \text{ is even}\Big\}\bigg).\end{aligned}$$

Suppose $u_n = \sum_{\phi\in\Phi_n^{norm}} y_\phi \phi$. Let A_n be the matrix $(a(\sigma,\phi))_{\sigma,\phi\in\Phi_n^{norm}}$, and let ξ_n be the column vector $(\langle f,\phi\rangle)_{\phi\in\Phi_n^{norm}}$. Then the column vector $y_n = (y_\phi)_{\phi\in\Phi_n^{norm}}$ is the solution of the system of linear equations

$$A_n y_n = \xi_n. \tag{2.4.3}$$

This linear system is ill-conditioned, i.e., the condition number $\kappa(A_n)$ of the matrix A_n increases rapidly as n increases. Hence, it would be very difficult to solve (2.4.3) when n is large.

Now we employ the wavelet basis Ψ_n^{norm} to solve (2.4.2). Suppose $u_n = \sum_{\psi\in\Psi_n^{norm}} z_\psi \psi$. We obtain the following linear system:

$$B_n z_n = \eta_n. \tag{2.4.4}$$

Here B_n is the matrix $(a(\chi,\psi))_{\chi,\psi\in\Psi_n^{norm}}$, whereas η_n is the column vector $(\langle f,\psi\rangle)_{\psi\in\Psi_n^{norm}}$, and z_n is the column vector $(z_\psi)_{\psi\in\Psi_n^{norm}}$.

We use $\lambda_{max}(B_n)$ and $\lambda_{min}(B_n)$ to denote the maximal and minimal eigenvalues of B_n, respectively. Then $\kappa(B_n) := \lambda_{max}(B_n)/\lambda_{min}(B_n)$ gives the condition number of B_n. An application of proposition 1.1 and theorem 2.2 gives the following theorem.

Theorem 2.3. *The condition number of the stiffness matrix associated with Ψ_n^{norm}, i.e., $B_n := (a(\chi,\psi))_{\chi,\psi\in\Psi_n^{norm}}$, is uniformly bounded (independent of n).*

For the model problem, i.e., (2.1.1) with $a(x) = 1$, $b(x) = 0$ and $c(x) = 0$, the condition number of A_n increases like $O(2^{4n})$. However, the condition number of B_n is always 1 since Ψ_n^{norm} is an orthonormal basis of V_n with respect to the H^2 semi-norm.

Note that Φ_n^{norm} and Ψ_n^{norm} are two bases of V_n. There exists a unique transformation between Φ_n^{norm} and Ψ_n^{norm}. To find the matrix representation of this transformation, we define

$$\Gamma_k^{norm} := \left\{ \frac{1}{8\sqrt{3}} 2^{-3k/2} \psi_{k,j}, j \text{ is odd} \right\} \bigcup \left\{ \frac{1}{8} 2^{-3k/2} \psi_{k,j}, j \text{ is even} \right\}.$$

Then $\Psi_n^{norm} = \bigcup_{k=0}^{n-1} \Gamma_k^{norm}$. We use the same notations Φ_n^{norm}, Ψ_n^{norm} and Γ_n^{norm} to denote the column vectors $(\phi)_{\phi \in \Phi_n^{norm}}$, $(\psi)_{\psi \in \Psi_n^{norm}}$ and $(\gamma)_{\gamma \in \Gamma_n^{norm}}$, respectively. Let I_n be the $n \times n$ identity matrix. Define

$$F := \begin{pmatrix} 2\sqrt{2} & 0 \\ 0 & \sqrt{2} \end{pmatrix}, \quad D := \begin{pmatrix} \sqrt{2} & -\dfrac{\sqrt{6}}{2} \\ \dfrac{\sqrt{6}}{4} & -\dfrac{\sqrt{2}}{4} \end{pmatrix}, \quad E := \begin{pmatrix} \sqrt{2} & \dfrac{\sqrt{6}}{2} \\ -\dfrac{\sqrt{6}}{4} & -\dfrac{\sqrt{2}}{4} \end{pmatrix}.$$

For fixed n and $2 \le k \le n$, by the refinement equations (2.2.1), we have

$$\begin{pmatrix} \Phi_{k-1}^{norm} \\ \Gamma_{k-1}^{norm} \end{pmatrix} = P_k \Phi_k^{norm},$$

where P_k is a $(2^{k+1}-2)\times(2^{k+1}-2)$ matrix in the form

$$\begin{pmatrix} E & F & D & 0 & 0 & \cdots & 0 \\ 0 & 0 & E & F & D & \cdots & 0 \\ \cdots & \cdots & \cdots & \cdots & \cdots & \cdots & \cdots \\ 0 & \cdots & \cdots & 0 & E & F & D \\ I_2 & 0 & 0 & 0 & \cdots & \cdots & 0 \\ 0 & 0 & I_2 & 0 & \cdots & \cdots & 0 \\ \cdots & \cdots & \cdots & \cdots & \cdots & \cdots & \cdots \\ 0 & \cdots & \cdots & \cdots & \cdots & 0 & I_2 \end{pmatrix}.$$

In this matrix, there are $2^{k-1}-1$ blocks of D, E and F, respectively. And there are 2^{k-1} blocks of I_2.

Therefore, the matrix representation S_n of the transformation between Φ_n^{norm} and Ψ_n^{norm} satisfies

$$\Psi_n^{norm} = S_n \Phi_n^{norm},$$

where

$$S_n = \begin{pmatrix} P_2 & 0 \\ 0 & I_{P_2} \end{pmatrix} \begin{pmatrix} P_3 & 0 \\ 0 & I_{P_3} \end{pmatrix} \cdots \begin{pmatrix} P_n & 0 \\ 0 & I_{P_n} \end{pmatrix}$$

for identity matrix I_{P_k} of size $(2^{n+1}-2^{k+1})\times(2^{n+1}-2^{k+1})$.

Consequently, the linear system (2.4.4) is equivalent to

$$S_n A_n S_n^T z_n = S_n \xi_n$$

since $B_n = S_n A_n S_n^T$ and $\eta_n = S_n \xi_n$. If we use conjugate gradient (CG) algorithm to solve $S_n A_n S_n^T z_n = S_n \xi_n$, the iterations needed to reach a fixed tolerance τ would not increase as the mesh size decreases since the condition number of B_n is uniformly bounded. By letting $y_n = S_n^T z_n$, the CG algorithm for solving $S_n A_n S_n^T z_n = S_n \xi_n$ is equivalent to the preconditioned conjugate gradient (PCG) algorithm for solving $A_n y_n = \xi_n$ using preconditioner S_n.

The CG and PCG algorithms for solving $A_n y_n = \xi_n$ are introduced as follows.

Algorithm 2.1 CG Algorithm for $A_n y_n = \xi_n$

Given initial guess y_n^0, $r_0 \leftarrow \xi_n - A_n y_n^0$
$p_0 \leftarrow r_0$
for $k = 1, 2, \ldots$ **do**
  $\alpha_{k-1} \leftarrow r_{k-1}^T p_{k-1} / p_{k-1}^T A_n p_{k-1}$
  $y_n^k \leftarrow y_n^{k-1} + \alpha_{k-1} p_{k-1}$
  $r_k \leftarrow r_{k-1} - \alpha_{k-1} A_n p_{k-1}$
  If $\|r_k\|_2 < \tau$, stop
  else $p_k \leftarrow r_k - \dfrac{r_k^T A_n p_{k-1}}{p_{k-1}^T A_n p_{k-1}} p_{k-1}$
end for

Algorithm 2.2 PCG Algorithm for $A_n y_n = \xi_n$ with preconditioner S_n

```
Given initial guess y_n^0, r_0 ← ξ_n − A_n y_n^0
p_0 ← r_0
for k = 1, 2, ... do
    α_{k−1} ← r_{k−1}^T p_{k−1} / p_{k−1}^T A_n p_{k−1}
    y_n^k ← y_n^{k−1} + α_{k−1} p_{k−1}
    r_k ← r_{k−1} − α_{k−1} A_n p_{k−1}
    If ||r_k||_2 < τ, stop
    else
    s_k ← S_n^T S_n r_k
    p_k ← s_k − (s_k^T A_n p_{k−1} / p_{k−1}^T A_n p_{k−1}) p_{k−1}
end for
```

Now we apply the wavelet bases to numerical solution to the Euler-Bernoulli bean equation (2.1.2).

Example 2.1. *Consider equation (2.1.2) with* $a(x) = 1 + 0.5\sin(x)$ *and right hand side* f *given by*

$$f(x) = -6x^2 \sin(x) + 24x \cos(x) + 6x \sin(x) + 11 \sin(x) - 12 \cos(x) + 24.$$

In this example, the exact solution $u(x) = x^2(1-x)^2$. We first use the finite element basis Φ_n^{norm} to discretize the corresponding variational problem and solve the resulting linear system $A_n y_n = \xi_n$ by CG algorithm (2.1). Next, we employ the wavelet basis Ψ_n^{norm} to solve the same problem, i.e., solve $A_n y_n = \xi_n$ by PCG algorithm (2.2) with preconditioner S_n. We set the tolerance τ to be $1e-10$ and use the zero vector as the initial guess. N_{CG} and N_{PCG} denote the number of CG and PCG iterations, respectively.

Table 2.1: CG vs PCG for Example 2.1, $\tau = 1e-10$

Level n	6	7	8	9	10	11
N_{CG}	255	807	2900	11024	44215	180897
N_{PCG}	10	10	9	8	8	7

In this table, the first row gives the level. The second and third rows give the number of iterations to achieve the tolerance $1e-10$ for CG and PCG algorithms, respectively. Since the linear system $A_n y_n = \xi_n$ is ill-conditioned, the CG iterations increase rapidly as the level n increases. However, the system $S_n A_n S_n^T z_n = S_n \xi_n$ (or $B_n z_n = \eta_n$) is well conditioned. The condition number of B_n is uniformly bounded, which guarantees that the PCG iterations would not increase as mesh size decreases. This is confirmed by our numerical results. In fact, more is true. We see from the last row of table 2.1 that the PCG iterations decrease as n increases. From this table, it is clear that the preconditioning technique is effective.

Let y_n and y_n^* be the numerical and exact solutions of $A_n y_n = \xi_n$. Then $u_n = \sum_{\phi \in \Phi_n^{norm}} y_\phi \phi$ is the numerical solution of example 2.1. Let $e_n := \|u_n'' - u''\|_{L_2}$ be the error estimated in the H^2 semi-norm. Suppose $u_n^* = \sum_{\phi \in \Phi_n^{norm}} y_\phi^* \phi$, then $e_n^* := \|(u^*)_n'' - u''\|_{L_2}$ is the discretization error in the H^2 semi-norm. We list the number of PCG iterations needed to achieve the discretization error in the H^2 semi-norm in the following table. In order to compute the discretization error, we simply perform sufficiently many PCG iterations to get y_n^*. The rate of convergence in the H^2 semi-norm is computed by $\log_2(\frac{e_{n-1}^*}{e_n^*})$. Note that $e_5^* = 8.73e-4$.

Table 2.2: Numerical Results of Example 2.1

Level n	6	7	8	9	10	11
N_{PCG}	7	7	8	8	8	8
e_n^*	2.18e-4	5.46e-5	1.36e-5	3.41e-6	8.54e-7	2.13e-7
$\log_2(\frac{e_{n-1}^*}{e_n^*})$	2.00	2.00	2.01	2.00	2.00	2.00

It is well known that the convergence rate provided by cubic splines is 2 in the H^2 semi-norm. This is confirmed by our numerical results. We also notice that the number of PCG iterations needed to achieve the discretization error remains stable under mesh refinement. Therefore, the wavelet Galerkin method may have advantages over many other methods if the problem needs to be discretized on a mesh with small size. For instance, the problem has a highly oscillating solution.

Example 2.2. *Consider equation (2.1.2) with $a(x) = x + 1$ and right hand side f given by*

$$f(x) = -8k^3\pi^3 \sin(2k\pi x) - 8(x+1)k^4\pi^4 \cos(2k\pi x),$$

where $k = 37$.

In this case, the exact solution $u(x) = (1 - \cos(2k\pi x))/2$. Note that $e_{12}^* = 2.29$.

Table 2.3: Numerical Results of Example 2.2

Level n	13	14	15	16
N_{PCG}	11	10	11	12
e_n^*	5.73e-1	1.43e-1	3.58e-2	9.08e-3
$\log_2(\frac{e_{n-1}^*}{e_n^*})$	2.00	2.00	2.00	1.98

Since the exact solution has a high-frequency component, we need to solve the problem at a high level n to get an approximate solution with small error. We see that the rate of convergence is 2 from the last row of this table. For large n, the convergence of CG method is extremely slow. But the PCG method has good performance.

In fact, to further improve the numerical performance, we may use the multilevel PCG method which will be discussed in the next two chapters.

For the model problem, i.e.,

$$\begin{cases} u''''(x) = f(x) \ \text{ for } \ x \in (0,1), \\ u(0) = u(1) = u'(0) = u'(1) = 0, \end{cases} \tag{2.4.5}$$

we know that the stiffness matrices associated with the wavelet bases are identity matrices. Hence no other preconditioning techniques could be better.

Bramble, Pasciak and Xu [3] proposed the BPX method for preconditioning. Based on their work, Liu constructed additive Schwarz-type preconditioners using Hermite cubic splines in [29], which is suitable for the following problem.

$$\begin{cases} u''''(x) + u(x) = f(x) \ \text{ for } \ x \in (0,1), \\ u(0) = u(1) = u'(0) = u'(1) = 0. \end{cases} \tag{2.4.6}$$

The condition numbers of the corresponding preconditioned matrices are listed as follows:

Table 2.4: Condition Numbers of Liu's Preconditioned Matrices

Level n	6	7	8	9	10	11
κ	7.57	7.75	7.88	7.98	8.06	8.12

However, using the wavelet preconditioning technique, the condition numbers of the preconditioned matrices are only about 1.002 for $6 \leq n \leq 11$.

In the one-dimensional space, the orthogonality to the energy norm results in orthonormal wavelet bases in the Sobolev space $H_0^m(0,1)$, where m is a positive integer. However, this way of construction cannot apply to the two- or higher-dimensional cases. Therefore, we propose different constructions of Riesz bases of wavelets in the Sobolev spaces to deal with second-order and fourth-order elliptic equations in chapter 3 and 4.

Chapter 3

The Wavelet Galerkin Method for Second-order Elliptic Problems

3.1 Introduction

Throughout this chapter, we will consider the second-order elliptic equation with Dirichlet boundary condition,

$$\begin{cases} -\frac{\partial}{\partial x}(a\frac{\partial}{\partial x}u) - \frac{\partial}{\partial y}(b\frac{\partial}{\partial y}u) = f & \text{in } \Omega, \\ u = 0 & \text{on } \partial\Omega, \end{cases} \tag{3.1.1}$$

where $\Omega = (0,1)^2$. a and b are two real-valued continuous functions on $[0,1]^2$ satisfying $a_1 \leq a(x,y) \leq a_2$ and $b_1 \leq b(x,y) \leq b_2$, where a_1, a_2, b_1 and b_2 are positive constants.

For the Poisson equation with Dirichlet boundary condition (i.e., problem (3.1.1) with $a = b = 1$)

$$\begin{cases} -\dfrac{\partial^2 u}{\partial x^2} - \dfrac{\partial^2 u}{\partial y^2} = f \ \text{ in } \Omega, \\ u = 0 \qquad\qquad\qquad\quad \text{on } \partial\Omega, \end{cases} \tag{3.1.2}$$

and on uniform discretizations, wavelet preconditioning techniques are known to be less efficient than multigrid algorithms. But the classical multigrid methods are usually not effective when the coefficients a and b are rough. For instance, a and b are anisotropic or highly oscillatory (see, e.g., [39], [6] and [18]). Line Gauss-Seidel (see, e.g., [4]), semi-coarsening (see, e.g., [33]) and algebraic multigrid (see, e.g., [2]) are designed to deal with some of these cases.

An advantage of the wavelet Galerkin method is that, as long as wavelets have been constructed such that the condition number of the associated stiffness matrix of the model problem is relatively small, these wavelets are applicable to a class of general elliptic equations. In particular, if proper wavelet bases have been constructed to solve the model problem (3.1.2) efficiently, to solve (3.1.1), we can still expect fast convergence of the numerical scheme based on the same wavelet bases without modifying our algorithm according to the properties (oscillation, anisotropy, etc.) of the variable coefficients a and b, given $\max\{a_2, b_2\}/\min\{a_1, b_1\}$ is not too big.

We relate the finite difference and finite element methods for solving the Poisson equation, and show that our wavelet bases constructed in section 3.2 are also applicable in the finite difference method for numerical solutions of equation (3.1.1). As a result, the associated numerical scheme becomes simpler and more efficient because numerical integrations are avoided.

3.2 Construction of Wavelets

In this section, we construct wavelets on the unit square on the basis of bi-linear splines.

Let $\phi(x)$ be the hat function, that is,

$$\phi(x) = \begin{cases} 1+x & \text{for} \quad -1 \le x < 0, \\ 1-x & \text{for} \quad 0 \le x \le 1, \\ 0 & \text{for} \quad \mathbb{R} \setminus [-1,1]. \end{cases}$$

ϕ satisfies the following refinement equation:

$$\phi(x) = \frac{1}{2}\phi(2x+1) + \phi(2x) + \frac{1}{2}\phi(2x-1), \;\; x \in \mathbb{R}. \tag{3.2.1}$$

For $n \ge 1$, consider the following set,

$$\Phi_n = \{\phi_{n,(j_1,j_2)}(x,y) : (j_1,j_2) \in J_n, \;\; (x,y) \in \Omega\},$$

where

$$J_n = \{(j_1,j_2) : j_1 = 1,2,\ldots 2^n - 1; j_2 = 1,2,\ldots 2^n - 1\}$$

and

$$\phi_{n,(j_1,j_2)}(x,y) = 2^n \phi(2^n x - j_1)\phi(2^n y - j_2), \;\; (x,y) \in \Omega.$$

For $(j_1, j_2) \in J_n$, $\phi_{n,(j_1,j_2)}$ is supported on $[0,1]^2$ and by (3.2.1), we have

$$\begin{aligned}\phi_{n,(j_1,j_2)} = \frac{\phi_{n+1,(2j_1,2j_2)}}{2} + \\ \frac{(\phi_{n+1,(2j_1-1,2j_2)} + \phi_{n+1,(2j_1,2j_2-1)} + \phi_{n+1,(2j_1,2j_2+1)} + \phi_{n+1,(2j_1+1,2j_2)})}{4} + \\ \frac{(\phi_{n+1,(2j_1-1,2j_2-1)} + \phi_{n+1,(2j_1-1,2j_2+1)} + \phi_{n+1,(2j_1+1,2j_2-1)} + \phi_{n+1,(2j_1+1,2j_2+1)})}{8}.\end{aligned} \tag{3.2.2}$$

Let V_n be the linear span of Φ_n. Φ_n has the following property:

Proposition 3.1. *Φ_n is a Riesz basis of V_n in the L_2 space for $n \geq 1$.*

The dimension of V_n is $(2^n - 1)^2$. By (3.2.2), we have

$$V_1 \subset V_2 \subset \cdots \subset V_n \subset \cdots .$$

Moreover, $\bigcup_{n=1}^{\infty} V_n$ is dense in $H_0^1(\Omega)$.

Let $Q_k : L_2(\Omega) \to V_k$ be the L_2-orthogonal projection onto V_k $(k \geq 1)$ with $\langle Q_k u, v\rangle = \langle u, v\rangle, u, v \in L_2(\Omega)$ and $Q_0 := 0$. Several authors (see, e.g., [40] and [43]) have proved that there exist two positive constants C_1 and C_2 such that

$$C_1 |f|_{H^1}^2 \leq \sum_{k=1}^{n} 4^k \|(Q_k - Q_{k-1}) f\|_{L_2}^2 \leq C_2 |f|_{H^1}^2, \;\; f \in V_n. \tag{3.2.3}$$

Now, we construct subspace W_n of V_{n+1} such that $V_{n+1} = V_n + W_n$ for $n \geq 1$. First we introduce the following seven index sets:

$$
\begin{aligned}
K_n^1 :=& \ \big\{(k_1,k_2) : k_1 = 1,3,\ldots,2^{n+1}-1, k_2 = 1,3,\ldots,2^{n+1}-1\big\};\\
K_n^2 :=& \ \big\{(k_1,1) : k_1 = 2,4,\ldots,2^{n+1}-2\big\};\\
K_n^3 :=& \ \big\{(k_1,k_2) : k_1 = 2,4,\ldots,2^{n+1}-2, k_2 = 3,\ldots,2^{n+1}-3\big\};\\
K_n^4 :=& \ \big\{(k_1,2^{n+1}-1) : k_1 = 2,4,\ldots,2^{n+1}-2\big\};\\
K_n^5 :=& \ \big\{(1,k_2) : k_2 = 2,4,\ldots,2^{n+1}-2\big\};\\
K_n^6 :=& \ \big\{(k_1,k_2) : k_1 = 3,\ldots,2^{n+1}-3, k_2 = 2,4,\ldots,2^{n+1}-2\big\};\\
K_n^7 :=& \ \big\{(2^{n+1}-1,k_2) : k_2 = 2,4,\ldots,2^{n+1}-2\big\}.
\end{aligned}
$$

They are subsets of J_{n+1}.

Correspondingly, define

$$
\begin{aligned}
\Gamma_n^1 :=& \ \Big\{\psi_{n,(k_1,k_2)} := \phi_{n+1,(k_1,k_2)}, (k_1,k_2) \in K_n^1\Big\};\\
\Gamma_n^2 :=& \ \Big\{\psi_{n,(k_1,k_2)} := \phi_{n+1,(k_1,k_2)} - \frac{1}{2}\phi_{n+1,(k_1,k_2+1)}, (k_1,k_2) \in K_n^2\Big\};\\
\Gamma_n^3 :=& \ \Big\{\psi_{n,(k_1,k_2)} := -\frac{1}{2}\phi_{n+1,(k_1,k_2-1)} + \phi_{n+1,(k_1,k_2)} - \frac{1}{2}\phi_{n+1,(k_1,k_2+1)},\\
& \ (k_1,k_2) \in K_n^3\Big\};\\
\Gamma_n^4 :=& \ \Big\{\psi_{n,(k_1,k_2)} := -\frac{1}{2}\phi_{n+1,(k_1,k_2-1)} + \phi_{n+1,(k_1,k_2)}, (k_1,k_2) \in K_n^4\Big\};\\
\Gamma_n^5 :=& \ \Big\{\psi_{n,(k_1,k_2)} := \phi_{n+1,(k_1,k_2)} - \frac{1}{2}\phi_{n+1,(k_1+1,k_2)}, (k_1,k_2) \in K_n^5\Big\};\\
\Gamma_n^6 :=& \ \Big\{\psi_{n,(k_1,k_2)} := -\frac{1}{2}\phi_{n+1,(k_1-1,k_2)} + \phi_{n+1,(k_1,k_2)} - \frac{1}{2}\phi_{n+1,(k_1+1,k_2)},\\
& \ (k_1,k_2) \in K_n^6\Big\};\\
\Gamma_n^7 :=& \ \Big\{\psi_{n,(k_1,k_2)} := -\frac{1}{2}\phi_{n+1,(k_1-1,k_2)} + \phi_{n+1,(k_1,k_2)}, (k_1,k_2) \in K_n^7\Big\}.
\end{aligned}
\tag{3.2.4}
$$

Let $K_n := \bigcup_{i=1}^{7} K_n^i$, $\Gamma_n := \bigcup_{i=1}^{7} \Gamma_n^i$ and W_n be the linear span of Γ_n.

It is easy to show that the functions in Φ_n and Γ_n are linearly independent and $W_n \subset V_{n+1}$ by definition, hence $V_{n+1} = V_n + W_n$ and

$$\mathrm{dim}W_n = \mathrm{dim}V_{n+1} - \mathrm{dim}V_n = 2^n(3 \cdot 2^n - 2).$$

Consequently,

$$V_{n+1} = V_1 + W_1 + W_2 + \ldots + W_n.$$

To avoid treating the term V_1 every time separately, we define $W_0 := V_1$, $K_0 := J_1$, $\Gamma_0 := \Phi_1$ and $\psi_{0,(1,1)} := \phi_{1,(1,1)}$. Γ_n has the following property:

Proposition 3.2. *For $n \geq 0$, Γ_n is a Riesz basis of W_n in the L_2 space.*

Proof. It is easily seen that Γ_0 is a Riesz basis of W_0. For $n \geq 1$, suppose $f = \sum_{(k_1,k_2)\in K_n} a_{n,(k_1,k_2)}\psi_{n,(k_1,k_2)}$ where $a_{n,(k_1,k_2)} \in \mathbb{R}$. By the construction of Γ_n, we have

$$\begin{aligned} f = &\sum_{(k_1,k_2)\in K_n} a_{n,(k_1,k_2)}\phi_{n+1,(k_1,k_2)} - \\ &\sum_{(k_1,k_2)\in J_{n+1}\setminus K_n} \frac{\big(a_{n,(k_1-1,k_2)} + a_{n,(k_1+1,k_2)} + a_{n,(k_1,k_2-1)} + a_{n,(k_1,k_2+1)}\big)\phi_{n+1,(k_1,k_2)}}{2} \end{aligned}$$

Note that Φ_{n+1} is a Riesz basis of V_{n+1} for $n \geq 0$, thus

$$\begin{aligned} \|f\|_{L_2}^2 &\geq C_1\Bigg(\sum_{(k_1,k_2)\in K_n} a_{n,(k_1,k_2)}^2 + \\ &\qquad \sum_{(k_1,k_2)\in J_{n+1}\setminus K_n} \frac{\big(a_{n,(k_1-1,k_2)} + a_{n,(k_1+1,k_2)} + a_{n,(k_1,k_2-1)} + a_{n,(k_1,k_2+1)}\big)^2}{4}\Bigg) \\ &\geq C_1 \sum_{(k_1,k_2)\in K_n} a_{n,(k_1,k_2)}^2, \end{aligned} \tag{3.2.5}$$

where C_1 is a positive constant independent of n. On the other hand,

$$\begin{aligned}
\|f\|_{L_2}^2 &\leq C_2\Bigg(\sum_{(k_1,k_2)\in K_n} a_{n,(k_1,k_2)}^2 + \\
&\sum_{(k_1,k_2)\in J_{n+1}\setminus K_n} \frac{\big(a_{n,(k_1-1,k_2)} + a_{n,(k_1+1,k_2)} + a_{n,(k_1,k_2-1)} + a_{n,(k_1,k_2+1)}\big)^2}{4}\Bigg) \\
&\leq C_2 \sum_{(k_1,k_2)\in K_n} a_{n,(k_1,k_2)}^2 + \\
&C_3 \sum_{(k_1,k_2)\in J_{n+1}\setminus K_n} \big(a_{n,(k_1-1,k_2)}^2 + a_{n,(k_1+1,k_2)}^2 + a_{n,(k_1,k_2-1)}^2 + a_{n,(k_1,k_2+1)}^2\big) \\
&\leq C_4 \sum_{(k_1,k_2)\in K_n} a_{n,(k_1,k_2)}^2,
\end{aligned} \tag{3.2.6}$$

where C_2, C_3 and C_4 are positive constants independent of n. Combining (3.2.5) and (3.2.6), we have

$$C_1 \sum_{(k_1,k_2)\in K_n} a_{n,(k_1,k_2)}^2 \leq \|f\|_{L_2}^2 \leq C_4 \sum_{(k_1,k_2)\in K_n} a_{n,(k_1,k_2)}^2.$$

Therefore, Γ_n is a Riesz basis of W_n. $\square$

3.3 Stability of Wavelets in the Sobolev Space H_0^1

In this section, we establish the stability of the wavelets constructed in the previous section in the Sobolev space $H_0^1(\Omega)$. Let

$$\Xi_k := \big\{\tau_{k,(k_1,k_2)} : (k_1,k_2) \in E_k\big\},$$

where $E_k := \{(k_1, k_2) : k_1 = 1, 2, \ldots, 2^k, k_2 = 1, 2, \ldots, 2^k\}$ and

$$\tau_{k,(k_1,k_2)} := \left[\frac{k_1 - 1}{2^k}, \frac{k_1}{2^k}\right] \times \left[\frac{k_2 - 1}{2^k}, \frac{k_2}{2^k}\right].$$

Consider the following bilinear form:

$$\langle f, g\rangle_{V_{k+1}} = \sum_{\tau_{k,(k_1,k_2)} \in \Xi_k} \langle f|_{\tau_{k,(k_1,k_2)}}, g|_{\tau_{k,(k_1,k_2)}}\rangle_{V_{k+1},\tau_{k,(k_1,k_2)}} \quad \text{for } f, g \in V_{k+1},$$

where

$$\begin{aligned}
&\langle f|_{\tau_{k,(k_1,k_2)}}, g|_{\tau_{k,(k_1,k_2)}}\rangle_{V_{k+1},\tau_{k,(k_1,k_2)}} \\
&= \frac{2^{-2(k+1)}}{4}\Big[f\Big(\frac{2k_1}{2^{k+1}}, \frac{2k_2}{2^{k+1}}\Big)g\Big(\frac{2k_1}{2^{k+1}}, \frac{2k_2}{2^{k+1}}\Big) \\
&+f\Big(\frac{2k_1 - 2}{2^{k+1}}, \frac{2k_2 - 2}{2^{k+1}}\Big)g\Big(\frac{2k_1 - 2}{2^{k+1}}, \frac{2k_2 - 2}{2^{k+1}}\Big) \\
&+f\Big(\frac{2k_1 - 2}{2^{k+1}}, \frac{2k_2}{2^{k+1}}\Big)g\Big(\frac{2k_1 - 2}{2^{k+1}}, \frac{2k_2}{2^{k+1}}\Big) \\
&+f\Big(\frac{2k_1}{2^{k+1}}, \frac{2k_2 - 2}{2^{k+1}}\Big)g\Big(\frac{2k_1}{2^{k+1}}, \frac{2k_2 - 2}{2^{k+1}}\Big) \qquad (3.3.1) \\
&+2f\Big(\frac{2k_1 - 1}{2^{k+1}}, \frac{2k_2 - 2}{2^{k+1}}\Big)g\Big(\frac{2k_1 - 1}{2^{k+1}}, \frac{2k_2 - 2}{2^{k+1}}\Big) \\
&+2f\Big(\frac{2k_1}{2^{k+1}}, \frac{2k_2 - 1}{2^{k+1}}\Big)g\Big(\frac{2k_1}{2^{k+1}}, \frac{2k_2 - 1}{2^{k+1}}\Big) \\
&+2f\Big(\frac{2k_1 - 1}{2^{k+1}}, \frac{2k_2}{2^{k+1}}\Big)g\Big(\frac{2k_1 - 1}{2^{k+1}}, \frac{2k_2}{2^{k+1}}\Big) \\
&+2f\Big(\frac{2k_1 - 2}{2^{k+1}}, \frac{2k_2 - 1}{2^{k+1}}\Big)g\Big(\frac{2k_1 - 2}{2^{k+1}}, \frac{2k_2 - 1}{2^{k+1}}\Big)\Big].
\end{aligned}$$

Indeed,

$$\langle f, g\rangle_{V_{k+1}} = 2^{-2(k+1)} \sum_{(k_1,k_2) \in J_{k+1} \setminus K_k^1} f\Big(\frac{k_1}{2^{k+1}}, \frac{k_2}{2^{k+1}}\Big)g\Big(\frac{k_1}{2^{k+1}}, \frac{k_2}{2^{k+1}}\Big) \qquad (3.3.2)$$

for $f, g \in V_{k+1}$.

Let $\mathrm{BL}(\tau)$ be the space of bi-linear polynomials on a square τ. If we assume that there exist two positive constants C_3 and C_4 independent of k and z such that

$$C_3\|z\|^2_{L_2(\tau_{k,(k_1,k_2)})} \leq \langle z, z\rangle_{V_{k+1},\tau_{k,(k_1,k_2)}} \leq C_4\|z\|^2_{L_2(\tau_{k,(k_1,k_2)})} \tag{3.3.3}$$

for $z \in \mathrm{BL}(\tau_{k,(k_1,k_2)})$, $k \geq 0$ and $(k_1, k_2) \in E_k$ at this moment, then it is easy to see that

$$C_1\|f\|^2_{L_2} \leq \langle f, f\rangle_{V_{k+1}} \leq C_2\|f\|^2_{L_2} \quad \text{on } V_k, \tag{3.3.4}$$

where C_1 and C_2 are two positive constants independent of f and k.

For $f \in V_{k+1}$, we write $\|f\|^2_{V_{k+1}}$ and $\|f|_{\tau_{k,(k_1,k_2)}}\|^2_{V_{k+1},\tau_{k,(k_1,k_2)}}$ for $\langle f, f\rangle_{V_{k+1}}$ and $\langle f|_{\tau_{k,(k_1,k_2)}}, f|_{\tau_{k,(k_1,k_2)}}\rangle_{V_{k+1},\tau_{k,(k_1,k_2)}}$, respectively. By (3.3.4), we know that $\|\cdot\|_{V_{k+1}}$ is a norm on V_k. Hence we have the following multiscale decomposition

$$V_{n+1} = \widetilde{W_0} + \widetilde{W_1} + \widetilde{W_2} + \ldots + \widetilde{W_n},$$

where $\widetilde{W_0} := V_1$ and $\widetilde{W_k} := \{g \in V_{k+1} : \langle g, f\rangle_{V_{k+1}} = 0 \ \ \forall f \in V_k\}$.

The following lemma implies (3.3.3).

Lemma 3.3. *Suppose $z \in BL(\tau_{k,(k_1,k_2)})$, then*

$$\frac{3}{4}\|z\|^2_{L_2(\tau_{k,(k_1,k_2)})} \leq \langle z, z\rangle_{V_{k+1},\tau_{k,(k_1,k_2)}} \leq \frac{9}{4}\|z\|^2_{L_2(\tau_{k,(k_1,k_2)})} \tag{3.3.5}$$

Proof. A simple transformation of coordinates shows that it is sufficient to prove

$$\frac{3}{4}\|z\|^2_{L_2(\tau_{0,(1,1)})} \leq \langle z, z\rangle_{V_1,\tau_{0,(1,1)}} \leq \frac{9}{4}\|z\|^2_{L_2(\tau_{0,(1,1)})}$$

for $z \in \mathrm{BL}(\tau_{0,(1,1)})$.

By definition, $\tau_{0,1,1} = [0,1]^2$. Suppose $z(0,0) = a$, $z(1,0) = b$, $z(0,1) = c$ and $z(1,1) = d$, where $a, b, c, d \in \mathbb{R}$. Since $z \in \mathrm{BL}([0,1]^2)$,

$$z(x,y) = (b-a)x + (c-a)y + (a+d-b-c)xy + a \text{ for } (x,y) \in [0,1]^2.$$

On one hand,

$$\|z\|^2_{L_2(\tau_{0,(1,1)})} = \frac{1}{18}(2a^2 + 2b^2 + 2c^2 + 2d^2 + 2ab + 2ac + ad + bc + 2bd + 2cd).$$

On the other hand, $a(0,1/2) = (a+c)/2$, $a(1/2,0) = (a+b)/2$, $a(1,1/2) = (b+d)/2$ and $a(1/2,1) = (c+d)/2$. Hence,

$$\langle z, z\rangle_{V_1,\tau_{0,(1,1)}} =$$
$$\frac{1}{16}\Big\{a^2 + b^2 + c^2 + d^2 + 2\Big[\Big(\frac{a+c}{2}\Big)^2 + \Big(\frac{a+b}{2}\Big)^2 + \Big(\frac{b+d}{2}\Big)^2 + \Big(\frac{c+d}{2}\Big)^2\Big]\Big\}$$
$$= \frac{1}{16}\Big(2a^2 + 2b^2 + 2c^2 + 2d^2 + ab + ac + bd + cd\Big).$$

Consequently,

$$\frac{\|z\|^2_{L_2(\tau_{0,(1,1)})}}{\langle z, z\rangle_{V_1,\tau_{0,(1,1)}}} =$$
$$\frac{16a^2 + 16b^2 + 16c^2 + 16d^2 + 16ab + 16ac + 8ad + 8bc + 16bd + 16cd}{18a^2 + 18b^2 + 18c^2 + 18d^2 + 9ab + 9ac + 9bd + 9cd}. \tag{3.3.6}$$

Let

$$y = \begin{pmatrix} y_1 \\ y_2 \\ y_3 \\ y_4 \end{pmatrix} = \begin{pmatrix} \frac{3}{2} & -\frac{3}{2} & -\frac{3}{2} & \frac{3}{2} \\ -3 & 0 & 0 & 3 \\ 0 & -3 & 3 & 0 \\ \frac{3\sqrt{3}}{2} & \frac{3\sqrt{3}}{2} & \frac{3\sqrt{3}}{2} & \frac{3\sqrt{3}}{2} \end{pmatrix} \begin{pmatrix} a \\ b \\ c \\ d \end{pmatrix},$$

then

$$\begin{pmatrix} a \\ b \\ c \\ d \end{pmatrix} = \begin{pmatrix} \frac{1}{6} & -\frac{1}{6} & 0 & \frac{1}{6\sqrt{3}} \\ -\frac{1}{6} & 0 & -\frac{1}{6} & \frac{1}{6\sqrt{3}} \\ -\frac{1}{6} & 0 & \frac{1}{6} & \frac{1}{6\sqrt{3}} \\ \frac{1}{6} & \frac{1}{6} & 0 & \frac{1}{6\sqrt{3}} \end{pmatrix} \begin{pmatrix} y_1 \\ y_2 \\ y_3 \\ y_4 \end{pmatrix}. \tag{3.3.7}$$

Substituting (3.3.7) in (3.3.6), we have

$$\frac{\|z\|^2_{L_2(\tau_{0,(1,1)})}}{\langle z, z\rangle_{V_1,\tau_{0,(1,1)}}} = \frac{y^T A y}{y^T y},$$

where

$$A = \begin{pmatrix} \frac{4}{9} & 0 & 0 & 0 \\ 0 & \frac{2}{3} & 0 & 0 \\ 0 & 0 & \frac{2}{3} & 0 \\ 0 & 0 & 0 & \frac{4}{3} \end{pmatrix}.$$

The maximal and minimal eigenvalues of A are $4/3$ and $4/9$, respectively. Therefore, (3.3.5) holds true. □

Although we define $\widetilde{W}_k$ and W_k in different ways, they are exactly the same, i.e.,

Proposition 3.4. *$\widetilde{W}_k = W_k$ for $k \geq 0$.*

Proof. If $k = 0$, $\widetilde{W}_0 = V_1 = W_0$. For $k \geq 1$, $\widetilde{W}_k$ and W_k are both complements of V_k in V_{k+1}, thus $\dim \widetilde{W}_k = \dim W_k$. It is sufficient to prove Γ_k is orthogonal to Φ_k under $\langle \cdot, \cdot \rangle_{V_{k+1}}$.

For $\psi \in \bigcup_{i=2}^{7} \Gamma_k^i$ and $\phi \in \Phi_k$, by simple computation, we know

$$\sum_{(k_1,k_2)\in J_{k+1}} \psi\Big(\frac{k_1}{2^{k+1}}, \frac{k_2}{2^{k+1}}\Big)\phi\Big(\frac{k_1}{2^{k+1}}, \frac{k_2}{2^{k+1}}\Big) = 0.$$

Note that ψ is zero at $(k_1/2^{k+1}, k_2/2^{k+1})$ for $(k_1, k_2) \in K_k^1$, therefore

$$\begin{aligned} \langle \psi, \phi \rangle_{V_{k+1}} &= 2^{-2(k+1)}\Big[\sum_{(k_1,k_2)\in J_{k+1}} \psi\Big(\frac{k_1}{2^{k+1}}, \frac{k_2}{2^{k+1}}\Big)\phi\Big(\frac{k_1}{2^{k+1}}, \frac{k_2}{2^{k+1}}\Big) \\ &- \sum_{(k_1,k_2)\in K_k^1} \psi\Big(\frac{k_1}{2^{k+1}}, \frac{k_2}{2^{k+1}}\Big)\phi\Big(\frac{k_1}{2^{k+1}}, \frac{k_2}{2^{k+1}}\Big)\Big] = 0 \end{aligned}$$

For $\psi \in \Gamma_k^1$, ψ is zero at $(k_1/2^{k+1}, k_2/2^{k+1})$ for $(k_1, k_2) \in J_{k+1} \setminus K_k^1$. Thus $\langle \psi, \phi \rangle_{V_{k+1}} = 0$ for $\phi \in \Phi_k$.

Consequently, $\Gamma_k = \bigcup_{i=1}^{7} \Gamma_k^i$ is orthogonal to Φ_k under $\langle \cdot, \cdot \rangle_{V_{k+1}}$. □

For $k \geq 1$, the mapping $P_k : V_{k+1} \to V_k$ satisfying $(I - P_k)V_{k+1} = W_k$ is then the linear projection onto V_k that is orthogonal with respect to $\langle \cdot, \cdot \rangle_{V_{k+1}}$. And W_k is the kernel of P_k. Let $P_0 := 0$. Fix $n \in \mathbb{N}$ for the time being. For each integer k with $0 \leq k \leq n$, let $T_k := P_k \cdots P_{n-1}$ and T_n be the identity operator on V_n. Then T_k is a linear projection from V_n to V_k.

According to theorem 4.9, to verify the stability of our wavelet basis, we only need to check whether the four conditions of theorem 4.9 are satisfied by taking $H_\mu = H_0^1(\Omega)$ and $H = L_2(\Omega)$.

It is easily seen that the first two conditions of theorem 4.9 are fulfilled because of (3.2.3). Proposition 3.2 implies that the last condition of theorem 4.9 holds true. The following lemma indicates that the third condition of theorem 4.9 is satisfied.

Lemma 3.5.

$$\|T_k f\|_{L_2} \leq C 2^{\lambda(j-k)} \|f\|_{L_2} \ \textit{for}\ f \in V_j \tag{3.3.8}$$

where $k, j \in \mathbb{N}$ with $k < j \leq n$, $\lambda < 1$ and C is a constant independent of k, j.

Proof. For $k < j \leq n$ with $k, j \in \mathbb{N}$ and $f \in V_j$,

$$\|T_k f\|_{L_2} = \|P_k P_{k+1} \cdots P_{j-1} f\|_{L_2}.$$

By (3.3.4), we have

$$\begin{aligned} \|P_k P_{k+1} \cdots P_{j-1} f\|_{L_2} &\leq C_1 \|P_k P_{k+1} \cdots P_{j-1} f\|_{V_{k+1}} \\ &= C_1 \frac{\|P_k P_{k+1} \cdots P_{j-1} f\|_{V_{k+1}}}{\|P_{k+1} \cdots P_{j-1} f\|_{V_{k+2}}} \cdots \frac{\|P_{j-1} f\|_{V_j}}{\|f\|_{V_{j+1}}} \|f\|_{V_{j+1}} \\ &\leq C \frac{\|P_k P_{k+1} \cdots P_{j-1} f\|_{V_{k+1}}}{\|P_{k+1} \cdots P_{j-1} f\|_{V_{k+2}}} \cdots \frac{\|P_{j-1} f\|_{V_j}}{\|f\|_{V_{j+1}}} \|f\|_{L_2}, \end{aligned} \tag{3.3.9}$$

where C and C_1 are positive constants independent of j and k.

If we assume that

$$\|P_l g\|_{V_{l+1}} \leq \sqrt{3} \|g\|_{V_{l+2}} \text{ for } l \in \mathbb{N}_0 \text{ and } g \in V_{l+1}, \tag{3.3.10}$$

then

$$\|P_k P_{k+1} \cdots P_{j-1} f\|_{L_2} \leq C \sqrt{3}^{j-k} \|f\|_{L_2} = C 2^{\lambda(j-k)} \|f\|_{L_2},$$

where $\lambda < 1$, we are done.

In order to verify (3.3.10), we follow the method used in [36].

For each $\tau_l \in \Xi_l$, note that $\mathrm{BL}(\tau_l)$ is a subspace of $V_{l+1}|_{\tau_l}$. Define

$$\mathrm{BL}^c(\tau_l) := \{h \in V_{l+1}|_{\tau_l} : \langle h, f \rangle_{V_{l+1,\tau_l}} = 0 \ \ \forall f \in \mathrm{BL}(\tau_l)\}.$$

Recall that $\langle \cdot, \cdot \rangle_{V_{l+1,\tau_l}}$ is not an inner product on $V_{l+1}|_{\tau_l}$, but $\| \cdot \|_{V_{l+1,\tau_l}}$ is a norm on $\mathrm{BL}(\tau_l)$. Hence, the mapping $P_{l,\tau_l} : V_{l+1}|_{\tau_l} \to \mathrm{BL}(\tau_l)$ satisfying

$(I - P_{l,\tau_l})V_{l+1}|_{\tau_l} = \mathrm{BL}^c(\tau_l)$ is then a linear projection onto $\mathrm{BL}(\tau_l)$ that is orthogonal with respect to $\langle \cdot, \cdot \rangle_{V_{l+1},\tau_l}$.

Letting $w = g|_{\tau_l}$, we have

$$\begin{aligned}
\|P_l g\|^2_{V_{l+1}} &= \|g\|^2_{V_{l+1}} - \|(I - P_l)g\|^2_{V_{l+1}} \\
&= \sum_{\tau_l \in \Xi_l} \left\{ \|g|_{\tau_l}\|^2_{V_{l+1},\tau_l} - \|g|_{\tau_l} - (P_l g)|_{\tau_l}\|^2_{V_{l+1},\tau_l} \right\} \\
&\leq \sum_{\tau_l \in \Xi_l} \left\{ \|w\|^2_{V_{l+1},\tau_l} - \|w - P_{l,\tau_l} w\|^2_{V_{l+1},\tau_l} \right\}.
\end{aligned}$$

On the other hand, by the first inequality of Lemma 3.3

$$\begin{aligned}
\|g\|^2_{V_{l+2}} &= \sum_{\tau_l \in \Xi_l} \left\{ \sum_{\tau_{l+1} \in \Xi_{l+1}, \tau_{l+1} \subset \tau_l} \|g|_{\tau_{l+1}}\|^2_{V_{l+2},\tau_{l+1}} \right\} \\
&= \sum_{\tau_l \in \Xi_l} \left\{ \sum_{\tau_{l+1} \in \Xi_{l+1}, \tau_{l+1} \subset \tau_l} \|w|_{\tau_{l+1}}\|^2_{V_{l+2},\tau_{l+1}} \right\} \\
&\geq \sum_{\tau_l \in \Xi_l} \left\{ \sum_{\tau_{l+1} \in \Xi_{l+1}, \tau_{l+1} \subset \tau_l} \frac{3}{4} \|w\|^2_{L_2(\tau_{l+1})} \right\} \\
&= \sum_{\tau_l \in \Xi_l} \left\{ \frac{3}{4} \|w\|^2_{L_2(\tau_l)} \right\}
\end{aligned}$$

Therefore,

$$\frac{\|P_l g\|^2_{V_{l+1}}}{\|g\|^2_{V_{l+2}}} \leq \sup_{\tau_l \in \Xi_l} \frac{\|w\|^2_{V_{l+1},\tau_l} - \|w - P_{l,\tau_l} w\|^2_{V_{l+1},\tau_l}}{\frac{3}{4}\|w\|^2_{L_2(\tau_l)}} \tag{3.3.11}$$

A simple transformation of coordinates shows that, to estimate the right hand side of (3.3.11), it is sufficient to consider the case $\tau_l = [0,1]^2$ and

$$\begin{aligned} V_{l+1}|_{\tau_l} = \;& \{w \in \mathbf{R}([0,1]^2) \;\; w \text{ is bilinear on } [0,1/2]\times[0,1/2], \\ & [0,1/2]\times[1/2,1], [1/2,1]\times[0,1/2] \text{ and } [1/2,1]\times[1/2,1]\}. \end{aligned}$$

Suppose

$$\begin{aligned} &w(0,0) = a_1, && w(1/2,0) = a_2, && w(1,0) = a_3, \\ &w(0,1/2) = a_4, && w(1/2,1/2) = a_5, && w(1,1/2) = a_6, \\ &w(0,1) = a_7, && w(1/2,1) = a_8, && w(1,1) = a_9, \end{aligned}$$

then $\|w\|^2_{L_2(\tau_l)}$ can be found to be

$$\begin{aligned} &\frac{1}{4}\Big[\frac{1}{18}a_1a_5 + \frac{1}{9}a_1a_2 + \frac{1}{9}a_1a_4 + \frac{1}{18}a_2a_4 + \frac{2}{9}a_5a_2 + \frac{2}{9}a_5a_4 \\ &+\frac{1}{18}a_2a_6 + \frac{1}{9}a_2a_3 + \frac{1}{18}a_3a_5 + \frac{1}{9}a_6a_3 + \frac{2}{9}a_6a_5 + \frac{1}{18}a_4a_8 \\ &+\frac{1}{9}a_4a_7 + \frac{1}{18}a_5a_7 + \frac{2}{9}a_8a_5 + \frac{1}{9}a_9^2 + \frac{1}{9}a_1^2 + \frac{4}{9}a_5^2 + \frac{2}{9}a_2^2 \\ &+\frac{2}{9}a_4^2 + \frac{2}{9}a_6^2 + \frac{1}{9}a_3^2 + \frac{2}{9}a_8^2 + \frac{1}{9}a_7^2 + \frac{1}{9}a_8a_7 + \frac{1}{18}a_5a_9 \\ &+\frac{1}{18}a_6a_8 + \frac{1}{9}a_9a_6 + \frac{1}{9}a_9a_8\Big]. \end{aligned}$$

Hence

$$\frac{3}{4}\|w\|^2_{L_2(\tau_l)} = \frac{1}{16}\vec{a}^T B\vec{a},$$

where $\vec{a}^T = (a_1, a_2, a_3, a_4, a_5, a_6, a_7, a_8, a_9)$ and

$$B = \begin{pmatrix} \frac{1}{3} & \frac{1}{6} & 0 & \frac{1}{6} & \frac{1}{12} & 0 & 0 & 0 & 0 \\ \frac{1}{6} & \frac{2}{3} & \frac{1}{6} & \frac{1}{12} & \frac{1}{3} & \frac{1}{12} & 0 & 0 & 0 \\ 0 & \frac{1}{6} & \frac{1}{3} & 0 & \frac{1}{12} & \frac{1}{6} & 0 & 0 & 0 \\ \frac{1}{6} & \frac{1}{12} & 0 & \frac{2}{3} & \frac{1}{3} & 0 & \frac{1}{6} & \frac{1}{12} & 0 \\ \frac{1}{12} & \frac{1}{3} & \frac{1}{12} & \frac{1}{3} & \frac{4}{3} & \frac{1}{3} & \frac{1}{12} & \frac{1}{3} & \frac{1}{12} \\ 0 & \frac{1}{12} & \frac{1}{6} & 0 & \frac{1}{3} & \frac{2}{3} & 0 & \frac{1}{12} & \frac{1}{6} \\ 0 & 0 & 0 & \frac{1}{6} & \frac{1}{12} & 0 & \frac{1}{3} & \frac{1}{6} & 0 \\ 0 & 0 & 0 & \frac{1}{12} & \frac{1}{3} & \frac{1}{12} & \frac{1}{6} & \frac{2}{3} & \frac{1}{6} \\ 0 & 0 & 0 & 0 & \frac{1}{12} & \frac{1}{6} & 0 & \frac{1}{6} & \frac{1}{3} \end{pmatrix}.$$

Next we calculate the numerator. By (3.3.1), we have

$$\|w\|^2_{V_{l+1},\tau_l} = \frac{1}{16}\big(a_1^2 + a_3^2 + a_7^2 + a_9^2 + 2(a_2^2 + a_4^2 + a_6^2 + a_8^2)\big) \qquad (3.3.12)$$

$\mathrm{BL}(\tau_l)$ is equivalent to the linear space spaned by $(1, 1/2, 0, 1/2, 1/4, 0, 0, 0)^T$, $(0, 1/2, 1, 0, 1/4, 1/2, 0, 0, 0)^T$, $(0, 0, 0, 1/2, 1/4, 0, 1, 1/2, 0)^T$ and $(0, 0, 0, 0, 1/4, 1/2, 0, 1/2, 1)^T$ since every $w \in \mathrm{BL}(\tau_l)$ is determined by $w(0, 0)$, $w(1, 0)$, $w(0, 1)$ and $w(1, 1)$. $(1, -1, 1, 0, 0, 0, 0, 0, 0)$, $(0, 0, 0, 0, 1, 0, 0, 0, 0)$, $(1, 0, 0, -1, 0, 0, 1, 0, 0)$, $(0, 1, 0, -1, 0, -1, 0, 1, 0)$ and $(-1, 1, 0, 0, 0, -1, 0, 0, 1)$ are orthogonal to the above linear space with respect to $\langle \cdot, \cdot \rangle_{V_{l+1},\tau_l}$ and all these nine vectors span the linear space equivalent to $V_{l+1}|_{\tau_l}$. Therefore the representation of P_{l,τ_l}, denoted by the same notation P_{l,τ_l}, satisfies the following linear system:

$$P_{l,\tau_l} X = Y,$$

where

$$X = \begin{pmatrix} 1 & 0 & 0 & 0 & 1 & 0 & 1 & 0 & -1 \\ \frac{1}{2} & \frac{1}{2} & 0 & 0 & -1 & 0 & 0 & 1 & 1 \\ 0 & 1 & 0 & 0 & 1 & 0 & 0 & 0 & 0 \\ \frac{1}{2} & 0 & \frac{1}{2} & 0 & 0 & 0 & -1 & -1 & 0 \\ \frac{1}{4} & \frac{1}{4} & \frac{1}{4} & \frac{1}{4} & 0 & 1 & 0 & 0 & 0 \\ 0 & \frac{1}{2} & 0 & \frac{1}{2} & 0 & 0 & 0 & -1 & -1 \\ 0 & 0 & 1 & 0 & 0 & 0 & 1 & 0 & 0 \\ 0 & 0 & \frac{1}{2} & \frac{1}{2} & 0 & 0 & 0 & 1 & 0 \\ 0 & 0 & 0 & 1 & 0 & 0 & 0 & 0 & 1 \end{pmatrix}$$

and

$$Y = \begin{pmatrix} 1 & 0 & 0 & 0 & 0 & 0 & 0 & 0 & 0 \\ \frac{1}{2} & \frac{1}{2} & 0 & 0 & 0 & 0 & 0 & 0 & 0 \\ 0 & 1 & 0 & 0 & 0 & 0 & 0 & 0 & 0 \\ \frac{1}{2} & 0 & \frac{1}{2} & 0 & 0 & 0 & 0 & 0 & 0 \\ \frac{1}{4} & \frac{1}{4} & \frac{1}{4} & \frac{1}{4} & 0 & 0 & 0 & 0 & 0 \\ 0 & \frac{1}{2} & 0 & \frac{1}{2} & 0 & 0 & 0 & 0 & 0 \\ 0 & 0 & 1 & 0 & 0 & 0 & 0 & 0 & 0 \\ 0 & 0 & \frac{1}{2} & \frac{1}{2} & 0 & 0 & 0 & 0 & 0 \\ 0 & 0 & 0 & 1 & 0 & 0 & 0 & 0 & 0 \end{pmatrix}.$$

Solving this linear system, we get

$$P_{l,\tau_l} = \begin{pmatrix} \frac{7}{12} & \frac{5}{12} & -\frac{1}{6} & \frac{5}{12} & 0 & -\frac{1}{12} & -\frac{1}{6} & -\frac{1}{12} & \frac{1}{12} \\ \frac{5}{24} & \frac{5}{12} & \frac{5}{24} & \frac{1}{6} & 0 & \frac{1}{6} & -\frac{1}{24} & -\frac{1}{12} & -\frac{1}{24} \\ -\frac{1}{6} & \frac{5}{12} & \frac{7}{12} & -\frac{1}{12} & 0 & \frac{5}{12} & \frac{1}{12} & -\frac{1}{12} & -\frac{1}{6} \\ \frac{5}{24} & \frac{1}{6} & -\frac{1}{24} & \frac{5}{12} & 0 & -\frac{1}{12} & \frac{5}{24} & \frac{1}{6} & -\frac{1}{24} \\ \frac{1}{12} & \frac{1}{6} & \frac{1}{12} & \frac{1}{6} & 0 & \frac{1}{6} & \frac{1}{12} & \frac{1}{6} & \frac{1}{12} \\ -\frac{1}{24} & \frac{1}{6} & \frac{5}{24} & -\frac{1}{12} & 0 & \frac{5}{12} & -\frac{1}{24} & \frac{1}{6} & \frac{5}{24} \\ -\frac{1}{6} & -\frac{1}{12} & \frac{1}{12} & \frac{5}{12} & 0 & -\frac{1}{12} & \frac{7}{12} & \frac{5}{12} & -\frac{1}{6} \\ -\frac{1}{24} & -\frac{1}{12} & -\frac{1}{24} & \frac{1}{6} & 0 & \frac{1}{6} & \frac{5}{24} & \frac{5}{12} & \frac{5}{24} \\ \frac{1}{12} & -\frac{1}{12} & -\frac{1}{6} & -\frac{1}{12} & 0 & \frac{5}{12} & -\frac{1}{6} & \frac{5}{12} & \frac{7}{12} \end{pmatrix}.$$

Consequently, a straightforward computation gives

$$\begin{aligned} \|w - P_{l,\tau_l} w\|^2_{V_{l+1},\tau_l} \;&=\; \frac{1}{16}\Big[-\frac{5}{6}a_1a_2 + \frac{1}{3}a_1a_3 - \frac{5}{6}a_1a_4 + \frac{1}{6}a_1a_6 \\ &+\; \frac{1}{3}a_1a_7 + \frac{1}{6}a_1a_8 - \frac{1}{6}a_1a_9 + \frac{7}{6}a_2^2 - \frac{5}{6}a_2a_3 \\ &-\; \frac{2}{3}a_2a_4 - \frac{2}{3}a_2a_6 + \frac{1}{6}a_2a_7 + \frac{1}{3}a_2a_8 + \frac{1}{6}a_2a_9 \\ &+\; \frac{5}{12}a_3^2 + \frac{1}{6}a_3a_4 - \frac{5}{6}a_3a_6 - \frac{1}{6}a_3a_7 + \frac{1}{6}a_3a_8 \\ &+\; \frac{1}{3}a_3a_9 + \frac{7}{6}a_4^2 + \frac{1}{3}a_4a_6 - \frac{5}{6}a_4a_7 - \frac{2}{3}a_4a_8 \\ &+\; \frac{1}{6}a_4a_9 + \frac{7}{6}a_6^2 + \frac{1}{6}a_6a_7 - \frac{2}{3}a_6a_8 - \frac{5}{6}a_6a_9 \\ &+\; \frac{5}{12}a_7^2 - \frac{5}{6}a_7a_8 + \frac{1}{3}a_7a_9 + \frac{7}{6}a_8^2 - \frac{5}{6}a_8a_9 \\ &+\; \frac{5}{12}a_9^2 + \frac{5}{12}a_1^2\Big]. \end{aligned} \tag{3.3.13}$$

Combining (3.3.12) and (3.3.13), we have

$$\|w\|^2_{V_{l+1},\tau_l} - \|w - P_{l,\tau_l} w\|^2_{V_{l+1},\tau_l} = \frac{1}{16}\vec{a}^T A \vec{a}, \tag{3.3.14}$$

where

$$A = \begin{pmatrix} \frac{7}{12} & \frac{5}{12} & -\frac{1}{6} & \frac{5}{12} & 0 & -\frac{1}{12} & -\frac{1}{6} & -\frac{1}{12} & \frac{1}{12} \\ \frac{5}{12} & \frac{5}{6} & \frac{5}{12} & \frac{1}{3} & 0 & \frac{1}{3} & -\frac{1}{12} & -\frac{1}{6} & -\frac{1}{12} \\ -\frac{1}{6} & \frac{5}{12} & \frac{7}{12} & -\frac{1}{12} & 0 & \frac{5}{12} & \frac{1}{12} & -\frac{1}{12} & -\frac{1}{6} \\ \frac{5}{12} & \frac{1}{3} & -\frac{1}{12} & \frac{5}{6} & 0 & -\frac{1}{6} & \frac{5}{12} & \frac{1}{3} & -\frac{1}{12} \\ 0 & 0 & 0 & 0 & 0 & 0 & 0 & 0 & 0 \\ -\frac{1}{12} & \frac{1}{3} & \frac{5}{12} & -\frac{1}{6} & 0 & \frac{5}{6} & -\frac{1}{12} & \frac{1}{3} & \frac{5}{12} \\ -\frac{1}{6} & -\frac{1}{12} & \frac{1}{12} & \frac{5}{12} & 0 & -\frac{1}{12} & \frac{7}{12} & \frac{5}{12} & -\frac{1}{6} \\ -\frac{1}{12} & -\frac{1}{6} & -\frac{1}{12} & \frac{1}{3} & 0 & \frac{1}{3} & \frac{5}{12} & \frac{5}{6} & \frac{5}{12} \\ \frac{1}{12} & -\frac{1}{12} & -\frac{1}{6} & -\frac{1}{12} & 0 & \frac{5}{12} & -\frac{1}{6} & \frac{5}{12} & \frac{7}{12} \end{pmatrix}.$$

Therefore,

$$\frac{\|P_l g\|^2_{V_{l+1}}}{\|g\|^2_{V_{l+2}}} \le \sup_{\vec{a}\in\mathbb{R}^9} \frac{\vec{a}^T A \vec{a}}{\vec{a}^T B \vec{a}}.$$

The eigenvalues of the matrix $\sqrt{B}^{-T} A \sqrt{B}^{-1}$ can be found directly to be $3, 8/3, 2, 2, 0, 0, 0, 0$ and 0. Hence

$$\frac{\|P_l g\|^2_{V_{l+1}}}{\|g\|^2_{V_{l+2}}} \le 3,$$

which implies (3.3.10). This completes the proof. □

Suppose S is a nonempty set of complex-valued functions and $a \in \mathbb{C}$, we define

$$aS := \{af : f \in S\}.$$

Let $\Psi_n := \bigcup_{k=0}^{n-1} 2^{-k}\Gamma_k$ and $\Psi := \bigcup_{k=0}^{\infty} 2^{-k}\Gamma_k$.

Consequently, by theorem 4.9, we have

Theorem 3.6. *Ψ is a Riesz basis of $H_0^1(\Omega)$.*

3.4 The Finite Element and Finite Difference Methods

If we use the finite element method to solve (3.1.2), we are seeking $u \in H_0^1(\Omega)$ satisfying the variational form

$$\langle \nabla u, \nabla v \rangle = \langle f, v \rangle \quad \forall v \in H_0^1(\Omega).$$

The corresponding Galerkin approximation problem is the following: find $u_n \in V_n$ such that

$$\langle \nabla u_n, \nabla v \rangle = \langle f, v \rangle \quad \forall v \in V_n. \tag{3.4.1}$$

Note that Φ_n is a basis of V_n, so is $2^{-n}\Phi_n$. Thus we are seeking $u_n = \sum_{\phi \in 2^{-n}\Phi_n} y_\phi \phi$, such that

$$\langle \nabla u_n, \nabla \phi \rangle = \langle f, \phi \rangle \quad \forall \phi \in 2^{-n}\Phi_n.$$

This linear system can be written as:

$$A_n y_n = \xi_n. \tag{3.4.2}$$

Here A_n is the matrix $(\langle\nabla\phi,\nabla\sigma\rangle)_{\phi,\sigma\in 2^{-n}\Phi_n}$, whereas ξ_n and y_n are the column vectors $(\langle f,\phi\rangle)_{\phi\in 2^{-n}\Phi_n}$ and $(y_\phi)_{\phi\in 2^{-n}\Phi_n}$, respectively. Therefore, solving (3.4.1) is equivalent to solving (3.4.2).

Note that Ψ_n is another basis of V_n, we may also seek u_n in the form $\sum_{\psi\in\Psi_n} z_\psi\psi$ such that

$$\langle\nabla u_n,\nabla\psi\rangle = \langle f,\psi\rangle \quad \forall\psi\in\Psi_n.$$

Similarly, we can write this linear system as follows:

$$B_n z_n = \eta_n. \tag{3.4.3}$$

Here B_n is the matrix $(\langle\nabla\psi,\nabla\chi\rangle)_{\psi,\chi\in\Psi_n}$, whereas η_n and z_n stand for the column vectors $(\langle f,\psi\rangle)_{\psi\in\Psi_n}$ and $(z_\psi)_{\psi\in\Psi_n}$, respectively. Then solving (3.4.1) is also equivalent to solving (3.4.3).

We consider the relation of the above two equivalent linear systems (3.4.2) and (3.4.3). By (3.2.2) and (3.2.4), we know that there exists a unique matrix S_n transforming the basis $2^{-n}\Phi_n$ to the other basis Ψ_n, therefore,

$$\begin{aligned} B_n &= S_n A_n S_n^T, \\ \eta_n &= S_n\xi_n. \end{aligned}$$

This shows the linear system (3.4.3) is exactly

$$S_n A_n S_n^T z_n = S_n\xi_n. \tag{3.4.4}$$

In the previous section, we established the stability of Ψ in $H_0^1(\Omega)$. Thus the condition number of B_n, i.e. $S_n A_n S_n^T$, is uniformly bounded. S_n is called the preconditioner of A_n. Without preconditioning, the condition number of A_n increases like $O(2^{2n})$. The uniform boundedness of the condition number of B_n is also confirmed by the following numerical results:

TABLE 3.1: Condition Numbers of $(B_n)_{2\leq n\leq 9}$

n	size of B_n	$\lambda_{max}(B_n)$	$\lambda_{min}(B_n)$	$\kappa(B_n)$
2	9×9	4.54	2.49	1.82
3	49×49	5.16	1.73	2.98
4	225×225	5.40	1.40	3.86
5	961×961	5.50	1.25	4.40
6	3969×3969	5.76	1.19	4.84
7	16129×16129	5.93	1.14	5.20
8	65025×65025	6.07	1.11	5.47
9	261121×261121	6.19	1.10	5.63

where $\lambda_{max}(B_n)$, $\lambda_{min}(B_n)$ and $\kappa(B_n) = \lambda_{max}(B_n)/\lambda_{min}(B_n)$ are the maximal, minimal eigenvalue and condition number of the stiffness matrix B_n, respectively.

Stevenson constructed wavelets on the basis of bi-linear splines in [35]. If (3.4.1) is discretized by Stevenson's wavelet bases, the condition numbers of the stiffness matrices, $(B_n^{Stv})_{2\leq n\leq 9}$, are listed in table 3.2.

TABLE 3.2: Condition Numbers of $(B_n^{Stv})_{2\leq n\leq 9}$

n	size of B_n^{Stv}	$\lambda_{max}(B_n^{Stv})$	$\lambda_{min}(B_n^{Stv})$	$\kappa(B_n^{Stv})$
2	9×9	7.16	2.26	3.17
3	49×49	11.96	2.08	5.76
4	225×225	13.71	1.83	7.50
5	961×961	14.20	1.69	8.38
6	3969×3969	14.71	1.60	9.19
7	16129×16129	15.55	1.55	10.02
8	65025×65025	16.04	1.52	10.53
9	261121×261121	16.46	1.51	10.93

We see that the condition numbers of the stiffness matrices associated with our wavelet bases are much smaller than those provided by Stevenson.

As we know, the numerical integration consumes lots of CPU time to solve the general second-order elliptic problem (3.1.1), if finite element method is applied. To avoid numerical integration, we consider the finite difference method, whose performance could also be improved by our wavelet preconditioning.

We first discretize the Poisson equation (3.1.2) on the uniform grid with $h = 1/2^n$.

For a function g, let $g_{i,j} = g(ih, jh), 1 \leq i, j \leq 2^n - 1$. A second order scheme is given by the 9-point stencil

$$\frac{1}{3h^2}\begin{pmatrix} 1 & 1 & 1 \\ 1 & -8 & 1 \\ 1 & 1 & 1 \end{pmatrix},$$

i.e., we discretize (3.1.2) as follows:

$$\begin{aligned} - \quad & (u_{i-1,j} + u_{i+1,j} + u_{i,j-1} + u_{i,j+1} - 8u_{i,j} + \\ & u_{i-1,j-1} + u_{i+1,j-1} + u_{i-1,j+1} + u_{i+1,j+1})/(3h^2) = f_{i,j}, \end{aligned} \tag{3.4.5}$$

where $1 \leq i, j \leq 2^n - 1$. This linear system could be written in the matrix form:

$$\widetilde{A}_n U_n = h^2 F_n, \tag{3.4.6}$$

where

$$U_n = (u_1, \ldots, u_{2^n-1})^T \text{ with } u_j = (u_{j,1}, \ldots, u_{j,2^n-1}), 1 \leq j \leq 2^n - 1$$

and

$$F_n = (f_1, \ldots, f_{2^n-1})^T \text{ with } f_j = (f_{j,1}, \ldots, f_{j,2^n-1}), 1 \leq j \leq 2^n - 1.$$

Note that $\widetilde{A}_n$ in (3.4.6) and A_n in (3.4.2) are exactly the same by straightforward computation. Hence to solve (3.1.2) numerically, we may solve the linear system (3.4.6) with S_n being the preconditioner. Furthermore, S_n is also a good preconditioner for proper difference scheme of the general second-order elliptic equation (3.1.1) if $\max\{a_2, b_2\}/\min\{a_1, b_1\}$ is not too big.

3.5 Numerical Schemes and Algorithms

In this section, we will show the efficiency of our wavelet preconditioning on solving general second-order elliptic equation (3.1.1) using the finite difference method.

A second-order difference scheme for discretizing (3.1.1) is

$$
\begin{aligned}
&\Big[\Big(b_{i,j-1/2}+b_{i,j+1/2}+a_{i-1/2,j}+a_{i+1/2,j}\\
&+\frac{a_{i-1/2,j-1/2}+b_{i-1/2,j-1/2}}{2}+\frac{a_{i-1/2,j+1/2}+b_{i-1/2,j+1/2}}{2}\\
&+\frac{a_{i+1/2,j-1/2}+b_{i+1/2,j-1/2}}{2}+\frac{a_{i+1/2,j+1/2}+b_{i+1/2,j+1/2}}{2}\Big)u_{i,j}\\
&-\Big(a_{i-1/2,j}+\frac{a_{i-1/2,j-1/2}-b_{i-1/2,j-1/2}}{2}+\frac{a_{i-1/2,j+1/2}-b_{i-1/2,j+1/2}}{2}\Big)u_{i-1,j}\\
&-\Big(a_{i+1/2,j}+\frac{a_{i+1/2,j+1/2}-b_{i+1/2,j+1/2}}{2}+\frac{a_{i+1/2,j-1/2}-b_{i+1/2,j-1/2}}{2}\Big)u_{i+1,j}\\
&-\Big(b_{i,j-1/2}+\frac{-a_{i-1/2,j-1/2}+b_{i-1/2,j-1/2}}{2}+\frac{-a_{i+1/2,j-1/2}+b_{i+1/2,j-1/2}}{2}\Big)u_{i,j-1}\\
&-\Big(b_{i,j+1/2}+\frac{-a_{i+1/2,j+1/2}+b_{i+1/2,j+1/2}}{2}+\frac{-a_{i-1/2,j+1/2}+b_{i-1/2,j+1/2}}{2}\Big)u_{i,j+1}\\
&-\frac{a_{i-1/2,j-1/2}+b_{i-1/2,j-1/2}}{2}u_{i-1,j-1}\\
&-\frac{a_{i-1/2,j+1/2}+b_{i-1/2,j+1/2}}{2}u_{i-1,j+1}\\
&-\frac{a_{i+1/2,j-1/2}+b_{i+1/2,j-1/2}}{2}u_{i+1,j-1}\\
&-\frac{a_{i+1/2,j+1/2}+b_{i+1/2,j+1/2}}{2}u_{i+1,j+1}\Big]\Big/3=\frac{1}{2^{2n}}f_{i,j} \quad \text{for} \quad 1\le i,j\le 2^n-1,\\
&u_{0,j}=u_{2^n,j}=u_{i,0}=u_{i,2^n}=0, \qquad\qquad \text{for} \quad 0\le i,j\le 2^n.
\end{aligned}
\tag{3.5.1}
$$

Here we take the values of a and b as follows:

$$
\begin{aligned}
&a_{i-1/2,j-1/2} = a(x_{i-1/2}, y_{j-1/2}), \quad &&b_{i-1/2,j-1/2} = b(x_{i-1/2}, y_{j-1/2}),\\
&a_{i,j-1/2} = a(x_i, y_{j-1/2}), &&b_{i,j-1/2} = b(x_i, y_{j-1/2}),\\
&a_{i-1/2,j} = a(x_{i-1/2}, y_j), &&b_{i-1/2,j} = b(x_{i-1/2}, y_j),
\end{aligned}
$$

where $x_{i-1/2} = (i-1/2)/2^n$ and $y_{j-1/2} = (j-1/2)/2^n$ for $1 \le i, j \le 2^n$.

Note that if $a(x, y) = b(x, y) = 1$, (3.5.1) reduces to (3.4.5). We write (3.5.1) in the following matrix form:

$$
A_n^{a,b} U_n = \frac{1}{2^{2n}} F_n. \tag{3.5.2}
$$

The condition number of $S_n A_n S_n^T$ is uniformly bounded, so is the condition number of $S_n A_n^{a,b} S_n^T$ given $0 < a_1 < a(x, y) < a_2$ and $0 < b_1 < b(x, y) < b_2$. Hence (3.5.2) can be solved by PCG algorithm with S_n being the preconditioner.

In order to further improve the numerical performance, we use the multi-level algorithm based on the PCG algorithm.

We first introduce some notations to describe the accuracy of our numerical solutions. For $n \ge 2$, let

$$
U_n = (u_1^n, \ldots, u_{2^n-1}^n)^T \text{ with } u_j^n = (u_{j,1}^n, \ldots, u_{j,2^n-1}^n), 1 \le j \le 2^n - 1,
$$

be the approximate solution to (3.5.2). Similarly,

$$
U_n^* = (u_1^{n,*}, \ldots, u_{2^n-1}^{n,*})^T \text{ with } u_j^{n,*} = (u_{j,1}^{n,*}, \ldots, u_{j,2^n-1}^{n,*}), 1 \le j \le 2^n - 1,
$$

represents the exact solution of (3.5.2). Suppose u^{exa} is the exact solution to (3.1.1). Let $u^{n,exa}_{i,j} := u^{exa}(i/2^n, j/2^n)$, $1 \le i, j \le 2^n - 1$. We define

$$\|e_n\|_{D_2^n} := h\Big(\sum_{i=1}^{2^n-1}\sum_{j=1}^{2^n-1}(u^n_{i,j} - u^{n,exa}_{i,j})^2\Big)^{1/2};$$

$$\|e^*_n\|_{D_2^n} := h\Big(\sum_{i=1}^{2^n-1}\sum_{j=1}^{2^n-1}(u^{n,*}_{i,j} - u^{n,exa}_{i,j})^2\Big)^{1/2}.$$

Indeed, $\|\cdot\|_{D_2^n}$ is the discrete L_2 norm of functions defined on Ω_h where $h = 1/2^n$, i.e., given a function $f : \Omega_h \to \mathbb{R}$,

$$\|f\|_{D_2^n} = h\Big(\sum_{(x,y)\in\Omega_h} f^2(x,y)\Big)^{1/2}$$

(see, e.g., [6]). Then $\|e^*_n\|_{D_2^n}$ represents the discretization error in the discrete L_2 norm.

If $\|e_n\|_{D_2^n} \le K\|e^*_n\|_{D_2^n}$, where K is a constant close to 1, we say that the error of an approximate solution U_n achieves the level of discretization error in the discrete L_2 norm.

For $k \ge 3$, let I^k_{k-1} and I^{k-1}_k be the bilinear interpolation and full weighting operators, respectively. These two notations agree with the notations I^h_{2h} and I^{2h}_h in the case $h = 1/2^k$ in [6].

In order to solve the linear system $A^{a,b}_n U_n = \frac{1}{2^{2n}} F_n$, we apply the following multilevel algorithm. Note that $A^{a,b}_2$ is a matrix of size 9×9. We first solve the equation $A^{a,b}_2 U_2 = \frac{1}{2^4} F_2$ exactly and get the solution U_2. Then for $3 \le k \le n$, perform m_k PCG iterations, with initial guess $I^k_{k-1} U_{k-1}$, for the linear system $A^{a,b}_k U_k = \frac{1}{2^{2k}} F_k$ to get U_k. Finally, the U_n is the approximate solution we want.

Note that m_k $(3 \le k \le n)$ iterations at level k are equivalent to $m_k/4^{n-k}$ iterations at level n. Thus, the total number of equivalent iterations at level n is computed by the following formula.

$$N_{it} = \sum_{k=3}^{n} \frac{m_k}{4^{n-k}}. \tag{3.5.3}$$

3.6 Numerical Examples

In this section, we apply our algorithm to solve (3.1.1) with coefficients $a(x,y)$ and $b(x,y)$. In comparison, we also solve the following examples by multigrid $V(2,1)$-cycle and full multigrid (FMG) algorithms based on $V(2,1)$-cycle since these two algorithms are commonly seen in multigrid books. For the multigrid algorithms, we choose usually used Gauss-Seidel relaxation, bilinear interpolation operator, full weighting restriction operator and grid 4×4 as the coarsest grid. See [6] for details.

Example 3.1. *Consider the Poisson equation, i.e., (3.1.1) with*

$$a(x,y) = b(x,y) = 1$$

where $(x,y) \in \Omega$. *Let the right hand side*

$$f(x,y) = 30(2x^2 - 2x + 2y^2 - 2y) \ \ (x,y) \in \Omega.$$

In this case, the exact solution is

$$u(x,y) = 30(x - x^2)(y - y^2) \ \ (x,y) \in \Omega.$$

Note that $\|f\|_{L_2} = 1$. The numerical results are listed in the following table.

Table 3.3: Numerical Results of Example 3.1

Level n	Grid $2^n \times 2^n$	N_{it}	$\|e_n\|_{D_2^n}$	$\|e_n^*\|_{D_2^n}$
5	32×32	3.94	1.63e-4	1.61e-3
6	64×64	3.98	4.17e-4	4.03e-4
7	128×128	4.00	1.03e-4	1.01e-4
8	256×256	4.00	2.66e-5	2.52e-5
9	512×512	4.00	6.51e-6	6.30e-6
10	1024×1024	4.00	1.73e-6	1.57e-6
11	2048×2048	4.00	4.12e-7	3.94e-7

In the above table, the first column lists the level. Given n, the size of the matrix $A_n^{a,b}$ is $(2^n-1)^2 \times (2^n-1)^2$. For example, at level 11, $A_{11}^{a,b}$ is a 4190209×4190209 matrix. The second column gives the grid to discretize (3.1.1).

The total number N_{it} of equivalent iterations at level n is computed by (3.5.3) and listed in the third column. For instance, for $n = 11$ and $3 \leq k \leq n$, $m_k = 3$. By (3.5.3) we have

$$N_{it} = \sum_{k=3}^{11} \frac{m_k}{4^{n-k}} \approx 3 \times \frac{4}{3} = 4.00.$$

We compare our approximate solution with the exact solution on the grid points and list the error $\|e_n\|_{D_2^n}$ in the fourth column. In comparison, the fifth column gives the discretization error in the discrete L_2 norm. In practice, we simply perform sufficient PCG iterations to get U_n^*. For

$5 \leq n \leq 11$, we have

$$\|e_n\|_{D_2^n} \leq 1.11 \|e_n^*\|_{D_2^n},$$

which shows that the level of discretization error is achieved. Moreover,

$$\|e_{n+1}^*\|_{D_2^{n+1}} / \|e_n^*\|_{D_2^n} \approx 1/4 \text{ for } 5 \leq n \leq 10.$$

Hence the rate of convergence is 2.

In comparison, we use both multigrid $V(2,1)$-cycle and FMG $V(2,1)$-cycle to solve the linear system $A_n^{a,b} U_n = \frac{1}{2^{2n}} F_n$. We measure the computational cost of multigrid algorithm by work unit (WU). A work unit is the cost of performing one relaxation sweep on the finest grid. For instance, we estimate one $V(2,1)$-cycle by $(3 + 0.5) \times \frac{4}{3} \approx 4.67$ WU. In the bracket, 3 WU denotes the computational cost for the three relaxation sweep on the finest grid. And the restriction and interpolation operations on the finest grid cost 0.5 WU. Since the algorithm is multilevel, a factor $4/3$ is multiplied to the computational cost on the finest grid. Similarly, one FMG $V(2,1)$-cycle costs $4.67 \times 4/3 \approx 6.23$ WU. Since our wavelets are simple, the computational cost of one PCG iteration is about 2.5 WU according to the PCG algorithm (2.2) introduced in the previous chapter. In fact, we run the PCG and multigrid $V(2,1)$-cycle algorithms on the same computer. At level 10, one PCG and one $V(2,1)$-cycle consume 0.16 and 0.31 seconds, respectively. This confirms that our estimation is reasonable for the PCG algorithm.

At level 11, 5 $V(2,1)$-cycles are needed to achieve the discretization error, which costs $5 \times 4.67 = 23.35$ WU. Only 1 FMG $V(2,1)$-cycle is required to reach the discretization error, and the computational cost is $1 \times 6.23 = 6.23$ WU. From the above table, it is easily seen that our algorithm costs $4.00 \times 2.5 = 10$ WU. Therefore, on solving the Poisson equation, our wavelet algorithm is less efficient than FMG algorithm, but more efficient than multigrid $V(2,1)$-cycle.

Example 3.2. *Consider (3.1.1) with*

$$a(x,y) = 1 + 0.95\sin(kx)$$

and

$$b(x,y) = 1 + 0.95\sin(ky)$$

where $(x,y) \in \Omega$ *and* $k = 610$. *Suppose the exact solution of the equation is*

$$u(x,y) = t\sin(\pi x)\sin(\pi y)(x^2 + y^2), (x,y) \in \Omega,$$

where $t > 0$ *is so chosen that the* f *obtain from (3.1.1) with* a, b *and* u *given above satisfying:* $\|f\|_{L_2} = 1$.

TABLE 3.4: Numerical Results of Example 3.2

Level n	Grid $2^n \times 2^n$	N_{it}	$\|e_n\|_{D_2^n}$	$\|e_n^*\|_{D_2^n}$
8	256×256	17.32	3.07e-4	3.07e-4
9	512×512	17.33	6.82e-5	6.48e-5
10	1024×1024	17.33	1.81e-5	1.60e-5
11	2048×2048	17.33	4.45e-6	3.96e-6

In this example, the coefficients $a(x,y)$ and $b(x,y)$ are different. They oscillate significantly along x and y axes, respectively.

The approximate solution obtained by our algorithm achieves the level of discretization error since

$$\|e_n\|_{D_2^n} \leq 1.13\|e_n^*\|_{D_2^n} \text{ for } 8 \leq n \leq 11.$$

Note that

$$\|e_{n+1}^*\|_{D_2^{n+1}}/\|e_n^*\|_{D_2^n} \approx 1/4 \text{ for } 9 \leq n \leq 10,$$

which indicates that the rate of convergence is of order 2 when n is large. This is reasonable because we have to discretize (3.1.1) with very small mesh size $h = 1/2^n$ to obtain an effective solution when a and b are oscillating.

In comparison, at level 11, 25 V(2,1)-cycles are needed to achieve $\|e_{11}\|_{D_2^n} = 4.49e-6$, and the computational cost is about 116.75 WU. Our algorithm costs only about 43.33 WU. The multigrid $V(2,1)$-cycle algorithm diverges for $5 \leq n \leq 8$, hence the FMG $V(2,1)$-cycle is not applicable. In order to apply FMG algorithms, one has to increase the coarsest level, raise the number of relaxation or change the coarser grid operator. Further discussion on this issue is beyond the scope of this thesis.

Example 3.3. *Consider (3.1.1) with*

$$a(x,y) = 1 + 0.95\sin(kx)$$

and

$$b(x,y) = 1 + 0.95\sin(ky)$$

where $(x,y) \in \Omega$ *and* $k = 1000$*. Suppose the exact solution of the equation is*

$$u(x,y) = t\sin(\pi x)\sin(\pi y)(x^2+y^2), (x,y) \in \Omega,$$

where $t > 0$ *is so chosen that the* f *obtain from (3.1.1) with* a*,* b *and* u *given above satisfying:* $\|f\|_{L_2} = 1$.

TABLE 3.5: Numerical Results of Example 3.3

Level n	Grid $2^n \times 2^n$	N_{it}	$\|e_n\|_{D_2^n}$	$\|e_n^*\|_{D_2^n}$
9	512×512	18.67	1.19e-5	1.19e-4
10	1024×1024	18.67	2.87e-5	2.66e-5
11	2048×2048	18.67	7.17e-6	6.48e-6

Here we raise the number k to 1000. The variable coefficients $a(x, y)$ and $b(x, y)$ are more oscillating than those in example 3.2. Both the multigrid $V(2, 1)$-cycle and FMG $V(2, 1)$-cycle diverge. Thus other techniques should be used in the multigrid algorithms to achieve convergence.

Note that

$$\|e_n\|_{D_2^n} \leq 1.11\|e_n^*\|_{D_2^n} \text{ for } 9 \leq n \leq 11.$$

This shows that our wavelet algorithm still works well, and the computational cost does not increase much to achieve the level of discretization error.

Example 3.4. *Consider (3.1.1) with a and b given by*

$$a(x, y) = b(x, y) = 1.0 + 0.95 \sin(50.7\pi(x - y)), (x, y) \in \Omega.$$

Suppose the exact solution of the equation is

$$u(x, y) = t \sin(\pi x) \sin(\pi y)(x^2 + y^2), (x, y) \in \Omega,$$

where $t > 0$ is so chosen that the f obtain from (3.1.1) with a, b and u given above satisfying: $\|f\|_{L_2} = 1$.

Table 3.6: Numerical Results of Example 3.4

Level n	Grid $2^n \times 2^n$	N_{it}	$\|e_n\|_{D_2^n}$	$\|e_n^*\|_{D_2^n}$
7	128×128	10.63	1.72e-4	1.72e-4
8	256×256	13.32	5.22e-5	5.04e-5
9	512×512	13.33	1.43e-5	1.30e-5
10	1024×1024	13.33	3.45e-6	3.24e-6
11	2048×2048	12.00	8.08e-7	8.08e-7

In this example, the coefficients $a(x, y)$ and $b(x, y)$ are the same and oscillating diagonally. This table also indicates that the level of discretization error is achieved and the convergence rate is 2.

At level 11, 25 $V(2, 1)$-cycles are needed to reach $\|e_{11}\|_{D_2^{11}} = 8.08e - 7$, whereas 13 FMG $V(2, 1)$-cycles are required to achieve the same error. Hence the computational costs of multigrid $V(2, 1)$-cycle and FMG $V(2, 1)$-cycle are 116.75 WU and 80.99 WU, respectively. From the above table, the level of discretization error is achived by 12.00 equivalent PCG iterations which costs $12 \times 2.5 = 30$ WU. This shows that our algorithm is much more efficient than both multigrid $V(2, 1)$-cycle and FMG $V(2, 1)$-cycle.

From the above examples, we observe that classical multigrid algorithms are not efficient on solving (3.1.1) when the coefficients a and b are rough. Special techniques need to be applied according to the properties of these coefficients. But the wavelet Galerkin method has good performance, and the convergence of the corresponding numerical schemes is always guaranteed.

Chapter 4

Riesz Bases of Wavelets and Applications to Fourth-order Elliptic Equations

4.1 Introduction

Many practical problems in elasticity and fluid dynamics are modeled by biharmonic equation. Here we consider the bending plate problem in the case all edges are built-in [38]. This problem is modeled by the two dimensional biharmonic equation with homogeneous boundary conditions. That is,

$$\begin{cases} \Delta^2 u(x,y) = f(x,y) & (x,y) \in \Omega, \\ u(x,y) = \dfrac{\partial}{\partial n} u(x,y) = 0 & (x,y) \in \partial\Omega, \end{cases} \tag{4.1.1}$$

where u and f denote the deflection of the plate and distributed load, respectively, and Ω denotes the unit square $(0,1) \times (0,1)$. As usual, Δ

stands for the Laplace operator: $\Delta = \frac{\partial^2}{\partial x^2} + \frac{\partial^2}{\partial y^2}$, and $\frac{\partial}{\partial n}$ represents the normal derivative.

Many numerical methods have been employed to solve the biharmonic equation. Altas et al [1] introduced a vector difference scheme of fourth order and solved the resulting linear system by geometric multigrid method. Algebraic multigrid method was used by Chang and Huang in [7] and Chang, Wong and Fu in [8] for the linear system arising from a second-order difference scheme. To apply the finite element methods, Oswald [32] designed multilevel preconditioners for the biharmonic equation discretized by bicubic C^1 splines, while Sun in [37] considered preconditioning techniques for the linear system based on quadratic splines' discretization. In the literature, (4.1.1) is often decoupled into two Poisson equations as follows:

$$\left.\begin{aligned} -\Delta u &= \omega \\ -\Delta \omega &= f \end{aligned}\right\} \text{ in } \Omega, \quad u = \frac{\partial u}{\partial n} = 0 \text{ on } \partial\Omega. \tag{4.1.2}$$

Silvester and Mihajlovic [34] applied multigrid preconditioning to the linear system resulting from discretizations of the above decoupled system.

As is well-known, the linear system arising from usual discretizations of the biharmonic equation is ill conditioned. Under mesh refinement, the condition number of the stiffness matrix deteriorates rapidly like h^{-4} in general. Thus, it is a challenging problem to efficiently solve the large linear system. In this chapter, we investigate stable wavelet bases in Sobolev spaces. We will show theoretically and numerically that the condition numbers of the stiffness matrices associated with our wavelet bases are uniformly bounded and relatively small. Thus, classical iterative methods could have good performance on solving the resulting linear system. By the use of multilevel idea, we further improve the efficiency of our algorithms. These wavelet bases are also applicable to numerical solutions of general fourth-order elliptic equations, and our numerical schemes still have superb performance.

Suppose Ω is a (nonempty) open subset of $\mathbb{R}^s$. In the first chapter, we defined Sobolev spaces $H^m(\Omega)$ and $H_0^m(\Omega)$ for $m \in \mathbb{N}$. Here we introduce Sobolev spaces $H^\mu(\Omega)$ and $H_0^\mu(\Omega)$ where μ is a nonnegative real number.

The Fourier transform of a function $f \in L_1(\mathbb{R}^s)$ is defined by

$$\hat{f}(\xi) := \int_{\mathbb{R}^s} f(x) e^{-ix\cdot\xi} dx, \ \ \xi \in \mathbb{R}^s,$$

where i denotes the imaginary unit. The Fourier tansform can be naturally extended to functions in $L_2(\mathbb{R}^s)$. By Plancherel theorem (see, e.g., [41]), we have $\|\hat{f}\|_{L_2} = (2\pi)^{s/2}\|f\|_{L_2}$.

For $\mu \geq 0$, we denote by $H^\mu(\mathbb{R}^s)$ the Sobolev space of all functions $f \in L_2(\mathbb{R}^s)$ such that the semi-norm

$$|f|_{H^\mu(\mathbb{R}^s)} := \left[\frac{1}{(2\pi)^s}\int_{\mathbb{R}^s} |\hat{f}(\xi)|^2 |\xi|^{2\mu} d\xi\right]^{1/2}$$

is finite. The space $H^\mu(\mathbb{R}^s)$ is a Hilbert space with the inner product given by

$$\langle f, g\rangle_{H^\mu(\mathbb{R}^s)} := \frac{1}{(2\pi)^s}\int_{\mathbb{R}^s} \hat{f}(\xi)\overline{\hat{g}(\xi)}(1 + |\xi|^{2\mu}) d\xi, \ \ f, g \in H^\mu(\mathbb{R}^s).$$

The norm in $H^\mu(\mathbb{R}^s)$ is given by $\|f\|_{H^\mu(\mathbb{R}^s)} = (\langle f, f\rangle_{H^\mu(\mathbb{R}^s)})^{1/2}$. This newly defined $H^\mu(\mathbb{R}^s)$ for $\mu \in \mathbb{N}_0$ agrees with the Sobolev space defined in the first chapter. For a (nonempty) open subset Ω of $\mathbb{R}^s$, we use $H_0^\mu(\Omega)$ to denote the closure of $C_c^\infty(\Omega)$ in $H^\mu(\mathbb{R}^s)$.

4.2 Wavelets in the One-dimensional Space

In this section we construct stable wavelet basis of $H_0^2(0,1)$, and then in the next section adapt it to the unit square Ω by tensor product so that we obtain a stable wavelet basis of $H_0^2(\Omega)$.

For a positive integer m, let M_m be the B-spline of order m, which is the convolution of m copies of $\chi_{[0,1]}$, the characteristic function of the interval $[0,1]$. More precisely, $M_1 := \chi_{[0,1]}$ and, for $m \geq 2$,

$$M_m(x) = \int_0^1 M_{m-1}(x-t)dt, \quad x \in \mathbb{R}.$$

We use cubic splines to construct the approximate space $\widetilde{V}_n$ of $H_0^2(0,1)$. Consider the B-spline of order four

$$M_4(x) = \begin{cases} \frac{1}{6}x^3 & \text{for} \quad 0 \leq x < 1, \\ -\frac{1}{2}x^3 + 2x^2 - 2x + \frac{2}{3} & \text{for} \quad 1 \leq x < 2, \\ \frac{1}{2}x^3 - 4x^2 + 10x - \frac{22}{3} & \text{for} \quad 2 \leq x < 3, \\ -\frac{1}{6}x^3 + 2x^2 - 8x + \frac{32}{3} & \text{for} \quad 3 \leq x \leq 4, \\ 0 & \text{for} \quad \mathbb{R} \setminus [0,4], \end{cases}$$

and the boundary element

$$\phi_b(x) = \begin{cases} \frac{1}{12}(-11x^3 + 18x^2) & \text{for} \quad 0 \leq x < 1, \\ \frac{1}{12}(7x^3 - 36x^2 + 54x - 18) & \text{for} \quad 1 \leq x < 2, \\ \frac{1}{6}(-x^3 + 9x^2 - 27x + 27) & \text{for} \quad 2 \leq x \leq 3, \\ 0 & \text{for} \quad \mathbb{R} \setminus [0,3]. \end{cases}$$

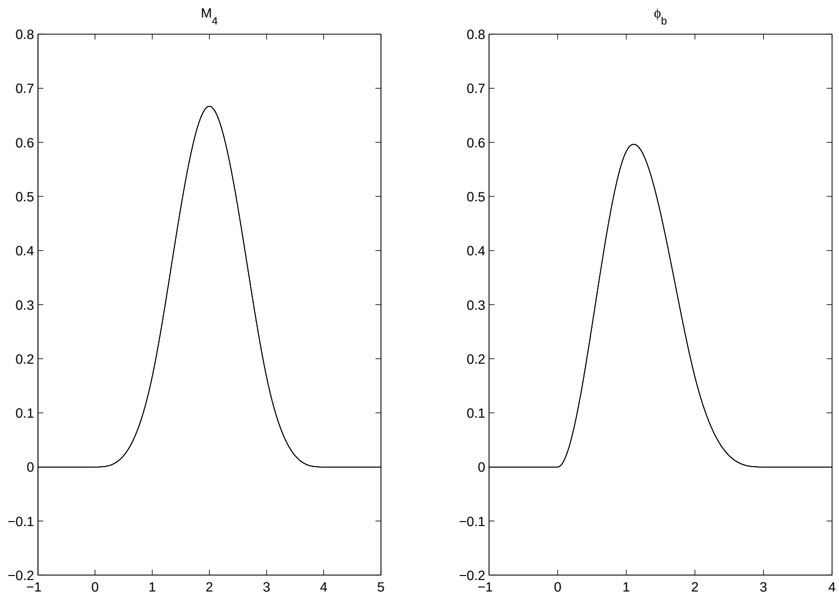

FIGURE 4.1: B-spline of Order 4 and Boundary Element

Note that

$$M_4(1) = 1/6, M_4(2) = 2/3, M_4(3) = 1/6$$
$$\phi_b(1) = 7/12, \phi_b(2) = 1/6. \tag{4.2.1}$$

Furthermore,

$$M_4(x) = \frac{1}{8}\big(M_4(2x)+4M_4(2x-1)+6M_4(2x-2)+4M_4(2x-3)+M_4(2x-4)\big),$$

$$\phi_b(x) = \frac{1}{16}\big(4\phi_b(2x) + 11M_4(2x) + 8M_4(2x-1) + 2M_4(2x-2)\big).$$

These two refinement equations guarantee that the following approximate subspaces $\widetilde{V}_n$'s are nested. For $x \in [0,1]$, $n \geq 3$, define

$$\widetilde{\phi}_{n,j}(x) := \begin{cases} 2^{n/2}\phi_b(2^n x) & j = 1, \\ 2^{n/2}M_4(2^n x - j + 2) & j = 2, \ldots, 2^n - 2, \\ 2^{n/2}\phi_b(2^n(1-x)) & j = 2^n - 1. \end{cases}$$

Let $\widetilde{\Phi}_n := \{\widetilde{\phi}_{n,j}, j = 1, 2, \ldots, 2^n - 1\}$ and $\widetilde{V}_n := \operatorname{span}\{\widetilde{\Phi}_n\}$. Note that $\phi_b \in H^\mu(\mathbb{R})$ for $0 < \mu < 5/2$, $M_4 \in H^\mu(\mathbb{R})$ for $0 < \mu < 7/2$, and both ϕ_b and M_4 are compactly supported. Hence $\widetilde{V}_n \subset H_0^\mu(0,1)$ for $0 < \mu < 5/2$. It is easily seen that

- $\widetilde{V}_3 \subset \widetilde{V}_4 \subset \widetilde{V}_5 \cdots$;
- $\displaystyle\bigcup_{n=3}^{\infty} \widetilde{V}_n$ is dense in $H_0^\mu(0,1)$ for $0 < \mu < 5/2$;
- $\dim(\widetilde{V}_n) = 2^n - 1$.

Moreover,

Proposition 4.1. *For $n \geq 3$, $\widetilde{\Phi}_n$ is a Riesz basis of $\widetilde{V}_n$ in the L_2 space.*

Next we need to construct suitable wavelet space $\widetilde{W}_n$ such that $\widetilde{V}_{n+1} = \widetilde{V}_n + \widetilde{W}_n$ for all $n \geq 3$. For this end, let $\widetilde{P}_n$ be the linear projection from $\widetilde{V}_{n+1}$ onto $\widetilde{V}_n$ given as follows: For $f_{n+1} \in \widetilde{V}_{n+1}$, $f_n := \widetilde{P}_n f_{n+1}$ is the unique element in $\widetilde{V}_n$ determined by the interpolation condition

$$f_n(k/2^n) = f_{n+1}(k/2^n) \quad k = 1, 2, \ldots, 2^n - 1.$$

Then the following proposition holds.

Proposition 4.2. *For $3 \leq m < n$, $\|\widetilde{P}_m \cdots \widetilde{P}_{n-1}\| \leq C2^{(n-m)/2}$, where C is a constant independent of m and n.*

See section 6 in [27] for the proof.

Let $\widetilde{W}_n$ be the kernel $\ker(\widetilde{P}_n)$ of $\widetilde{P}_n$ in $\widetilde{V}_{n+1}$. $\widetilde{W}_n$ is generated by the following wavelets:

$$\psi(x) := -\frac{1}{4}M_4(2x) + M_4(2x-1) - \frac{1}{4}M_4(2x-2),$$

$$\psi_b(x) := \phi_b(2x) - \frac{1}{4}M_4(2x).$$

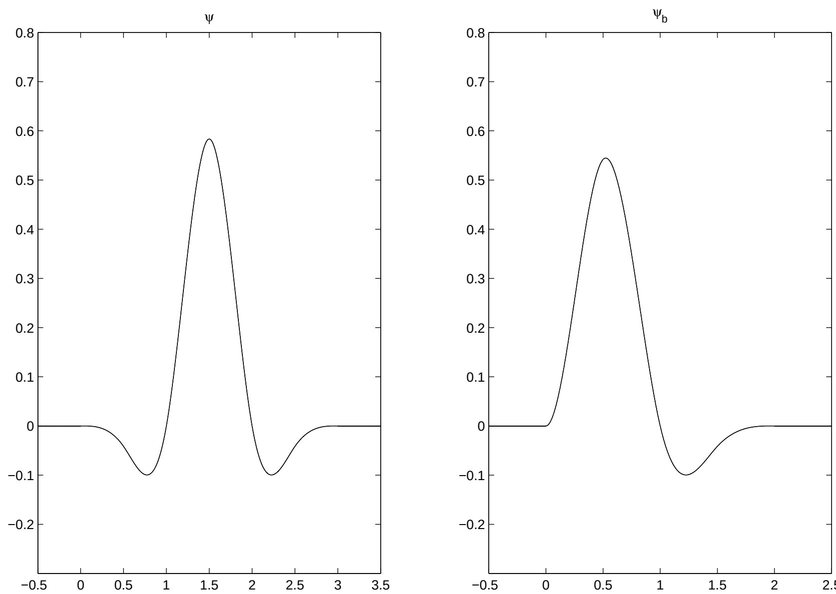

FIGURE 4.2: Wavelets ψ and ψ_b

In other words, $\widetilde{W}_n = \text{span}\{\widetilde{\Gamma}_n\} := \text{span}\{\widetilde{\psi}_{n,j}, j = 1, 2, \ldots, 2^n\}$ where

$$\widetilde{\psi}_{n,j}(x) := \begin{cases} 2^{n/2}\psi_b(2^n x) & j = 1, \\ 2^{n/2}\psi(2^n x - j + 2) & j = 2, \ldots, 2^n - 1, \\ 2^{n/2}\psi_b(2^n(1-x)) & j = 2^n \end{cases}$$

for $x \in [0, 1]$ and $n \geq 3$. Indeed, $\{\widetilde{\psi}_{n,j}, j = 1, 2, \ldots, 2^n\}$ is linearly independent. By (4.2.1), we know that $\psi(i) = \psi_b(i) = 0$ for all $i \in \mathbb{Z}$, thus $\widetilde{P}_n \widetilde{\psi}_{n,j} = 0$.

Furthermore,

Proposition 4.3. *For $n \geq 3$, $\widetilde{\Gamma}_n$ is a Riesz basis of $\widetilde{W}_n$ in the L_2 space.*

An application of theorem 4.9 gives the following result.

Theorem 4.4. *For $1/2 < \mu < 5/2$, the set*

$$\{2^{-3\mu}\widetilde{\Phi}_3\} \bigcup \bigcup_{n=3}^{\infty} \{2^{-n\mu}\widetilde{\Gamma}_n\}$$

forms a Riesz basis of $H_0^{\mu}(0, 1)$.

Since $1/2 < 2 < 5/2$, in particular, $\{2^{-6}\widetilde{\Phi_3}\} \bigcup \bigcup_{n=3}^{\infty} \{2^{-2n}\widetilde{\Gamma_n}\}$ is a stable wavelet basis of $H_0^2(0, 1)$.

4.3 Wavelets in the Two-dimensional Space

In order to obtain a stable wavelet basis of $H_0^2(\Omega)$, we use the tensor product denoted by $\otimes$. For two functions v and w defined on $[0, 1]$, we use $v \otimes w$ to denote the function on $[0,1]^2$ given by

$$v \otimes w(x,y) := v(x)w(y), \quad 0 \le x, y \le 1.$$

For $n \ge 3$, let $J_n := \{j = (j_1, j_2) \in \mathbb{Z}^2 : 1 \le j_1, j_2 \le 2^n - 1\}$. Define

$$\begin{aligned} &\phi_{n,j} := \widetilde{\phi}_{n,j_1} \otimes \widetilde{\phi}_{n,j_2}, \ \ j \in J_n; \\ &\Phi_n := \{\phi_{n,j}, j \in J_n\}; \\ &V_n := \operatorname{span}\{\Phi_n\}. \end{aligned} \tag{4.3.1}$$

V_n's have similar properties as their counterparts $\widetilde{V}_n$'s, i.e.,

- $V_3 \subset V_4 \subset V_5 \cdots$;
- $\bigcup_{n=3}^{\infty} V_n$ is dense in $H_0^{\mu}(\Omega)$ for $0 < \mu < 5/2$;
- $\dim(V_n) = (2^n - 1)(2^n - 1)$.

Furthermore,

Proposition 4.5. *For $n \ge 3$, Φ_n is a Riesz basis of V_n in the L_2 space.*

Let P_n be the linear projection from V_{n+1} onto V_n given as follows: For $f_{n+1} \in V_{n+1}$, $f_n := P_n f_{n+1}$ is the unique element in V_n determined by the interpolation condition

$$f_n(k/2^n) = f_{n+1}(k/2^n) \quad k \in J_n.$$

Similarly, the following proposition holds.

Proposition 4.6. *For $3 \le m < n$, $\|P_m \cdots P_{n-1}\| \le C2^{(n-m)}$, where C is a constant independent of m and n.*

The wavelet space is constructed as $W_n := \ker(P_n)$. Let

$$\Gamma_n' := \big\{\widetilde{\phi}_{n,j_1} \otimes \widetilde{\psi}_{n,k_2} : 1 \le j_1 \le 2^n - 1, 1 \le k_2 \le 2^n\big\};$$

$$\Gamma_n'' := \big\{\widetilde{\psi}_{n,k_1} \otimes \widetilde{\phi}_{n,j_2} : 1 \le j_2 \le 2^n - 1, 1 \le k_1 \le 2^n\big\};$$

$$\Gamma_n''' := \big\{\widetilde{\psi}_{n,k_1} \otimes \widetilde{\psi}_{n,k_2} : 1 \le k_1, k_2 \le 2^n\big\}.$$

Then

Proposition 4.7. *For $n \ge 3$, $\Gamma_n := \Gamma_n' \bigcup \Gamma_n'' \bigcup \Gamma_n'''$ is a Riesz basis of W_n in the L_2 space.*

An application of theorem 4.9 gives the following result.

Theorem 4.8. *For $1 < \mu < 5/2$, the set*

$$\{2^{-3\mu}\Phi_3\} \bigcup \bigcup_{n=3}^{\infty} \{2^{-n\mu}\Gamma_n\}$$

forms a Riesz basis of $H_0^\mu(\Omega)$.

In particular, $\{2^{-6}\Phi_3\} \bigcup \bigcup_{n=3}^{\infty} \{2^{-2n}\Gamma_n\}$ is a Riesz basis of $H_0^2(\Omega)$. This wavelet basis will be used to solve the biharmonic equation on Ω.

Note that the upper bound of $\|P_m \cdots P_{n-1}\|$ is $C2^{(n-m)}$ which is slightly different from the upper bound $C2^{(n-m)/2}$ of $\|\widetilde{P}_m \cdots \widetilde{P}_{n-1}\|$ in the one-dimensional case. This results in the difference of the lower bound 1 of μ in this theorem and the lower bound $1/2$ of μ in theorem 4.4.

4.4 Stable Wavelet Bases in Hilbert Spaces

In this section, we give a characterization of Riesz bases of Hilbert spaces equipped with some induced norms.

Let H be a Hilbert space equipped with norm $\|\cdot\|$. Suppose that $V_0 = 0$ and $(V_n)_{n=1,2,\ldots}$ is a nested family of closed subspaces of H, i.e., $V_n \subset V_{n+1}$ for all $n \in \mathbb{N}$. Assume that $\bigcup_{n=1}^{\infty} V_n$ is dense in H. Fix $\mu > 0$ and let H_μ be a linear subspace of H. Suppose H_μ itself is a normed linear space with norm $\|\cdot\|_{H_\mu}$. For $n \in \mathbb{N}_0$, let P_n be a linear projection from V_{n+1} onto V_n, and W_n be the kernel space of P_n. Then V_{n+1} is the direct sum of V_n and W_n. The following theorem characterizes the Riesz basis of H_μ.

Theorem 4.9. *If the following four conditions are satisfied:*

- *If $f \in H_\mu$ has a decomposition $f = \sum_{n=1}^{\infty} f_n$ with $f_n \in V_n$, then*

$$\|f\|_{H_\mu} \leq A_1 \Big(\sum_{n=1}^{\infty} [2^{n\mu} \|f_n\|]^2 \Big)^{1/2},$$

  where A_1 is a positive constant independent of n;

- *For each $f \in H_\mu$, there exists a decomposition $f = \sum_{n=1}^{\infty} f_n$ with $f_n \in V_n$ such that*

$$A_2 \Big(\sum_{n=1}^{\infty} [2^{n\mu} \|f_n\|]^2 \Big)^{1/2} \leq \|f\|_{H_\mu},$$

  where A_2 is a positive constant independent of n;

- *Suppose that $0 < \nu < \mu$ and there exists a positive constant B such that*

$$\|P_m \cdots P_{n-1}\| \leq B 2^{\nu(n-m)}$$

  for all $m, n \in \mathbb{N}$ with $m < n$;

- *$\{\psi_{n,k} : k \in K_n\}$ is a Riesz basis of W_n in H.*

Then $\{2^{-m\mu} \psi_{m,k} : m \in \mathbb{N}_0, k \in K_m\}$ is a Riesz basis of H_μ.

See section 5 in [27] for the proof of this theorem.

Let $\widetilde{Q}_n : L_2(0,1) \to \widetilde{V}_n$ be the L_2-orthogonal projection onto $\widetilde{V}_n$ $(n \geq 3)$ with $\langle \widetilde{Q}_n \widetilde{u}, \widetilde{v} \rangle = \langle \widetilde{u}, \widetilde{v} \rangle, \tilde{u}, \tilde{v} \in L_2(0,1)$ and $\widetilde{Q}_0 := 0$. Similarly, in the two-dimensional space, let $Q_n : L_2(\Omega) \to V_k$ be the L_2-orthogonal projection onto V_n $(n \geq 3)$ with $\langle Q_n u, v \rangle = \langle u, v \rangle, u, v \in L_2(\Omega)$ and $Q_0 := 0$.

The following inequalities have been established in section 4 of [27].

$$\widetilde{C}_1 \|\widetilde{f}\|_{H^\mu} \leq \Big([2^{3\mu} \|\widetilde{Q}_3 \widetilde{f}\|_{L_2}]^2 + \sum_{n=4}^{\infty} [2^{n\mu} \|(\widetilde{Q}_n - \widetilde{Q}_{n-1}) \widetilde{f}\|_{L_2}]^2 \Big)^{1/2} \leq \widetilde{C}_2 \|\widetilde{f}\|_{H^\mu} \tag{4.4.1}$$

hold for all $\widetilde{f} \in \widetilde{V}_n$ with $0 < \mu < 5/2$ where $\tilde{C}_1$ and $\tilde{C}_2$ are two positive constants independent of $\widetilde{f}$;

$$C_1 \|f\|_{H^\mu} \leq \Big([2^{3\mu} \|Q_3 f\|_{L_2}]^2 + \sum_{n=4}^{\infty} [2^{n\mu} \|(Q_n - Q_{n-1}) f\|_{L_2}]^2 \Big)^{1/2} \leq C_2 \|f\|_{H^\mu} \tag{4.4.2}$$

hold for all $f \in V_n$ with $0 < \mu < 5/2$ where C_1 and C_2 are two positive constants independent of f.

For $1/2 < \mu < 5/2$, we take $H_\mu = H_0^\mu(0,1)$ and $H = L_2(0,1)$ in the one-dimensional case. Let us check the four conditions of theorem 4.9.

The norm equivalence (4.4.1) and its proof in [27] indicate that the first two conditions are satisfied. Proposition 4.2 gives the third condition with $\nu = 1/2$. The last condition holds true because of proposition 4.3. Therefore, theorem 4.9 implies theorem 4.4.

Similarly, in the two-dimensional case, we take $H_\mu = H_0^\mu(\Omega)$ and $H = L_2(\Omega)$ for $1 < \mu < 5/2$. Then an application of theorem 4.9 with $\nu = 1$ gives theorem 4.8 since the four conditions are fulfilled because of the norm equivalence (4.4.2), proposition 4.6 and proposition 4.7.

4.5 Condition Numbers of the Stiffness Matrices

In this section, we apply the wavelet bases constructed in the previous section to numerical solutions of the biharmonic equation (4.1.1). We always assume $n \geq 3$.

The variational problem of the biharmonic equation (4.1.1) is to find $u \in H_0^2(\Omega)$ such that

$$a(u, v) = \langle f, v \rangle \quad \forall v \in H_0^2(\Omega), \tag{4.5.1}$$

where $a(u, v) = \langle \Delta u, \Delta v \rangle$. For $u, v \in H_0^2(\Omega)$, it is easy to verify that $a(u, v) \leq \|u\|_{H_0^2(\Omega)} \|v\|_{H_0^2(\Omega)}$ and $a(u, v) \geq C\|u\|^2_{H_0^2(\Omega)}$ where C is a constant independent of u. Hence $a(u, v)$ is continuous and coercive, and by the Lax-Milgram theorem, existence and uniqueness of the solution are guaranteed for (4.5.1).

In order to solve (4.5.1), we take the finite dimensional subspace V_n to approximate $H_0^2(\Omega)$ and seek $u_n \in V_n$ such that

$$\langle \Delta u_n, \Delta v \rangle = \langle f, v \rangle \quad \forall v \in V_n. \tag{4.5.2}$$

Recall that $\Phi_n = \{\phi_{n,j}, j \in J_n\}$ is a basis of V_n. The argument in the first chapter guides us to look for the column vector $y_n = (y_\phi)_{\phi \in \Phi_n}$ satisfying

$$A_n y_n = \xi_n, \tag{4.5.3}$$

where $A_n = (\langle \Delta\sigma, \Delta\phi \rangle)_{\sigma,\phi \in \Phi_n}$ and ξ_n is the column vector $(\langle f, \phi \rangle)_{\phi \in \Phi_n}$. Then we obtain an approximate solution $u_n = \sum_{\phi \in \Phi_n} y_\phi \phi$ in V_n. The condition number $\kappa(A_n)$ of the matrix A_n is of the size $O(2^{4n})$. Hence, it would be very difficult to solve the linear system (4.5.3) when n is large.

Now we employ the wavelet basis $\Psi_n := \{2^{-6}\Phi_3\} \bigcup \bigcup_{k=3}^{n-1}\{2^{-2k}\Gamma_k\}$ of V_n constructed in the previous section. Similarly, we are looking for the column vector $z_n = (z_\psi)_{\psi\in\Psi_n}$ satisfying

$$B_n z_n = \eta_n, \tag{4.5.4}$$

where $B_n = (\langle\Delta\chi, \Delta\psi\rangle)_{\chi,\psi\in\Psi_n}$ and η_n is the column vector $(\langle f, \psi\rangle)_{\psi\in\Psi_n}$. Then the approximate solution in V_n is $u_n = \sum_{\psi\in\Psi_n} z_\psi \psi$.

Note that Φ_n and Ψ_n are two bases of V_n, there exists a unique matrix S_n, called wavelet transform, which transforms Φ_n to Ψ_n. Therefore,

$$\begin{aligned} B_n &= S_n A_n S_n^T, \\ \eta_n &= S_n \xi_n. \end{aligned}$$

Hence linear systems (4.5.4) and (4.5.3) are equivalent if we set $y_n = S_n^T z_n$. Actually, we will use multilevel algorithm based on the following modified PCG algorithm.

Algorithm 4.1 Modified PCG Algorithm

Given initial guess y_n^0, $r_0 \leftarrow \xi_n - A_n y_n^0$
$p_0 \leftarrow r_0$
for $k = 1, 2, \ldots$ **do**
    $\alpha_{k-1} \leftarrow r_{k-1}^T p_{k-1} / p_{k-1}^T A_n p_{k-1}$
    $y_n^k \leftarrow y_n^{k-1} + \alpha_{k-1} p_{k-1}$
    $r_k \leftarrow r_{k-1} - \alpha_{k-1} A_n p_{k-1}$
    $s_k \leftarrow S_n r_k$
    If $\|s_k\|_2 < \tau$, stop
    else
    $s_k \leftarrow S_n^T s_k$
    $p_k \leftarrow s_k - \dfrac{s_k^T A_n p_{k-1}}{p_{k-1}^T A_n p_{k-1}} p_{k-1}$
end for

The difference between this modified PCG algorithm and the former PCG algorithm in the second chapter is the stopping criterion. This modified PCG algorithm stops when the l_2 norm of the residue of equation (4.5.4) is less than some tolerance τ. Whereas the former PCG algorithm stops when the l_2 norm of the residue of equation (4.5.3) is less than some tolerance τ.

Since $\{2^{-6}\Phi_3\} \bigcup \bigcup_{n=3}^{\infty} \{2^{-2n}\Gamma_n\}$ is a Riesz basis of $H_0^2(\Omega)$, the condition number $\kappa(B_n)$ of the matrix B_n is uniformly bounded by proposition 1.1. This is also confirmed by the numerical computation. The condition number $\kappa(B_n)$ is computed for $4 \leq n \leq 9$ and listed in table 4.1.

Table 4.1: Condition Numbers of the Preconditioned Matrices

n	size of B_n	$\lambda_{max}(B_n)$	$\lambda_{min}(B_n)$	$\kappa(B_n)$
4	225×225	2.7160	0.07996	33.97
5	961×961	2.7883	0.07995	34.88
6	3969×3969	2.8082	0.07994	35.13
7	16129×16129	2.8259	0.07994	35.35
8	65025×65025	2.8434	0.07994	35.57
9	261121×261121	2.8489	0.07994	35.64

A multigrid preconditioner was proposed in [34] for the decoupled biharmonic system (4.1.2). From tables 1, 2 and 3 in [34], we can see that the condition number of the preconditioned matrix grows like $O(h^{-1})$, where h is the mesh size. In particular, for piecewise linear approximation on the 48×48 grid, the condition number already exceeds 80. In comparison, the condition number $\kappa(B_n)$ of the stiffness matrix associated with our wavelet basis is uniformly bounded. For the 512×512 grid ($n = 9$), $\kappa(B_9) < 36$.

To estimate the accuracy of our numerical solutions, we introduce the following notations. Let $z_n^* := (z_\psi^*)_{\psi \in \Psi_n}$ be the exact solution to the equation $B_n z_n = \eta_n$ and $u_n^* = \sum_{\psi \in \Psi_n} z_\psi^* \psi$. Suppose u is the exact solution to the biharmonic equation (4.1.1). Let $e_n^* := u_n^* - u$. Then $\|\Delta e_n^*\|_{L_2}$ and $\|e_n^*\|_{L_2}$ represent the discretization errors in the energy norm and L_2 norm, respectively. Suppose $u_n = \sum_{\psi \in \Psi_n} z_\psi \psi$, where $z_n := (z_\psi)_{\psi \in \Psi_n}$ is an approximate solution to equation (4.5.4). Let $e_n := u_n - u$. Similarly, let $\tilde{e}_n^* := u_n^* - u_{n+1}^*$ and $\tilde{e}_n := u_n - u_{n+1}$. Then

Proposition 4.10. $\|\Delta e_n^*\|_{L_2} \leq \|\Delta e_n\|_{L_2}$.

Proof.

$$\begin{aligned}
\|\Delta e_n\|_{L_2} &= \langle \Delta(u_n - u), \Delta(u_n - u)\rangle \\
&= \langle \Delta(u_n - u_n^* + u_n^* - u), \Delta(u_n - u_n^* + u_n^* - u)\rangle \\
&= \|\Delta(u_n - u_n^*)\|_{L_2} + 2\langle \Delta(u_n^* - u), \Delta(u_n - u_n^*)\rangle + \|\Delta e_n^*\|_{L_2}
\end{aligned}$$

Note that $u_n, u_n^* \in V_n$, so is $u_n - u_n^*$. Since u and u_n^* satisfy the variational formulation (4.5.2), we have

$$\langle \Delta u_n^*, \Delta(u_n - u_n^*)\rangle = \langle f, u_n - u_n^*\rangle = \langle \Delta u, \Delta(u_n - u_n^*)\rangle.$$

Thus, $\langle \Delta(u_n^* - u), \Delta(u_n - u_n^*)\rangle = 0$. Consequently,

$$\|\Delta e_n\|_{L_2} = \|\Delta(u_n - u_n^*)\|_{L_2} + \|\Delta e_n^*\|_{L_2} \geq \|\Delta e_n^*\|_{L_2}$$

□

If $\|\Delta e_n\|_{L_2} \leq K\|\Delta e_n^*\|_{L_2}$, where K is a constant close to 1, we say that the error of an approximate solution u_n achieves the level of discretization error in the energy norm. Similarly, the error of u_n achieves the level of discretization error in the L_2 norm if $\|e_n\|_{L_2} \leq K\|e_n^*\|_{L_2}$ for K is close to 1.

4.6 Numerical Examples: Error Estimates in the Energy Norm

In physics, Δu has its own meaning where u is the solution of (4.1.1). For example, in fluid mechanics, $-\Delta u$ represents the vorticity of the fluid where u describes the stream function. In many cases, people only need to look for an approximation of Δu. Thus, it is important to design the efficient algorithms for computing approximate solutions that achieves the level of discretization error in the energy norm $\|\Delta e_n\|_{L_2}$. In this section, we will provide such algorithm and give sufficient examples to demonstrate its efficiency.

For $k > 3$, let $\mathcal{E}_k$ be the linear mapping from $\mathbb{R}^{\Psi_{k-1}}$ to $\mathbb{R}^{\Psi_k}$ that sends $(a_\psi)_{\psi\in\Psi_{k-1}}$ to $(b_\psi)_{\psi\in\Psi_k}$, where

$$b_\psi := \begin{cases} a_\psi & \text{for} \quad \psi \in \Psi_{k-1}, \\ 0 & \text{for} \quad \psi \in \Psi_k \setminus \Psi_{k-1}. \end{cases} \tag{4.6.1}$$

We use $\mathcal{P}_k$ to denote the mapping from $\mathbb{R}^{\Psi_k}$ to V_k that sends $(a_\psi)_{\psi\in\Psi_k}$ to $\sum_{\psi\in\Psi_k} a_\psi \psi$.

We wish to solve the linear system (4.5.4), i.e., $B_n z_n = \eta_n$, and then obtain an approximate solution u_n. For $4 \le k \le n$, let $z_k^{(l)}$ be the approximate solution to $B_k z_k = \eta_k$ when l^{th} PCG iteration is performed. Correspondingly, the residue $r_k^{(l)} = \eta_k - B_k z_k^{(l)}$. We apply the following multilevel algorithm.

Algorithm 4.2 Solving $B_n z_n = \eta_n$

1: Solve $B_3 z_3 = \eta_3$ exactly and denote the solution by $z_3^{(m_3)}$. Then $u_3 = \mathcal{P}_3 z_3^{(m_3)}$

2: Perform 2 PCG iterations for $B_4 z_4 = \eta_4$ with initial guess $\mathcal{E}_4 z_3^{(m_3)}$ to get $z_4^{(2)}$. $\|\Delta \tilde{e}_3\|_{L_2} \leftarrow \|\Delta(u_3 - \mathcal{P}_4 z_4^{(2)})\|_{L_2}$

3: **for** $k = 4$ to n **do**

4:
$$\epsilon_{n,k} \leftarrow \frac{k}{n} \frac{\|\Delta \tilde{e}_3\|_{L_2}}{2^{2n-5}}$$

5: Perform m_k PCG iterations for $B_k z_k = \eta_k$ with initial guess $\mathcal{E}_k z_{k-1}^{(m_{k-1})}$ to get $z_k^{(m_k)}$ such that $\|r_k^{(m_k)}\|_2 \le \epsilon_{n,k}$.

6: **end for**

Hence, $z_n^{(m_n)}$ is the approximate solution to $B_n z_n = \eta_n$ and $u_n = \mathcal{P}_n z_n^{(m_n)}$ is the approximate solution to the biharmonic equation. Set $r_n = r_n^{(m_n)}$.

Remark 1. The size of B_3 is only 49×49. We can solve $B_3 z_3 = \eta_3$ exactly. In practice, we could perform sufficient CG iterations with initial guess vector $\mathbf{0}$. Therefore, the initial residue for $B_n z_n = \eta_n$ is $r_n^0 = \eta_n$.

Remark 2. Since our numerical scheme is efficient, 2 PCG iterations are good enough to obtain an approximate solution to $B_4 z_4 = \eta_4$ with initial guess $\mathcal{E}_4 z_3^{(m_3)}$ for computing $\|\Delta \tilde{e}_3\|_{L_2}$.

Remark 3. The factor k/n in the threshold $\epsilon_{n,k}$ comes from the fact that more iterations performed on coarser grid lead to less iterations on finer grid. In practice, k/n could be replaced by a positive increasing function $a(k)$ with $a(n) = 1$.

Remark 4. Recall that the error of an approximate solution u_n achieves the level of discretization error in the energy norm, if $\|\Delta e_n\|_{L_2} \leq K \|\Delta e_n^*\|_{L_2}$ for some K close to 1. Since the rate of convergence is of order 2 for the energy norm, i.e., $\|\Delta e_n^*\|_{L_2} \leq M_1 2^{-2n}$ for some positive constant M_1 independent of n, then $\|\Delta e_n\|_{L_2} \leq M 2^{-2n}$ for some positive constant M independent of n. $\|\Delta e_n\|_{L_2} \leq M 2^{-2n}$ holds if the residue $\|r_n\|_2 \leq M_2 2^{-2n}$. This motivates us to choose the factor $\|\Delta \tilde{e}_3\|_{L_2}/2^{2n-5}$ in the threshold $\epsilon_{n,k}$. Indeed, recall that z_n and z_n^* are the approximate and exact solution to $B_n z_n = \eta_n$, respectively. Since $\{2^{-6}\Phi_3\} \bigcup \bigcup_{k=3}^{\infty} \{2^{-2k}\Gamma_k\}$ is a Riesz basis of $H_0^2(\Omega)$, we have

$$C_1 \|z_n - z_n^*\|_2 \leq \|\Delta(\mathcal{P}_n(z_n - z_n^*))\|_{L_2} \leq C_2 \|z_n - z_n^*\|_2,$$

i.e.,

$$C_1 \|z_n - z_n^*\|_2 \leq \|\Delta(u_n - u_n^*)\|_{L_2} \leq C_2 \|z_n - z_n^*\|_2, \tag{4.6.2}$$

Let the residue $r_n = \eta_n - B_n z_n$. Then $B_n(z_n - z_n^*) = B_n z_n - \eta_n = -r_n$. Since the condition number of B_n is uniformly bounded, there exist two positive numbers C_3 and C_4 independent of n such that

$$C_3\|z_n - z_n^*\|_2 \le \|r_n\|_2 \le C_4\|z_n - z_n^*\|_2,$$

This in connection with (4.6.2) gives

$$\frac{C_1}{C_4}\|r_n\|_2 \le \|\Delta(u_n - u_n^*)\|_{L_2} \le \frac{C_2}{C_3}\|r_n\|_2.$$

Note that $e_n - e_n^* = u_n - u_n^*$, thus

$$\|\Delta e_n\|_{L_2} - \|\Delta e_n^*\|_{L_2} \le \|\Delta(e_n - e_n^*)\|_{L_2} = \|\Delta(u_n - u_n^*)\|_{L_2} \le \frac{C_2}{C_3}\|r_n\|_2.$$

This shows

$$\|\Delta e_n\|_{L_2} \le \|\Delta e_n^*\|_{L_2} + \frac{C_2}{C_3}\|r_n\|_2.$$

Consequently, $\|r_n\|_2 \le M_2 2^{-2n}$ leads to $\|\Delta e_n\|_{L_2} \le M 2^{-2n}$.

Note that m_k $(4 \le k \le n)$ iterations at level k are equivalent to $m_k/4^{n-k}$ iterations at level n. Thus, the total number of equivalent iterations at level n is computed by the following formula.

$$N_{it} = \sum_{k=4}^{n} \frac{m_k}{4^{n-k}}. \tag{4.6.3}$$

We are in a position to give numerical examples to show that the above algorithm is efficient. The following computation is conducted on a Lenovo desktop with 2 GB memory and an Intel Core 2 CPU 6400 at 2.13 GHz.

Example 4.1. *Consider the biharmonic equation (4.1.1) on* Ω *with* f *given by*

$$f(x, y) = t\pi^4[4\cos(2\pi x)\cos(2\pi y) - \cos(2\pi x) - \cos(2\pi y)], (x, y) \in \Omega,$$

where $t > 0$ is so chosen that $\|f\|_{L_2} = 1$. The exact solution of the equation is

$$u(x,y) = t[1-\cos(2\pi x)][1-\cos(2\pi y)]/16, (x,y) \in \Omega.$$

TABLE 4.2: Numerical Results of Example 4.1

Level n	Grid $2^n \times 2^n$	N_{it}	$\|r_n^0\|_2$	$\|r_n\|_2$	$\|\Delta e_n\|_{L_2}$	$\|\Delta e_n^*\|_{L_2}$	Time(s)
5	32×32	1.75	5.64e-3	1.01e-5	2.23e-5	2.00e-5	0.001
6	64×64	1.81	5.64e-3	1.72e-6	5.21e-6	4.99e-6	0.002
7	128×128	1.88	5.64e-3	3.02e-7	1.28e-6	1.25e-6	0.007
8	256×256	1.80	5.64e-3	7.25e-8	3.22e-7	3.11e-7	0.029
9	512×512	1.81	5.64e-3	1.32e-8	8.02e-8	7.79e-8	0.133
10	1024×1024	1.50	5.64e-3	9.31e-9	2.12e-8	1.95e-8	0.531

In the above table, the third column gives the total number N_{it} of equivalent iterations at level n computed by (4.6.3). For instance, for $n = 10$ and $4 \le k \le n$, m_k iterations are required for the equation $B_k z_k = \eta_k$, where $m_4 = 15$, $m_5 = 13$, $m_6 = 8$, $m_7 = 5$, $m_8 = 2$, $m_9 = 1$, and $m_{10} = 1$. By (4.6.3) we have

$$N_{it} = \sum_{k=4}^{n} \frac{m_k}{4^{n-k}} = \frac{15}{4096} + \frac{13}{1024} + \frac{8}{256} + \frac{5}{64} + \frac{2}{16} + \frac{1}{4} + 1 \approx 1.50.$$

The fourth column of the above table lists the initial residue, and the fifth column lists the residue when the algorithm terminates. Note that $\|r_n^0\|_2$ depends on n. But the first three digits of $\|r_n^0\|_2$ are the same for $n \ge 5$.

The sixth column gives the err $\|\Delta e_n\|_{L_2}$ of the approximate solution in the energy norm. For the purpose of comparison, we lists the discretization error $\|\Delta e_n^*\|_{L_2}$ in the energy norm in the seventh column. Recall that $e_n^* = u_n^* - u$ and $u_n^* = \mathcal{P}_n z_n^*$, where z_n^* is the exact solution to equation (4.5.4), which is obtained by sufficiently many iterations. We find that

$$\|\Delta e_n\|_{L_2} \leq 1.12\|\Delta e_n^*\|_{L_2} \text{ for } 5 \leq n \leq 10.$$

This shows that the approximate solution obtained by our algorithm achieves the level of discretization error. Moreover, we see that

$$\|\Delta e_{n+1}^*\|_{L_2}/\|\Delta e_n^*\|_{L_2} < 0.2506 \approx 1/4 \text{ for } 5 \leq n \leq 9$$

which indicates that the rate of convergence is of order 2.

The last column gives the CPU time in seconds for solving the linear system of equations $B_n z_n = \eta_n$. At level $n = 10$, the matrix B_{10} has size 1046529×1046529. Our algorithm takes only 0.531 second to solve the equation $B_{10} z_{10} = \eta_{10}$.

Example 4.2. *For $(x, y) \in \mathbb{R}^2$, let $z := (x - 1/2)^2 + (y - 1/2)^2 - 1/4$. Consider the biharmonic equation (4.1.1) on Ω with f given by*

$$f(x, y) = t[(4z + 1)^2 \sin z + 16(4z + 1)(1 - \cos z) + 32(z - \sin z)]$$

for $z < 0$, and $f(x, y) = 0$ for $z \geq 0$, where $t > 0$ is so chosen that $\|f\|_{L_2} = 1$. The exact solution is given by $u(x, y) = t(\sin z - z + z^3/3)$ for $(x, y) \in \Omega$.

The following table lists the numerical results. Note that in this example, we have

$$\|\Delta e_n\|_{L_2} \leq 1.11\|\Delta e_n^*\|_{L_2} \text{ for } 5 \leq n \leq 10.$$

Thus the level of discretization error in the energy norm is achieved.

TABLE 4.3: Numerical Results of Example 4.2

Level n	Grid $2^n \times 2^n$	N_{it}	$\|r_n^0\|_2$	$\|r_n\|_2$	$\|\Delta e_n\|_{L_2}$	$\|\Delta e_n^*\|_{L_2}$	Time(s)
5	32×32	2.00	5.19e-3	9.35e-6	2.89e-5	2.77e-5	0.001
6	64×64	1.81	5.19e-3	2.32e-6	7.47e-6	6.78e-6	0.002
7	128×128	1.92	5.19e-3	3.72e-7	1.76e-6	1.69e-6	0.007
8	256×256	1.60	5.19e-3	1.35e-7	4.50e-7	4.21e-7	0.026
9	512×512	1.51	5.19e-3	2.95e-8	1.16e-7	1.05e-7	0.122
10	1024×1024	1.43	5.19e-3	9.61e-9	2.84e-8	2.63e-8	0.523

Example 4.3. *Consider the biharmonic equation (4.1.1) with f given by*

$$f(x,y) = te^{(3x-y)^2}, (x,y) \in \Omega,$$

where $t > 0$ is so chosen that $\|f\|_{L_2} = 1$.

In this case, the exact solution is unknown. We list the error $\|\Delta \tilde{e}_n\|_{L_2}$ of the approximate solutions between consecutive levels and $\|\Delta \tilde{e}_n^*\|_{L_2}$ for comparison.

TABLE 4.4: Numerical Results of Example 4.3

Level n	Grid $2^n \times 2^n$	N_{it}	$\|r_n^0\|_2$	$\|r_n\|_2$	$\|\Delta\tilde{e}_n\|_{L_2}$	$\|\Delta\tilde{e}_n^*\|_{L_2}$	Time(s)
5	32×32	2.75	1.15e-3	7.02e-6	3.58e-5	3.58e-5	0.001
6	64×64	3.13	1.15e-3	1.83e-6	8.89e-6	8.87e-6	0.002
7	128×128	3.25	1.15e-3	4.20e-7	2.20e-6	2.20e-6	0.009
8	256×256	3.31	1.15e-3	8.23e-8	5.51e-7	5.51e-7	0.048
9	512×512	2.27	1.15e-3	4.98e-8	1.38e-7	1.38e-7	0.157

The sixth column and seventh column are almost the same. Hence, the approximate solution achieves the level of discretization error.

Example 4.4. *Let* $(c_{i_1,i_2})_{0\le i_1,i_2\le 2^{10}}$ *be a random array of real numbers between 0 and 1. Consider the biharmonic equation (4.1.1) with* f *being a piecewise constant function given by*

$$f(x,y) = tc_{i_1,i_2} \text{ for } \frac{i_1}{2^{10}} < x < \frac{i_1+1}{2^{10}} \text{ and } \frac{i_2}{2^{10}} < y < \frac{i_2+1}{2^{10}}.$$

where $t > 0$ *is so chosen that* $\|f\|_{L_2} = 1$.

In this example, the exact solution is unknown. We list $\|\Delta\tilde{e}_n\|_{L_2}$ and $\|\Delta\tilde{e}_n^*\|_{L_2}$ in the following table showing the numerical results.

Table 4.5: Numerical Results of Example 4.4

Level n	Grid $2^n \times 2^n$	N_{it}	$\|r_n^0\|_2$	$\|r_n\|_2$	$\|\Delta\tilde{e}_n\|_{L_2}$	$\|\Delta\tilde{e}_n^*\|_{L_2}$	Time(s)
5	32×32	2.75	5.55e-3	8.78e-6	3.31e-5	3.31e-5	0.001
6	64×64	3.06	5.55e-3	2.01e-6	8.29e-6	8.29e-6	0.002
7	128×128	1.98	5.55e-3	9.55e-7	2.08e-6	2.08e-6	0.006
8	256×256	1.99	5.55e-3	2.04e-7	5.35e-7	5.35e-7	0.032
9	512×512	1.93	5.55e-3	6.20e-8	1.42e-7	1.42e-7	0.139

For relative residue reduction in the l_2 norm, the above numerical examples show that our algorithm requires considerably fewer iterations than those reported in [32] and [37]. Let us discuss relative residue reduction in l_∞ norm given by the quantity $\tau_n := \|r_n\|_\infty / \|r_n^0\|_\infty$. In the following table, for $\epsilon = 10^{-4}$, 10^{-5} and 10^{-6}, we list the average number of iterations needed for $\tau_n < \epsilon$ in the above four examples.

Table 4.6: Relative Residue Reduction in l_∞ Norm

Level n	Grid $2^n \times 2^n$	$\tau_n < 10^{-4}$	$\tau_n < 10^{-5}$	$\tau_n < 10^{-6}$
8	256×256	1.8	3.0	5.0
9	512×512	1.4	2.0	2.9
10	1024×1024	1.3	1.5	1.9

The relative residue reduction in the l_∞ norm was discussed in [34] for the 258×258 grid discretized by piecewise linear elements. It required 4 BICGSTAB iterations to get $\tau_8 < 6.2 \times 10^{-4}$ and 20 BICGSTAB iterations to get $\tau_8 < 1.2 \times 10^{-6}$. Further, 3 multigrid $V(1,1)$ cycles per iteration were performed for preconditioning (see Table 4 iii in [34]). The algebraic multigrid method was used in [7] and [8]. It was reported in Table 10 of [7] that more than 40 iterations were needed for the relative residue reduction in the l_∞ norm to be less than 10^{-6}.

We remark that residue reductions are not fully comparable, because the corresponding matrices are different in different contexts. We think that it is more appropriate to compare the efficiency of numerical algorithms to achieve the level of discretization error. The wavelet Galerkin method we propose has the advantage that the number of iterations needed to achieve the level of discretization error will not increase as the mesh size decreases. In comparison, in most of the aforementioned papers, the number of iterations would increase as the mesh size decreases.

4.7 Numerical Examples: Error Estimates in the L_2 and L_∞ Norms

In this section we investigate numerical solutions of the biharmonic equation and estimate errors of the approximate solutions in the L_2 and L_∞ norms. We simply perform more iterations to achieve the level of discretization error. For the examples considered in this section, about 7 equivalent PCG iterations based on our wavelets will be sufficient.

The following example was considered in [1]. We define

$$\|e_n\|_\infty := \max\{|e_n(i_1/2^n, i_2/2^n)| : 0 \le i_1, i_2 \le 2^n\}$$

which agrees with the one given in [1].

Example 4.5. *Consider the biharmonic equation (4.1.1) with f given by*

$$f(x,y) = 16\pi^4[4\cos(2\pi x)\cos(2\pi y) - \cos(2\pi x) - \cos(2\pi y)], (x,y) \in \Omega,$$

The exact solution of the equation is

$$u(x,y) = [1 - \cos(2\pi x)][1 - \cos(2\pi y)], (x,y) \in \Omega.$$

The numerical results are listed in the following table.

Table 4.7: Error Estimates in the Maximum Norm

Level n	Grid $2^n \times 2^n$	$\|e_n^D\|_\infty$	Time (s)	$\|e_n^{LD}\|_\infty$	Time (s)	$\|e_n^*\|_\infty$
5	32×32	6.28e-6	0.003	6.28e-6	0.004	6.28e-6
6	64×64	3.90e-7	0.007	3.90e-7	0.013	3.90e-7
7	128×128	2.44e-8	0.026	2.44e-8	0.047	2.44e-8
8	256×256	4.19e-9	0.110	1.52e-9	0.198	1.52e-9
9	512×512	4.27e-8	0.507	8.34e-11	0.885	8.31e-11

In the above table, the third column gives the error $\|e_n^D\|_\infty$ by using the double precision arithmetic, and the fourth column lists the corresponding CPU time in seconds. The fifth column gives the error $\|e_n^{LD}\|_\infty$ by using the long double precision arithmetic, and the sixth column lists the corresponding CPU time in seconds. The last column provides the discretization error $\|e_n^*\|_\infty$ in the l_∞ norm for comparison.

We observe that, starting from level 8, the accuracy of the approximate solutions is affected by the roundoff errors if the double precision arithmetic is used. But the long double precision gives the desired accuracy at levels

8 and 9. We also find that $\|e_n^*\|_\infty / \|e_{n+1}^*\|_\infty < 0.626 \approx 2^{-4}$ for $n = 5, 6, 7, 8$. Thus, the rate of convergence is of order 4.

A vector difference scheme of order 4 was used in [1]. The matrix obtained from discretization using their scheme has size $3(2^n-1)^2 \times 3(2^n-1)^2$ at level n. In comparison, the matrix B_n has size $(2^n-1)^2 \times (2^n-1)^2$. But our discretization error $\|e_n^*\|_\infty$ is smaller. For instance, for $n = 7$ we have $\|e_7^*\|_\infty \approx 2.44 \times 10^{-8}$, while the corresponding discretization error in [1] is 4.2×10^{-8}. It was reported in [1] that 3 FMG (Full Multigrid) $W(3,2)$-cycles were used to achieve the level of discretization error. We estimate that a multiplication of their matrix with a vector costs as twice as much as a multiplication of our matrix (B_n) with a vector (see the above comparison of the matrix size). Consequently, we estimate that a multigrid $V(3,2)$-cycle costs as much as 5 PCG iterations of our scheme. The computational cost of a FMG $W(3,2)$-cycle is about twice of the cost of a simple $V(3,2)$-cycle (see [1]). Thus, the computational cost of 3 FMG $W(3,2)$-cycles is about the cost of 30 PCG iterations of our scheme.

Example 4.6. *Consider the biharmonic equation (4.1.1) on Ω with f given by*

$$f(x,y) = e^{(3x-y)^2}, (x,y) \in \Omega.$$

In this case, the exact solution is unknown. In the following table we list numerical results of the approximate solutions that achieve the level of discretization error in the L_2 norm. The numerical computation shows that the rate of convergence is of order 4.

Table 4.8: Error Estimates in the L_2 Norm

Level n	Grid $2^n \times 2^n$	$\|\tilde{e}_n^D\|_{L_2}$	Time(s)	$\|\tilde{e}_n^{LD}\|_{L_2}$	Time(s)	$\|\tilde{e}_n^*\|_{L_2}$
5	32×32	7.18e-7	0.003	7.18e-7	0.004	7.18e-7
6	64×64	4.18e-8	0.007	4.18e-8	0.013	4.18e-8
7	128×128	2.54e-9	0.026	2.54e-9	0.047	2.54e-9
8	256×256	1.67e-10	0.110	1.59e-10	0.198	1.58e-10
9	512×512	1.20e-9	0.507	1.00e-11	0.885	9.92e-12

4.8 General Fourth-order Elliptic Equations

In this section we extend our study to general elliptic equations of fourth order. If the Dirichlet form of a fourth-order elliptic operator is strictly coercive, then the wavelet bases constructed in this chapter are still applicable to numerical solutions of the corresponding fourth-order elliptic equation with homogeneous boundary conditions. For simplicity, we consider the following elliptic equation,

$$\begin{cases} \Delta(a(x,y)\Delta u)(x,y) = f(x,y) & \text{for} \quad (x,y) \in \Omega, \\ u(x,y) = \dfrac{\partial}{\partial n} u(x,y) = 0 & \text{for} \quad (x,y) \in \partial\Omega, \end{cases} \tag{4.8.1}$$

where $a(x,y)$ is a continuous function on Ω and there exist two positive constants K_1 and K_2 such that $K_1 \leq a(x,y) \leq K_2$ for all $(x,y) \in \Omega$. The variational form corresponding to this elliptic equation is

$$\langle a\Delta u, \Delta v \rangle = \langle f, v \rangle, \forall v \in H_0^2(\Omega)$$

We use our wavelet bases to discretize this equation and obtain the following linear system:

$$B_n^a z_n = \eta_n, \tag{4.8.2}$$

where $B_n^a = (\langle a\Delta\chi, \Delta\psi\rangle)_{\chi,\psi\in\Psi_n}$ and η_n is the column vector $(\langle f, \psi\rangle)_{\psi\in\Psi_n}$. Then the approximate solution in V_n is $u_n = \sum_{\psi\in\Psi_n} z_\psi \psi$.

Note that $K_1 \le a(x, y) \le K_2$, then $\langle a\Delta u, \Delta v\rangle$ is continuous and coercive. An application of proposition 1.1 gives the following theorem.

Theorem 4.11. *The condition number $\kappa(B_n^a)$ is uniformly bounded.*

Example 4.7. *Let $a(x, y) := (1 + x)(1 + y)$ for $(x, y) \in \Omega$. Suppose f is obtained by (4.8.1) with exact solution u given by*

$$u(x, y) = [1 - \cos(2\pi x)][1 - \cos(2\pi y)]/4, (x, y) \in \Omega. \tag{4.8.3}$$

The numerical results are listed in the following table.

TABLE 4.9: Numerical Results of Example 4.7

Level n	Grid $2^n \times 2^n$	$\|e_n\|_{L_2}$	$\|e_n^*\|_{L_2}$	Time (s)
5	32×32	7.38e-7	7.38e-7	0.017
6	64×64	4.57e-8	4.57e-8	0.053
7	128×128	2.85e-9	2.85e-9	0.196
8	256×256	1.78e-10	1.78e-10	0.806
9	512×512	1.10e-11	1.10e-11	3.524

Example 4.8. *Let $a(x, y) := 1+0.5 \sin[10.8(x-y)]$ for $(x, y) \in \Omega$. Suppose f is obtained by (4.8.1) with exact solution u given by (4.8.3).*

The numerical results are listed in the following table.

Table 4.10: Numerical Results of Example 4.8

Level n	Grid $2^n \times 2^n$	$\|e_n\|_{L_2}$	$\|e_n^*\|_{L_2}$	Time (s)
5	32×32	8.25e-7	8.25e-7	0.017
6	64×64	5.11e-8	5.11e-8	0.053
7	128×128	3.21e-9	3.18e-9	0.196
8	256×256	2.04e-10	1.99e-10	0.806
9	512×512	1.26e-11	1.21e-11	3.524

From the numerical examples, we see that our numerical schemes also have superb performance on solving general elliptic equations of fourth order.

Chapter 5

Conclusions and Future Work

In this thesis, we present new constructions of spline wavelet bases, establish their stability in Sobolev spaces and demonstrate their effectiveness for numerical solutions of elliptic equations.

We provide different ways to construct wavelet bases. All of these constructions are simple. Consequently, the corresponding numerical schemes are easily implemented. On one hand, we prove that the condition numbers of the stiffness matrices associated with our wavelet bases are uniformly bounded. This guarantees that the number of iterations needed to achieve the level of discretization error will not increase under mesh refinement. Therefore, the wavelet Galerkin method is suitable for large scale computation. On the other hand, we compute the condition numbers numerically. Numerical experiments confirm our theoretical results, and indicate that the condition numbers are relatively small compared with those provided by other preconditioning techniques. Thus our methods are efficient and competitive to the existing methods.

These wavelet bases are then applied to solve elliptic equations with homogeneous boundary conditions. Since our preconditioning techniques are effective, classical iterative algorithms have good performance. To further speed up these algorithms, we use the multilevel idea in the wavelet Galerkin method. In particular, we design extremely fast automatic multilevel algorithms based on PCG algorithm for computing approximate solutions that achieve the level of discretization error in the energy norm. Numerical examples demonstrate the advantages of the wavelet Galerkin method we propose over many other popular numerical methods.

Based on the theoretical and numerical results obtained in this thesis, we believe that the wavelet method has great potential in numerical solutions of partial differential equations.

In [30] and [31], Liu and Xu developed Galerkin methods for solving high-order singularly perturbed problems of reaction diffusion and convection diffusion types, respectively. They used Hermite splines with knots adapted to the singular behavior of the solution of the problems. In particular, fourth-order singularly perturbed problems were solved using Hermite cubic splines. We may consider employing wavelet bases on the adaptive mesh concentrated in the layers to improve the numerical performance. Kumar [28] applied the wavelet optimized finite difference method based on an interpolating wavelet transform using cubic spline to solve the singularly perturbed reaction diffusion equations of elliptic and parabolic types. Our wavelet bases constructed in Chapter 2 may also be used to generate adaptive mesh.

It is known that finite element methods have advantages over finite difference methods in solving high order PDEs on irregular domains. But for second-order problems on regular domains, especially with variable coefficients, finite difference methods could have better performance since they don't have to do numerical integrations. Let us consider using the general

9-point stencil

$$(1-\alpha)\begin{pmatrix} 0 & 1 & 0 \\ 1 & -4 & 1 \\ 0 & 1 & 0 \end{pmatrix} + \frac{\alpha}{2}\begin{pmatrix} 1 & 0 & 1 \\ 0 & -4 & 0 \\ 1 & 0 & 1 \end{pmatrix},$$

$0 \le \alpha \le 1$, to discretize equation (3.1.2). Note that the standard 5-point stencil is obtained with $\alpha = 0$. The 9-point stencil with $\alpha = 2/3$ is used in chapter 3. And we construct stable wavelet bases which provide efficient preconditioners for the resulting linear systems. In fact, more is true numerically. If we discretize the Poisson equation using the 9-point stencil with α other than $2/3$, those preconditioners still work well. For instance, the condition numbers of the preconditioned finite difference matrices are uniformly bounded by 13, 10, 9, 8 and 7 as $\alpha = 0, 1/4, 1/3, 1/2$ and $3/4$, respectively. But for $\alpha = 1$, it seems that the condition number grows as the mesh size decreases. From the numerical experiments, we guess that our wavelets are applicable in the case $0 \le \alpha < 1$. How to prove this theoretically is a specific problem I will work on. This work will broaden the applications of our wavelet bases in general difference schemes. In the long term, the application of wavelet preconditioning techniques in finite difference methods will be studied.

On regular domains such as rectangular domains, we have successfully applied the wavelet Galerkin method to numerical solutions of elliptic equations and presented numerical results to demonstrate their advantages. Stable wavelet bases on general meshes have been studied by many mathematicians (see, e.g., [17] and [25]). However, numerical schemes have yet to be implemented. On general domains, how to construct stable wavelet bases which are both easily implemented and effective still needs to be further investigated.

Bibliography

[1] I. Altas, J. Dym, M. M. Gupta, and R. P. Manohar, Multigrid solution of automatically generated high-order discretizations for the biharmonic equation, *SIAM J. Sci. Comput.* **19** (1998), 1575-1585.

[2] D. Braess, Towards algebraic multigrid for elliptic problems of second order, *Computing* **55** (1995), 379-393.

[3] J. H. Bramble, J. E. Pasciak and J. Xu, Parallel multilevel preconditioners, *Math. Comp.* **55** (1990), 1-22.

[4] A. Brandt, Multi-level adaptive solutions to boundary-value problem, *Math. Comp.* **31** (1977), 333-390.

[5] S. C. Brenner and L. R. Scott, The Mathematical Theory of Finite Element Methods, Second Edition, Springer-Verlag, New York, 2002.

[6] W. L. Briggs, V. E. Henson, S. F. McCormick, A Multigrid Tutorial, second edition, SIAM, Philadelphia, 2000.

[7] Q. Chang and Z. Huang, Efficient algebraic multigrid algorithms and their convergence, *SIAM J. Sci. Comput.* **24** (2002), 597-618.

[8] Q. Chang, Y. S. Wong and H. Fu, On the algebraic multigrid method, *J. Comput. Phys.* **125** (1996), 279-292.

[9] Z. Chen, B. Wu and Y. Xu, Multilevel augmentation methods for differential equations, *Adv. Comput. Math.* **24** (2006), 213-238.

[10] M. A. Christon and D. W. Roach, The numerical performance of wavelets for PDEs: the multi-scale finite element, *Comp. Mech.* **25** (2000), 230-244.

[11] C. K. Chui and E. Quak, Wavelets on a bounded interval, in Numerical Methods in Approximation Theory, Vol. 9, D. Braess and L. L. Schumaker (eds.), pp. 53-75, Birkhäser, Basel, 1992.

[12] C. K. Chui and J. Z. Wang, On compactly supported spline wavelets and a duality principle, *Trans. Amer. Math. Soc.* **330** (1992), 903-916.

[13] A. Cohen, I. Daubechies and P. Vial, Wavelets on the interval and fast wavelet transforms, *Appl. Comput. Harmon. Anal.* **1** (1993), 54-81.

[14] W. Dahmen, B. Han, R. Q. Jia and A. Kunoth, Biorthogonal multiwavelets on the interval: cubic Hermite splines, *Constr. Approx.* **16** (2000), 221-259.

[15] W. Dahmen and C. A. Micchelli, Biorthogonal wavelet expansions, *Constr. Approx.* **13** (1997), 293-328.

[16] I. Daubechies, Ten Lectures on Wavelets, SIAM, Philadelphia, 1992.

[17] O. Davydov and R. Stevenson, Hierachical Riesz bases for $H^s(\Omega)$, $1 < s < 5/2$, *Constr. Approx.* **22** (2005), 365-394.

[18] B. Engquist and E. Luo, Convergence of a multigrid method for elliptic equations with highly oscillatory coefficients, *SIAM J. Numer. Anal.* **34** (1997), 2254-2273.

[19] L. C. Evans, Partial Differential Equations, American Mathematical Society, Providence, 1998.

[20] P. Grisvard, Elliptic Problems in Nonsmooth Domains, Pitman Monographs and Studies in Mathematics, 24, Pitman, Boston, 1985.

[21] B. Han and Z. Shen, Wavelets with short support, *SIAM J. Math. Anal.* **38** (2006), 530-556.

[22] R. Q. Jia, Stable bases of spline wavelets on the interval, in Wavelets and Splines, G. R. Chen and M. J. Lai (eds.), pp. 243-259, Nashboro Press, Brentwood, 2006.

[23] R. Q. Jia, Spline wavelet on the interval with homogeneous boundary conditions, *Adv. Comput. Math.* **30** (2009), 177-200.

[24] R. Q. Jia and S. T. Liu, Wavelet bases of Hermite cubic splines on the interval, *Adv. Comput. Math.* **25** (2006), 23-39.

[25] R. Q. Jia and S. T. Liu, C^1 spline wavelets on triangulations, *Math. Comp.* **78** (2008), 287-312.

[26] R. Q. Jia, J. Wang and D. X. Zhou, Compactly supported wavelet bases for Sobolev spaces, *Appl. Comput. Harmon. Anal.* **15** (2003), 224-241.

[27] R. Q. Jia and W. Zhao, Riesz bases of wavelets and applications to numerical solutions of elliptic equations, *Math. Comp.*, to appear.

[28] V. Kumar, Solving singularly perturbed reaction diffusion problems using wavelet optimized finite difference and cubic spline adaptive wavelet scheme, *Int J. Numer. Anal. Model.* **5** (2008), 270-285.

[29] S. T. Liu, Additive Schwarz-type preconditioners for fourth-order elliptic problems using hermite cubic splines, *Numer. Methods Partial Differential Equations* **22** (2006), 69-78.

[30] S. T. Liu and Y. Xu, Galerkin methods based on hermite splines for singular perturbation problems, *SIAM J. Numer. Anal.* **43** (2006), 2607-2623.

[31] S. T. Liu and Y. Xu, Graded Galerkin methods for the high-order convection-diffusion problem, *Numer. Methods Partial Differential Equations* **25** (2009), 1261-1282.

[32] P. Oswald, Multilevel preconditioners for discretizations of the biharmonic equation by rectangular finite elements, *Numer. Linear Algebra Appl.* **2** (1995), 487-505.

[33] S. Schaffer, A semicoarsening multigrid method for elliptic partial differential equations with highly discontinuous and anisotropic coefficients, *SIAM J. Sci. Comput.* **20** (1998), 228-242.

[34] D. J. Silvester and M. D. Mihajlovic, Efficient preconditioning of the biharmonic equation, *Numerical Analysis Report* **362** (2000), Manchester Center for Computational Mathematics, University of Manchester.

[35] R. Stevenson, A robust hierarchical basis preconditioner on general meshes, *Numer. Math.* **78** (1997), 269-303.

[36] R. Stevenson, Stable three-point wavelet bases on general meshes, *Numer. Math.* **80** (1998), 131-158.

[37] J. C. Sun, Domain decompositions and multilevel PCG method for solving 3-D fourth order problems, *Contemp. Math.* **157** (1994), 71-78.

[38] S. Timoshenko and S. Woinowsky-Krieger, Theory of Plates and Shells, McGraw-Hill, New York, 1959.

[39] U. Trottenberg, C. W. Oosterlee, A. Schüller, Multigrid, Academic Press, London, 2001.

[40] J. Xu, Iterative methods by space decomposition and subspace correction, *SIAM Rev.* **34** (1992), 581-613.

[41] K. Yosida, Functional Analysis, Springer-Verlag, Berlin, 1968.

[42] R. M. Young, An Introduction to Nonharmonic Fourier Series, Academic Press, New York, 1980.

[43] X. Zhang, Multilevel Schwarz methods, *Numer. Math.* **63** (1992), 521-539.